Decoding protein phosphorylation during oocyte meiotic divisions using phosphoproteomics

Leonid Peshkin[1#]✉, Enrico Maria Daldello[2#], Elizabeth Van Itallie[1], Matthew Sonnett[1], Johannes Kreuzer[1], Wilhelm Haas[1], Marc W Kirschner[1] and Catherine Jessus[2]

[1] Systems Biology Department, Harvard Medical School, Boston, MA, 02115, USA

[2] Sorbonne Université, CNRS, Laboratoire de Biologie du Développement - Institut de Biologie Paris Seine, LBD - IBPS, F-75005 Paris, France

[#] Equal contribution

✉Corresponding author: Leonid_Peshkin@hms.harvard.edu

Running title: Protein phosphorylation during oocyte meiotic divisions

ABSTRACT

Oocyte meiotic divisions represent a critical process in sexual reproduction, as a diploid non-dividing oocyte is transformed into a haploid fertilizable egg, as a prelude for the subsequent embryonic divisions and differentiation. Although cell differentiation and proliferation are governed by transcription, oocyte maturation and early embryonic divisions depend entirely on changes in protein abundance and post-translational modifications. Here, we analyze the abundance and phosphorylation of proteins during *Xenopus* oocyte meiotic maturation. We reveal significant shifts in protein stability, related to spindle assembly, DNA replication and RNA-binding. Our analysis pinpoints broad changes in phosphorylation correlating with key cytological meiotic milestones, noteworthy changes in membrane trafficking, nuclear envelope disassembly and modifications in microtubule dynamics. Additionally, specific phosphorylation events target regulators of protein translation, Cdk1 and the Mos/MAPK pathway, thereby providing insight into the dynamics of Cdk1 activity, as related to the meiotic cell cycle. This study sheds light on the orchestration of protein dynamics and phosphorylation events during oocyte meiotic divisions, providing a rich resource for understanding the molecular pathways orchestrating meiotic progression in the frog, and most likely applicable to other vertebrate species.

Key Words: Meiotic divisions/Meiotic maturation/Protein phosphorylation/Phosphoproteome/*Xenopus* oocyte

INTRODUCTION

In mature females, the oocyte undergoes a long period of growth, during which meiosis is arrested at prophase I. In the *Xenopus* oocyte, transcription is switched off when the oocyte reaches the end of its growth phase (Dumont, 1972). The full-grown oocyte is transcriptionally silent and equipped with a stock of mRNAs and proteins that will support without transcription three critical embryonic processes: first, two meiotic divisions that transform the oocyte into a fertilizable haploid egg; second, the process of fertilization; and third, 13 embryonic divisions, after which transcription is initiated.

The transformation of a fully-grown oocyte arrested in prophase into a fertilizable cell, arrested in metaphase of the second meiotic division is a process called meiotic maturation. Meiotic maturation is triggered by progesterone, secretion by the follicle cells surrounding the oocyte. The secretion of progesterone is stimulated by Follicle Stimulating Hormone secreted by the pituitary. Progesterone initiates a molecular signaling cascade that lasts 3 to 4 hours and occurs with little change in oocyte morphology. Notably, this cascade leads to the activation of the Cdk1-Cyclin B kinase, the universal inducer of cell division in eukaryotes. Cdk1 phosphorylates many substrates that promote meiotic nuclear events: nuclear envelope breakdown (NEBD), the formation of the first meiotic spindle (MI), the completion of the first meiotic division with expulsion of a polar body, and formation of the second meiotic spindle (MII) (Fig. 1). As in all vertebrates, the frog oocyte arrests a second time in metaphase II, until fertilization stimulates the completion of the second meiotic division. The entire process of oocyte maturation occurs in the absence of transcription. The regulation of the two meiotic divisions and the 13 mitotic divisions that follow are thought to be largely regulated by changes in protein abundance and phosphorylation/dephosphorylation.

The prophase arrested oocyte contains a store of Cdk1-Cyclin B complexes that are kept inhibited by Cdk1 phosphorylation at Y15 and T14, which are substrates of the kinase, Myt1 (Mueller *et al*, 1995). In all vertebrates, the prophase arrest is maintained by high levels of cAMP and PKA (cAMP-activated protein kinase) activity (Fig. 1). The release of this prophase block is triggered by a drop in the levels of cAMP and the consequent inhibition of PKA, which occurs within 60 min after progesterone stimulation. The identity of the critical PKA substrates whose dephosphorylation is thought to induce the pathway leading to Cdk1 activation is still unknown, with the exception of Arpp19 whose mechanism of action is not completely understood (Dupré *et al*, 2014; Santoni *et al*, 2024). Nevertheless, a drop in PKA activity leads to the synthesis of new proteins from cytoplasmic stockpiles of mRNAs as well as increases in protein level through regulation of the ubiquitination machinery (Santoni *et al*, 2024). Among the accumulated proteins are Cyclin B1, the best-known activator of Cdk1 in mitotic cells, and

Mos, a kinase specific to the oocytes (Fig. 1). The newly synthesized B1-Cyclins bind to monomeric Cdk1 to form a small pool of active complexes that evade the inhibition of Myt1 (Hochegger *et al*, 2001; Gaffré *et al*, 2011). Subsequently, this small amount of active Cdk1 initiates a complex network of feedback loops, involving many kinases and phosphatases, thereby creating an auto-amplification loop (Jessus, 2010) (Fig. 1). Within this loop, the activation of the Cdc25 phosphatase that dephosphorylates Cdk1 and the inhibition of the PP2A phosphatase that counteracts Cdk1, lead to a rapid and full activation of Cdk1-Cyclin B (Jessus, 2010; Lemonnier *et al*, 2020). Another important player in this positive feedback loop is Mos, whose translation is induced by progesterone and which accumulates at the time of Cdk1 activation (Sagata *et al*, 1988, 1989a; Frank-Vaillant *et al*, 1999). Mos activates Erk1/2 (also known as MAPK) indirectly, which modulates the core regulators of Cdk1 (Haccard & Jessus, 2006) (Fig. 1). Cdk1 and the kinases activated under its control (Mos/MAPK, Aurora-A, Plk1, etc.) trigger a second wave of protein translation and accumulation, as well as mediating the structural changes of cell division: NEBD, chromosome condensation and formation of the Meiosis I spindle (Jessus, 2010; Santoni *et al*, 2024). They also activate the anaphase-promoting complex (APC), an E3 ubiquitin ligase, leading to the degradation of both Cyclin B and securin, thus enabling entry into anaphase I and chromosome separation and the expulsion of the 1st polar body (Fig. 1). The decrease in Cdk1 activity is rapidly followed by the inhibition of APC , which then allows the accumulation of B-Cyclins and increase of Cdk1 activity (Fig. 1). These events trigger the entry into metaphase II and the formation of the MII spindle. In all vertebrates as a result of the stabilization of cyclin B oocytes arrest in the middle of the meiotic division due to the stabilization of B-Cyclins, resulting from APC inhibition by the Emi2/Erp1 (Jessus, 2010) (Fig. 1).

The burst of phosphorylation, which occurs at NEBD when Cdk1 is activated, targets proteins belonging to three categories (Maller *et al*, 1977): first, regulators of translation and/or degradation of proteins that are essential for the progression of meiotic divisions; second, proteins directly involved in the intracellular reorganization of the oocyte, such as the components of meiotic spindles, the nuclear envelope or other cytoskeletal elements; third, proteins that do not have a role in meiotic divisions but regulate fertilization and early embryonic development. Notably, the sperm does not contribute any proteins or RNA except for its genome and its two centrioles. With fertilization there is extrusion of the 2nd polar body, the fusion of the male and female pronuclei. Within a few minutes after fertilization the first S-phase starts, followed by the first 13 embryonic division cycles, all occurring in the absence of transcription. Thus, these events depend exclusively on maternal proteins and mRNA. Since Phosphoregulation is a central and conserved mechanism that enables remodeling of the oocyte

proteome and supports cell division. It prepares the oocyte to transform into the egg and undertake development. In the absence transcription our knowledge of the dynamic patterns of phosphorylation of thousands of oocyte phosphosites represents an essential tool for study of oogenesis, embryogenesis, especially the unique meiotic and mitotic processes. Interestingly, two recent studies based on phosphoproteomics have revealed new insights into how phosphorylation dynamics regulate meiotic divisions in yeast(Celebic *et al*, 2024; Koch *et al*, 2024). We now extend this analysis to the physiological process of oogenesis specific to metazoans. The study of mitotic processes in somatic cells, which are short in duration requires exquisite synchronization, which is difficult. Although previous studies of protein phosphorylation during mitosis have revealed the identity of numerous players of cell division, especially those controlling the structural reorganization of the dividing cell and its checkpoints, they have not been able to fully elucidate the epistatic relationships between kinases and phosphatases, which are nonetheless crucial to understanding the temporal sequences regulating the various events of mitosis. This weakness is due to the fact that cell proliferation is a continuous phenomenon, without physiological arrest. Its duration varies from one cell to another within the same population. The necessity of using synchronizing agents induces non-physiological arrests, which activate checkpoints, leading to the resumption of the cell cycle not comparable to that of untreated cells. Moreover, these studies often use transformed cell lines accumulation of mutations makes it hard to compare with cells in a physiological cellular context. The exceptional features of oocyte maturation for experimental studies of mitosis and meiosis are: 1) the synchronicity of the process in the oocyte, initiated by a physiological signal, progesterone, 2) the natural oocyte arrests in oocyte maturation at either prophase I (equivalent to a late G2-arrest) or at MII (M-phase arrest), 3) and the large size of the oocyte (1.2 mm in diameter) and its high protein content (30 µg soluble proteins per cell), offering the rare opportunity of single-cell proteomics of events at the single cell level. For these reasons we performed time-resolved proteomics and phosphoproteomics in *Xenopus* oocytes from prophase I through the MII arrest of the unfertilized egg.

In this study, we have analyzed the changes in the phosphorylation in relation to three categories of events: specific periods of meiotic maturation, activities of the master regulators of meiosis and peculiar cellular features of meiosis. Our analysis confirms the high quality of our phosphoproteome by the detection of multiple phosphorylation events with previously-documented functional effects on meiotic divisions or early development. Through the detection of many new regulated phosphosites, it provides a rich pool of candidate proteins for multiple avenues of investigation of previously uncharacterized important players of the oocyte to embryo transition.

RESULTS

The temporal resolution of the events of meiotic divisions

Prophase-arrested oocytes (PRO) and oocytes resuming meiosis were collected at regular intervals after progesterone exposure (Movie EV1, Methods). To correlate the time-points of this experiment with the cytological events known to occur during meiosis resumption, a set of proteins whose accumulation had been extensively studied during *Xenopus* oocyte meiosis progression were used as markers. One of the first events following progesterone stimulation is the accumulation of Cyclin B1 that begins before and independently of Cdk1 activation (Santoni *et al*, 2024; Frank-Vaillant *et al*, 1999). In our experiments, Cyclin B1 accumulation starts at about 2 hours and increases linearly until MII arrest at 6.5 hours (Fig. 2A). It has been reported that Mos translation is stimulated by progesterone concomitant with the accumulation of Cyclin B1; however the Mos protein does not accumulate before NEBD because it turns over rapidly (Santoni *et al*, 2024; Frank-Vaillant *et al*, 1999). Another critical well documented event that occurs downstream to Cdk1 activation is the degradation of CPEB1 (Santoni *et al*, 2024; Mendez *et al*, 2002), an RNA-binding protein whose degradation activates protein translation in MI. Hence, Mos accumulation and the degradation of CPEB1 are well established markers for the timing of NEBD. After NEBD, activation of the anaphase-promoting complex (APC) leads to the ubiquitination and degradation of Cyclin B2, which marks the entry into anaphase I. During the MI-MII transition, multiple additional events take place: Cyclin B3 is degraded (Bouftas *et al*, 2022), Cdc6 (Lemaître *et al*, 2002; Whitmire *et al*, 2002; Daldello *et al*, 2015), Wee2 (Nakajo *et al*, 2000) and Cyclin E (Rempel *et al*, 1995) accumulate, reaching their maximal levels in MII. These four events mark the entry into MII. Based on these markers, the timing of cytological events in our experiment is as follows (Fig. 2A): NEBD and MI occur between 3 and 4 hours, the MI-MII transition takes place between 5 and 6 hours, and entry and arrest in MII are at 7 hours. This time course is in agreement with the cytological previously described events (Huchon *et al*, 1981; Gard, 1992). A physiological measure of MII arrest can be ascertained by the ability of the oocytes to be activated by an electric shock, a property that is acquired only in MII (Movie EV2).

Validation of the quantitative proteomic data

The quality of oocytes resuming meiosis is also confirmed by the dynamics of protein accumulation and degradation that occur during meiotic progression (Fig. 2B). A set of 34 proteins, whose changes in concentration have been previously studied during meiotic divisions was used to validate the quality of our quantitative proteomics data (Figs. 2B and EV1A). Our proteome correctly classifies 15 out of 18 proteins accumulating during *Xenopus* meiosis resumption (FC(MII/PRO) > 1.5), 11 out of 12 proteins

whose concentration is constant (0.75 < FC(MII/PRO) < 1.5), and 4 out of 4 proteins whose accumulation was reported to decrease (FC(MII/PRO) < 0.75) (Figs. 2B and EV1A). The concordance between our dataset (30/34 proteins) with the changes in the protein levels reported in the literature is substantially higher than in a previously published system-wide proteomic dataset from *Xenopus* oocytes where only 7 out of these 34 proteins were correctly measured (Peuchen *et al*, 2017) (Fig. EV1A-B). This also may explain why changes in protein concentration reported in that study poorly correlate with the one measured in our proteomic study (Fig. EV1B). The high quality of the new proteomic data is also confirmed by the strong correlation of the translational pattern of *Xenopus* allo-alleles (Fig. EV1C-D), which were derived by genome endoduplication (Session *et al*, 2016).

Protein homeostasis during meiotic divisions

Absolute concentrations of proteins during meiotic maturation

The absolute concentration of 7974 proteins identified in our proteome dataset was calculated (Dataset EV1, Appendix Supplementary Methods). We then performed a qualitative comparison of average oocyte abundance of proteins belonging to distinct functional groups (Appendix Fig. S1). As expected, the less abundant subgroups include signaling molecules and transcription factors. Perhaps of more surprise, E3 enzymes and kinases are not abundant. At the other end of the spectrum are glycolytic and tricarboxylic acid cycle enzymes, as well as proteasome and ribosome components. These observations are expected because the oocyte has a stock of nutrient molecules and all the enzymes linked to their metabolism, which are used in viviparous animals throughout embryonic and larval development. For instance, the glycolytic enzyme GAPDH that catalyzes an important energy-yielding step in carbohydrate metabolism, is a very abundant protein in the oocyte (average concentration of between 8.88 μM and 17.83 μM). The ribogenesis program, which takes place during the oocyte growth from stage III to stage VI, before meiosis resumption, allows the accumulation of very large quantities of ribosomal RNAs and proteins that are used during embryonic development, until the swimming tadpole stage (Woodland, 1974). Similarly, the components of the DNA replication machinery are quite abundant, probably in anticipation of the post-fertilization cell cycles. All these data are therefore consistent with biological understanding of their roles during embryonic development after post-fertilization (Peshkin *et al*, 2015).

Temporal profiles of protein levels

We clustered the relative data for protein abundance across subsequent hourly timepoints post-progesterone stimulation (see Methods). As illustrated in Appendix Fig. S2A, the majority of the 60 expression profiles are flat, demonstrating that most (over 80%) proteins are stable during meiotic

maturation. Our proteomic dataset allowed to identify 12% of proteins affected by changes in concentration during meiotic progression by applying the same fold change threshold: 413 proteins that accumulate and 562 proteins whose concentration decreases (Figs. 2B and EV1E; Dataset EV2). Although these changes only concern a minority of proteins, they are critical for the meiotic process. Since transcription is silent during this period, these documented changes must result from the regulation of translation or/and degradation (Meneau *et al*, 2020).

Protein accumulation: the machinery of cell division and DNA replication. Gene ontology analysis was used to characterize the functional significance of the 413 proteins whose level increases during meiosis. Proteins involved in spindle assembly and mitotic division were significantly enriched (Fig. 2C). Among these important regulators are the Targeting-protein-for-Xklp2 (Tpx2) and Protein-regulator-of-cytokinesis 1 (Prc1) that also accumulate during meiotic maturation in mouse oocytes[10,11]. We also find that the centrosomal maturation factor, SSX2IP, and two plus-end motors, the kinesins Kifc1 and Kif11 (Eg5) (Houliston *et al*, 1994), also accumulate significantly during meiotic maturation. Three of these proteins, Tpx2 and the two kinesins, play an important role in the assembly of both acentrosomal meiotic spindles and centrosomal mitotic spindles (Gruss, 2018; Kufer *et al*, 2002; Ems-McClung *et al*, 2020; Miller *et al*, 2019). Interestingly, the prophase oocyte is equipped with most of the proteins essential for the formation of division spindles. Hence these new results suggest that increases in the relative level of some components is required to support the meiotic and first rapid embryonic divisions.

Another protein category found to increase is the machinery of DNA replication initiation (Fig. 2C). Indeed, oocytes accumulate the components of the DNA replication machinery during meiosis resumption to support the 13 rapid rounds of cell cycles occurring during early embryogenesis, all of which occur in the absence of transcription. In *Xenopus*, it was shown that Cdc6 is the only missing factor of the pre-replicative (pre-RC) complex in the prophase-arrested oocyte and that its accumulation occurs during the MI-MII transition (Lemaître *et al*, 2002; Whitmire *et al*, 2002; Daldello *et al*, 2015) (Fig. 1). Translational and then post-translational mechanisms targeting Cdc6 prevent the pre-RC from functioning between the two meiotic divisions, thus ensuring the production of a haploid gamete. Our proteomic analysis shows that, even though the other pre-RC proteins, as ORC1, ORC2 and ORC6, are already expressed in prophase oocytes, they accumulate further during meiotic maturation, revealing a strong co-regulation of the components of the pre-RC.

Another process controlled by highly enriched proteins is vesicle tethering, which includes the family of exocyst proteins (Fig. 2C). Interestingly, exocyst proteins are involved in the completion of cell

division during the secretory-vesicle-mediated abscission (Gromley *et al*, 2005). The accumulation of these proteins during meiotic maturation could be important to support the extrusion of the polar bodies, as already suggested in *C. elegans* (Kumar *et al*, 2019) and the rapid cell divisions sustaining early embryogenesis.

Protein degradation: RNA-binding proteins (RBPs). Gene ontology analysis of the 562 proteins whose concentration decreases during meiosis reveals that 116 (21 %) are annotated to bind RNA. Among them, a large portion are RNA helicases (Fig. 2D). Among these RBPs, another important group are proteins that are involved in ribosome biogenesis. The ribogenesis program takes place during the oocyte growth, allowing the accumulation of ribosomal RNAs and proteins that are used during embryonic development (Woodland, 1974). This process is downregulated during meiotic maturation (Hyman & Wormington, 1988; Chen *et al*, 2011). The decrease in the concentration of proteins involved in rRNA synthesis and processing does not result in a general decrease of ribosomal proteins that are stable during meiotic divisions (Appendix Fig. S3A). Halting ribogenesis may allow the oocyte to re-allocate its energy resources to the production of other cellular components required for meiotic divisions and embryogenesis. Intriguingly, Rpl26 (Ribosomal protein L26) is the only ribosomal protein detected to decrease during meiotic divisions (Appendix Fig. S3A). Since this protein is known to be dispensable for ribosome formation in yeast (Babiano *et al*, 2012; Warner & McIntosh, 2009; Takagi *et al*, 2005), the distinct regulation of Rpl26 as compared to the other Rpls suggests that Rpl26 might have extra-ribosomal functions. This hypothesis is reinforced by its specific modification by the ubiquitin-like UFMylation modification (Walczak *et al*, 2019) and its role in the regulation of protein stability (Zhang *et al*, 2016). Another subgroup of RBPs that decrease during meiotic divisions is involved in the repression of translation during prophase arrest, such as CPEB1 (Mendez *et al*, 2002; Reverte *et al*, 2001; Piqué *et al*, 2008), PATL2 (Nakamura *et al*, 2010; Cao *et al*, 2021; Christou-Kent *et al*, 2018) and Zar1l(Zar2) (Charlesworth *et al*, 2012; Yamamoto *et al*, 2013; Rong *et al*, 2019). Remodeling the repertoire of RBPs in the oocyte could be a general mechanism to regulate translation during meiotic divisions. Among these RBPs is Serbp1, which in mouse is involved in the stabilization of mRNA involved in meiosis resumption (Chew *et al*, 2013), as well as Caprin2, whose degradation is also observed during meiotic maturation of human oocytes (Virant-Klun *et al*, 2016). Caprin2 is a RBP with unknown function and highly enriched in the oocyte Balbiani body (Boke *et al*, 2016), a non-membrane compartment specific to the early diplotene oocytes, which contains mitochondria, RNAs and endoplasmic reticulum. The functions of this organelle are not clear, although it is strongly correlated in *Xenopus* to the establishment of oocyte polarity and to the localization of maternal determinants (Jamieson-Lucy &

Mullins, 2019). In *Xenopus*, it disperses at the onset of vitellogenesis, leaving a wedge-shaped cytoplasmic region rich in mitochondria (Wilk *et al*, 2005) and promotes the formation of RNP condensates in the vegetal cortex of the oocyte (Yang *et al*, 2022). Interestingly, Rbpms2, another regulator of the Balbiani body (Kaufman *et al*, 2018), is strongly degraded during meiotic maturation, highlighting how dynamic during meiosis is the composition of this transient compartment specific to the oocyte.

Interestingly, distinct E3 ubiquitin ligases, mainly APC and SCF (Skp, Cullin, F-box containing complex) have been shown to be active at different time periods of meiosis resumption in *Xenopus* oocytes (Kinterová *et al*, 2022). 186 proteins (37%) identified as decreasing in our proteome include in their sequences one of the APC degrons (Appendix Fig. S3B). This group of proteins includes two known APC targets, Cyclin B2 (Glotzer *et al*, 1991) and Securin (Cohen-Fix *et al*, 1996). Additionally, 30 proteins (6%) whose concentration decreases in the oocytes have one SCF degron in their sequence (Appendix Fig. S3B), including CPEB1 (Reverte *et al*, 2001) and Cdc6 (Daldello *et al*, 2015), two characterized SCF-targets. Interestingly, 253 proteins (57%) of proteins that decrease during meiotic divisions do not bear in their sequence any of the degrons for the ubiquitination systems identified in *Xenopus* oocytes (Appendix Fig. S3B). Further research is therefore required to identify the sequences and the E3 enzymes and deubiquitinating enzymes that control the turnover of this important protein class.

The highly dynamic landscape of phosphorylation during meiotic maturation

We performed phosphoproteomic mass spectrometry analysis in order to measure the overall dynamics of protein phosphorylation taking place during meiotic divisions and to identify which specific proteins and which sites are phosphorylated during this process. We identified 6783 different phosphopeptides and quantified the dynamics of relative change across all time points (Dataset EV3). These peptides came from 2308 distinct proteins. When respective protein and un-phosphorylated peptide were also measured, we were able to compute the stoichiometry (see Methods). A list of all 415 phospho-sites for which it was possible to calculate the phospho-occupancy is provided as Dataset EV4.

We identified the human homologous counterparts of 5901 (87%) among the 6783 sites found to be phosphorylated during meiotic divisions. Interestingly, only 177 (3%) out of 5901 conserved sites were already known to be phosphorylated on phosphosite.org database. Thus, our phosphosite dataset identifies a very large number of novel phosphosites, never previously identified and characterized. We suspected that a reason why only such a small number of phosphorylations among those detected by our phosphoproteome was previously reported, might suggest that a large portion of these

phosphorylation events are related to cell division. Dividing cells generally account for a small fraction of tissue mass. This leads to a high dilution of the phosphorylation signature of cell division, as compared to the highly synchronous meiotic divisions of oocyte maturation. Interestingly, 60% of the phosphosites detected in oocytes are dynamically regulated during meiotic maturation, highlighting the importance of this post-translational regulation in controlling this last step of oogenesis and meiosis. Unbiased clustering reveals that changes in protein phosphorylation are pervasive and far more dynamic than changes in protein abundance (Appendix Fig. S2), which was also noted during yeast meiosis (Koch *et al*, 2024). Comparing the three stages of meiotic division (PRO, MI and MII) and based on the main cellular events of these stages, we can group phosphopeptide stoichiometry into 5 classes (Fig. 3A; Dataset EV3). Class I includes proteins bearing a phosphosite whose occupancy decreases during the first 2 hours following progesterone stimulation. This class includes only 136 phosphopeptides (2%) which might be involved in the early signaling pathway induced by progesterone and PKA downregulation. This small number was expected since there is a low level of phosphorylation detectable in prophase-arrested oocytes (Maller *et al*, 1977). This makes sense since there are presumably only a few substrates of PKA sufficient to initiate meiosis resumption. Class II is larger (39% of the phosphopeptides) and includes proteins whose phosphorylation increases between NEBD and MI and which remain highly phosphorylated in both MI and MII. The massive amount of Class II phosphosites presumably reflects the catalytic power of Cdk1 as well as its downstream kinases, to generate the thousands of substrates essential for cell division. Our measurements that most of the sites, which are phosphorylated in MI, remain stably phosphorylated during MI to MII transition is consistent with the observations made in yeast showing that most of Cdk1 motifs remain phosphorylated at the end of meiosis I (Celebic *et al*, 2024). Class III (5%) consists of proteins whose phosphorylation peaks in MI then decreases while oocytes progress throughout oocyte maturation. This is the most predominant class of phosphosites present during meiotic maturation in starfish (Swartz *et al*, 2021) and follow the peculiar pattern of Cdk1 activity peaking at MI in these oocytes (Okano-Uchida *et al*, 1998; Kishimoto, 2003). Class IV (9%) is composed of proteins whose phosphorylation progressively increases from MI to MII, hence potentially implicated in MII entry. Finally, Class V (5%) comprises proteins whose phosphorylation increases from MII and which could play a role in establishing the MII arrest. The phosphosites that are specific for either MI (Class III) or MII (Classes IV and V) are much less abundant (5%, 9% and 5% respectively, Fig. 3A) and might distinguish the biochemical state of the two meiotic divisions.

The release of the prophase arrest: receptors and membrane trafficking

Receptors. Since meiotic maturation signaling begins with the interaction of progesterone with membrane receptors, we first focused our analysis on these proteins (Josefsberg Ben-Yehoshua *et al*, 2007; Sadler & Maller, 1985). Progesterone signals through activation of a seven-pass-transmembrane progesterone receptor (mPRβ or PAQR8) that belongs to the progestin and adiponectin receptor family (Josefsberg Ben-Yehoshua *et al*, 2007; Nader *et al*, 2018, 2020) (Fig. 1). The release of the prophase block also involves the inactivation of an orphan constitutively active GPCR, GPR185, responsible for maintaining oocyte prophase arrest by ensuring high cAMP levels and PKA activity (Ríos-Cardona *et al*, 2008; Deng *et al*, 2008). Progesterone decreases GPR185 signaling either through its cleavage by a metalloproteinase (Deng *et al*, 2008) or through its endocytosis (Nader *et al*, 2014). One limitation of our dataset lies in the loss of some membrane proteins during the fractionation protocol, explaining why our proteomic workflow did not detect mPRβ and GPR185 or its close relative GPR12. Nevertheless, it does detect some proteins that interact with mPR, *i.e.* PGRMC1, VLDLR and APPL1. PGRMC1 is known to form a receptor complex with mPRα and is necessary for mediating progesterone signaling in zebrafish oocytes (Wu *et al*, 2018). Interestingly, our phosphorylation data reveals that PGRMC1 and its close relative PGRMC2 are phosphorylated on two homologous threonine residues during meiotic maturation, suggesting that these proteins may contribute to mPRβ activity in *Xenopus* oocytes. In the prophase-arrested oocyte, VLDLR regulates mPR trafficking from the endoplasmic reticulum through the Golgi to the plasma membrane, preparing the oocyte to be responsive to progesterone (Nader *et al*, 2018). In contrast, progesterone induces clathrin-dependent endocytosis of mPRβ into signaling endosomes, where mPR interacts transiently with APPL1 and Akt2 to induce meiosis (Nader *et al*, 2020). The phosphoproteomic data reveal that both APPL1 and Akt are phosphorylated in response to progesterone at the time of Cdk1 activation, suggesting that phosphorylation events regulate the traffic and activity of this receptor.

Membrane traffic. Vesicular trafficking at the cell membrane appears to be crucial for the maintenance and the release the prophase meiotic arrest, and may also function through early embryogenesis (Fig. 1). In the prophase-arrested oocyte, the accumulation of the GPR185 receptor at the plasma membrane maintains high cAMP levels (Nader *et al*, 2014) while the plasma membrane targeting of mPRβ renders the oocyte competent to respond to progesterone (Nader *et al*, 2018).

Exocytosis is also crucial for the formation of the fluid-filled blastocoele cavity during embryogenesis (Müller, 2001). Indeed, the apical membrane of the epithelium surrounding the blastula where the polarized activities of ion channels and transporters generate the blastocoele fluid is formed from the oocyte cell membrane (Müller, 2001). This requires further remodeling. Progesterone rapidly

blocks this exocytosis pathway (Colman *et al*, 1985; Leaf *et al*, 1990), leading to a decrease in membrane surface area, which is revealed by the disappearance of microvilli that are enriched in oocytes but almost absent in eggs (Dumont, 1972; Kado *et al*, 1981; Larabell & Chandler, 1989; Bluemink *et al*, 1983). Importantly, blocking exocytosis induces meiotic maturation, in the absence of hormonal stimulation (Mulner-Lorillon *et al*, 1995; El-Jouni *et al*, 2007). Furthermore, progesterone stimulates endocytosis of membrane proteins, such as GPR185, whose activity is suppressed by its internalization, and mPRβ, whose internalization is required to transduce its effects (Nader *et al*, 2018, 2020, 2014). The stimulation of endocytosis also converts plasma membrane into intracellular vesicles that can provide membrane reserves, necessary to support the rapid cell divisions, and hence the requirement for greater total membrane surface area, during embryogenesis (Angres *et al*, 1991; Gawantka *et al*, 1992). However, it is unknown whether PKA is responsible for the active secretory transport during the prophase arrest and how progesterone blocks exocytosis and stimulates endocytosis (Fig. 1).

To improve our understanding of vesicular trafficking and membrane organization, we analyzed the proteins involved in these processes whose phosphosites belong to Class I (Fig. 3B). Among these proteins, PI4KB deserves special attention. This protein is critical for the maintenance of the Golgi and trans-Golgi phosphatidylinositol-4-phosphate (PI4) pools. PI4KB regulates Golgi disintegration/reorganization during mitosis and is involved in Golgi-to-plasma membrane trafficking (De Matteis *et al*, 2013). The phosphoproteome reveals that PI4KB is dephosphorylated within 2 hours after progesterone stimulation, on a PKA consensus phosphorylation site conserved in vertebrates. The phosphorylation of this site by PKA is known to control the interaction of PI4KB with Armadillo-like helical domain-containing protein 3 (ARMH3), an interaction important for the Golgi membrane integrity (McPhail *et al*, 2020; Isobe *et al*, 2017; Blomen *et al*, 2015). PI4KB is also regulated by its interaction with ACBD3, an AKAP-like scaffold platform in Golgi, which directly binds the R regulatory subunit of PKA and regulates the traffic between Golgi and endoplasmic reticulum in a PKA-depending manner (Jia *et al*, 2023; Klima *et al*, 2016; Sasaki *et al*, 2012). The phosphoproteome reveals that ACBD3 is phosphorylated during meiotic maturation at the time of NEBD (Class II). PI4KB is therefore at the crossroad between PKA and intra-membrane endoplasmic reticulum-Golgi-plasma membrane trafficking. Since these are key events involved in meiosis resumption, PI4KB is a particularly attractive candidate as a PKA substrate for future functional studies of membrane relocalization.

Proteins involved in the actin cytoskeleton are also represented in Class I phosphosites (Fig. 3B). Their early post-translational modifications could regulate the reorganization of the actin cytoskeleton that is known to accompany the modification of the secretory/endocytosis pathways (Gard, 1999).

Among them, ITPRID2/KRAP tethers IP_3 receptors, which are located in the membrane of the endoplasmic reticulum, to the actin under the plasma membrane, to mediate Ca^{2+} signalling (Thillaiappan *et al*, 2021). During meiotic maturation, the endoplasmic reticulum, which is the major Ca^{2+} store, is enriched in the cortex of the oocyte (Campanella *et al*, 1984; Charbonneau & Grey, 1984; Terasaki *et al*, 2001). This remodeling brings the Ca^{2+} source close to its primary targets at fertilization, when Ca^{2+} release from endoplasmic reticulum activates the oocyte and blocks polyspermy. The proteins highlighted above (Fig. 3B) could participate to this critical reorganization of the endoplasmic reticulum.

Protein translation and accumulation orchestrate meiotic divisions

Two waves of translation take place in the oocytes: the first depends on PKA inactivation. It occurs upstream and independently of Cdk1 activity and is required for Cdk1 activation. The second translation wave takes place downstream Cdk1 activation (Santoni *et al*, 2024). Hence, in contrast to mitosis, a period when protein synthesis is repressed (Ross, 1997), translation is activated during meiotic maturation, indicating the existence of meiosis-specific controls of the process. However, the regulation of the two waves of protein translation and the identity of the newly translated proteins had not been unraveled. Interestingly, protein translation components are extensively regulated at the level of phosphorylation as demonstrated by the enrichment of the proteins regulating these processes among 3 of the 5 phosphopeptide classes (Fig. 4A).

RBPs and translational control. Interestingly, several proteins implicated in the control of translation bear phosphosites belonging to Class I, as eIF4ENIF1/4E-T, PATL1 and TACC3/Maskin (Figs. 3B and 4B). eIF4ENIF1/4E-T is required for eIF4e1b localization to P-bodies where mRNAs are stored in a dormant state in zebrafish oocytes (Lorenzo-Orts *et al*, 2023). Both 4E-T and eIF4e1b are extensively phosphorylated during meiotic divisions on multiple residues, suggesting a highly dynamic regulation of P-bodies during meiotic divisions (Fig. 4B). Many RBPs known to control translation in oocytes are also regulated at the phosphorylation level, including Pum proteins (Nakahata *et al*, 2003; Ota *et al*, 2011; Padmanabhan, 2006), Zar proteins (Charlesworth *et al*, 2012; Yamamoto *et al*, 2013; Rong *et al*, 2019; Heim *et al*, 2022) and PATL proteins (Christou-Kent *et al*, 2018; Zhang *et al*, 2023; Marnef *et al*, 2010). PATL1 is a RNA-binding protein required for cytoplasmic mRNA P-body assembly in oocytes (Marnef *et al*, 2010). PATL1 and PATL2 have mutually exclusive expression patterns in *Xenopus* oocytes: PATL2 is degraded while PATL1 accumulates during meiotic maturation (Marnef *et al*, 2010), as confirmed by our proteomic data (Figs. 2B,D and EV1). Although the role of PATL2 and the regulation of its stability by

phosphorylation have been well documented in the oocyte (Christou-Kent *et al*, 2018; Zhang *et al*, 2023), little is known about the role of PATL1 during meiosis. Both PATL1 and 2 inhibit translation when tethered to mRNA and assemble a complex that includes CPEB1, Xp54/DDX6, Rap55B/LSM14b (Marnef *et al*, 2010) (Fig. 4B). The early dephosphorylation of PATL1 detected in the phosphoproteome could modulate this inhibitory complex during early events of meiotic maturation, while the extensive phosphorylation of the other components of the complex could control its activity later during meiotic divisions (Fig. 4B). Another component of the repressive complex that interacts with CPEB1 is TACC3/Maskin, which is found widely regulated during meiotic divisions in the phosphoproteome (Fig. 4B). TACC3/Maskin plays a dual function, regulating the centrosome-mediated microtubule nucleation through γ-TuRC (Peset *et al*, 2005) but also translation (Barnard *et al*, 2005; Groisman *et al*, 2002). Eight residues in TACC3/Maskin, of which only two are conserved in human Maskin (214/228 and 298/317 in human/*Xenopus*), exhibit a complex profile of phosphorylation (Fig. 4B). Two sites identified in the phosphoproteome, S266 and S298, were previously found to be phosphorylated in egg extracts, regulating the function of TACC3/Maskin in the control of translation (Barnard *et al*, 2005). S626 was also reported to be phosphorylated in prophase oocytes and during oocyte meiotic maturation, although there is some controversy about the kinase (either PKA or Aurora-A) and the role of this phosphorylation in either the control of translation or centrosome attachment (Barnard *et al*, 2005; Pascreau *et al*, 2005). Interestingly, in our studies S240 is phosphorylated in the prophase oocyte and dephosphorylated early in response to progesterone (Class I) (Fig. 4B). Since the sequence surrounding S240 does not correspond to a PKA consensus motif, it is hard to establish the biological significance; nevertheless, such an early dephosphorylation deserves further attention.

The control of translation initiation. Translation regulation might not only depend on the expression and post-translational regulation of the RBPs but could also involve the regulation of the core translation initiation machinery, since we find that many of its components are phosphorylated (Fig. 4C). Indeed, eIF4b, an activator of the eIF4a helicase that facilitates ribosome scanning (Piqué *et al*, 2008), eIF2b/eIF2s2, a component of the molecular machinery recruitment on the met-tRNA (Piqué *et al*, 2008), and eIF4g, involved in the recognition of the mRNA 5'Cap, are among the proteins bearing sites whose phosphorylation peaks in MII (Appendix Fig. S4). These phosphorylation patterns correlate with the second wave of activation of translation that begins under the control of Cdk1 activity in MI and continues progressively through MII (Meneau *et al*, 2020; Santoni *et al*, 2024).

The control of ubiquitin ligases. The levels of specific proteins are also regulated by proteolysis at each step of meiotic maturation. Targeted regulation allows for the accumulation of key proteins

independently of any general increase in their translation, such as for Cyclin B1 (Santoni *et al*, 2024), or the well-studied degradation of proteins, such as Cyclin B2, securin or CPEB1 (Taieb *et al*, 2001; Wassmann, 2022; Setoyama *et al*, 2007). Interestingly, proteins controlling polyubiquitination display phosphopeptides enriched in Class II, strengthening the view that a major regulation of protein turnover takes place at NEBD in order to orchestrate meiotic divisions (Figs. 3 and 5A). APC is the key E3 ubiquitin ligase that promotes metaphase-anaphase transition. Although the phosphorylation status of some substrates determines their recognition by APC and influences the precise timing of their degradation, APC activity is also regulated by the phosphorylation of its core subunits (Bansal & Tiwari, 2019) (Fig. 5B).

Another important ubiquitination system that regulates stability of proteins during mitosis and meiosis is the SCF complex (Kinterová *et al*, 2022). SCF is composed of three main components: Cul1, a scaffold protein; Skp1, which interacts with specific F-box proteins that are involved in the substrate recognition; and Rbx1, which interacts with the E2-ubiquitin ligases (Kinterová *et al*, 2022) (Fig. 5C). SCF ligases play important roles during oocyte meiotic maturation, especially the $SCF^{\beta TrCP}$ complex. $SCF^{\beta TrCP}$-mediated degradation of Emi1, Emi2/Erp1, CPEB1 and BTG4 is essential for progression through MI and MII of mouse and *Xenopus* oocytes (Kinterová *et al*, 2022). This is very similar to the role of Emi1 in mitosis and is thought to set the time between binding of cyclin B and its destruction (Reimann *et al*, 2001).

Many F-Box proteins are also expressed in *Xenopus* oocytes, but they do not display high phosphorylation dynamics. An exception is Imo7/Fbox20, which is degraded during meiosis, and is dynamically phosphorylated (Fig. 5C). Interestingly, Imo7 overexpression causes defects at the spindle assembly checkpoint, affecting the progression through mitotic divisions (Tzeng *et al*, 2018). Additionally, many E2 enzymes were identified in our datasets as highly regulated at the translational/accumulation and post-translational levels during meiotic maturation (Fig. 5C). This layer of regulation of protein ubiquitination remains understudied. Interestingly, an E2/E3 hybrid ubiquitin-protein ligases, UBE2O, UBE4B (also known as UBOX3 or E4) and FAF2 (or UBXD8) display phosphorylation sites belonging to Class I (Figs. 3B and 5C). FAF2 is involved in stress granule clearance (Gwon *et al, 2021*). UBE2O is also known to be involved in the drastic proteome remodeling during erythroid differentiation (Nguyen *et al*, 2017) as well as quality control factor for orphans of multiprotein complexes (Yanagitani *et al*, 2017). Ribosomal proteins are known substrates of UBE2O which leads to their degradation (Nguyen *et al*, 2017). Whether UBE2O is involved in the downregulation of ribosome biogenesis that occurs during meiotic maturation (Hyman & Wormington,

1988), and in the decrease of Rpl26 (Appendix Fig. S3A), is an interesting question. The dephosphorylation of UBE2O, UBE4B and FAF2 could also be involved in the accumulation of Cyclin B1, which was recently shown to occur independently of any increase in translation but to result from protein stabilization (Santoni *et al*, 2024).

Another important regulator of the SCF system, DCUN1D5, is found regulated in our phosphoproteome. DCUN1D5 catalyzes the neddylation of all cullins, which is necessary for the activation of cullin-RING E3 ubiquitin ligases (Keuss *et al*, 2016). DCUN1D5 is dephosphorylated at S9, a PKA consensus site, and phosphorylated starting NEBD at S10 and S12 (Fig. 5C). These phosphorylations could control DCUN1D5 ability to activate SCF, especially since the inhibition of neddylation causes a meiotic arrest in MI in mouse oocytes (Yang *et al*, 2019). Altogether, our dataset provides attractive candidates to be involved in the regulation of both translation and protein stability that occur during meiotic maturation.

Activation of Cdk1 occurs through an intricate network of phosphorylation of Cdk1 regulators

The activation of Cdk1 during oocyte maturation relies on an intricate network of feedforward and feedback phosphorylation pathways mediated by kinases and phosphatases (Fig. 1). Indeed, components of the cell division machinery are highly enriched among Class II, III, IV and V (Fig. 6A). Some of the phosphorylation sites implicated in cell division control have been identified previously through detailed studies using site-specific mutagenesis and phospho-specific antibodies. Our phosphoproteomic analysis of oocyte maturation provides new regulatory elements (Fig. 6B). An important regulator of the Cdk1 auto-amplification loop is the kinase Plk1 that contributes to the phosphorylation of the two direct Cdk1 regulators, Cdc25 and Myt1 (Myt1, a membrane-bound protein, was not detected in our proteome). Plk1 is activated by Aurora-A, a kinase itself under the indirect control of Cdk1 in *Xenopus* oocyte (Maton *et al*, 2003), through the phosphorylation of T210 (T201 in *Xenopus*)(Macůrek *et al*, 2008), a residue localized in the activation T-loop of the kinase domain. We show here that Plk1 phosphorylation at T210 increases in MI and is then constant throughout meiotic maturation (Class II) (Figs. 6B and EV2A). This is consistent with the function of Plk1, which phosphorylates multiple proteins required for the mechanics of division, and which must logically be kept active throughout both meiotic divisions (Hansen *et al*, 2006; Solc *et al*, 2015). Interestingly, the phosphoproteome also detects additional phosphorylation sites of Plk1, S326 (S335 in human) and S340 (not conserved in human), which were previously found to be upregulated in response to okadaic acid (Wind *et al*, 2002), an inhibitor of PP2A that strongly induces M-phase. These two residues are located

between the two functional domains of Plk1, the kinase domain and the Polo-box domain (Cheng, 2003). This suggests that the phosphorylation of other critical residues than T210 of Plk1 could be essential for its catalytic activation. Aurora-A kinase is activated during meiotic maturation downstream Cdk1 (Maton *et al*, 2003; Castro *et al*, 2003; Maton *et al*, 2005). While our phosphoproteome does not detect Aurora-A autophosphorylation at T288 (T295 in *Xenopus*), it registers the extensive phosphorylation of Bora, an activator of Aurora-A involved in Plk1 activation (Thomas *et al*, 2016) (Fig. 6B and EV2B). Several phosphorylation sites of Bora have been reported to be important for its function as an Aurora-A activator: S41/38, S112/110, S137/135 and S252/S252 (human/*Xenopus*) (Thomas *et al*, 2016; Vigneron *et al*, 2018; Tavernier *et al*, 2015, 2021). Among these sites, S110 phosphorylation of Bora by Cdk1-Cyclin A is critical for mitotic entry in *Xenopus* egg extracts (Vigneron *et al*, 2018; Tavernier *et al*, 2015, 2021). Our phosphoproteome reveals that Bora belongs to Class II, being phosphorylated starting NEBD, but surprisingly on distinct sites that were never reported in the literature: S191/189, T294/287, S552/549, S-/521, T12/9 and T15/12 (human/*Xenopus*), with the exception of S278/285. In contrast to the situation in mitosis, Cyclin A is very weakly expressed in the prophase oocyte and accumulates during meiotic maturation (Kobayashi, 1991). Our proteome dataset reveals that Cyclin A accumulates after MI. Hence, the phosphorylation of Bora at MI cannot be catalyzed by Cdk1-Cyclin A in the *Xenopus* oocyte. Cdk1-Cyclin B is probably involved in these phosphorylations that take place concomitantly with its activity and at Cdk1 phosphorylation consensus sites for 5 of the 7 phosphosites (Fig. EV2B). Thus, this analysis reveals that Bora activation correlates with its phosphorylation at residues not previously identified in earlier studies of the oocyte. We also detect additional phosphorylation events on other players of the Cdk1 amplification loop, as Cdc25 and Gwl/MASTL (Figs. 6B and EV2C,D), whose extensive phosphorylation during M-phase is usually detected by a large electrophoretic shift (Dupré *et al*, 2014).

Phosphoregulation of the bimodal activity of Cdk1 during MI-MII transition

In *Xenopus* oocytes, Cdk1 is not fully inactivated at anaphase I and during extrusion of the 1st polar body. Indeed, the low Cdk1 activity that persists during the MI-MII transition is essential to avoid the reformation of a nucleus, chromosome decondensation and DNA replication (Huchon *et al*, 1993; Thibier *et al*, 1997). This short period is followed by a further increase of Cdk1 activity, due to a sustained synthesis of B-cyclins; the increased Cdk1 activity allows the formation of the MII spindle (Gerhart *et al*, 1984) (Fig. 1). Although this bimodal subtle regulation of Cdk1 activity is essential for the success of meiosis, *i.e*. linking two successive divisions without intervening DNA replication, it has never

been quantified precisely. Cdk1 activity can be measured by looking at the phosphorylation of one of its direct substrates, Cdc27, a core APC component, at S428 (S426 in human)(Patra & Dunphy, 1998). Our precise quantification of the phospho-occupancy of this site shows that its phosphorylation is virtually absent in prophase, increases by 40% in MI, decreases during the MI-MII transition to 20%, then increases again in MII by 60% (Fig. EV2E). Three other residues of Cdc27, T205/207, S435/437 and S438/440 (human/*Xenopus*), also known to be phosphorylated at M-phase (Kraft, 2003), follow the same bimodal pattern than S428. The subsequent increase in Cdk1 activity essential for MII entry requires that the kinase escapes inhibitory phosphorylations by Myt1 and Wee2. Both Myt1 and Wee2 are reported to be inhibited by phosphorylations, although the precise sites responsible for this inhibition are not precisely defined. Myt1, a membrane protein, was not detected in our proteome. In *Xenopus*, Wee2 is not expressed in prophase oocytes and accumulates after NEBD (Nakajo *et al*, 2000; Charlesworth *et al*, 2012) (Fig. 1). Our analysis reveals that newly synthesized Wee2 is immediately phosphorylated at 4 sites (Classes II and IV), one of them being not conserved in human, and none of them corresponding to the proposed inhibitory S53 and S123 sites (Figs. 6A and EV2F). Hence, these data provide exciting new avenues of research to discover unexpected new regulations of old players in Cdk1 activation.

The Mos/MAPK pathway activation

Mos plays a well-known role at the origin of a critical pathway controlling meiotic maturation (Yew *et al*, 1992; Furuno *et al*, 1994). It phosphorylates Mek1/2, which in turn phosphorylates Erk1/2 (also known as MAPK) which leads to Rsk1/2 activation (Fig. 6B). These play multiple essential roles, such as preventing the reformation of a replicating nucleus between MI and MII (Dupre *et al*, 2002), enabling arrest in MII (Sagata *et al*, 1989b), but also participating in Cdk1 activation (Sagata *et al*, 1989a) and the functioning of meiotic spindles (Araki *et al*, 1996; Choi *et al*, 1996; Bodart *et al*, 2005). The phosphoproteome detects the activation of the Mos-MAPK module, with the phosphorylation of Erk2 on T185 and Y187 (T188 and Y190 in *Xenopus*) by MEK1/2 (Payne *et al*, 1991), an event that begins in MI (Figs. 6B and EV3A). Interestingly, additional phosphorylation sites are identified in MEK1 and Rsk1/2, the latter being hyperphosphorylated during meiosis as detected by a large electrophoretic shift (Bhatt & Ferrell, 2000) (Figs. 6B and EV3B,E). Rsk1 auto-phosphorylation at S381 (S380 in human) is required for its activity (Vik & Ryder, 1997). Our phosphoproteome measures a highly-confident phospho-occupancy for this site demonstrating the switch-like activation of the MAPK pathway at NEBD, followed by the maintenance of a constant level of its activity (Fig. EV3F). The timing of activation of the Mos-

MAPK cascade has been controversial, one hypothesis being that it is activated before Cdk1 and participates in the activation of this kinase (Sagata *et al*, 1988; Gavin *et al*, 1999), while another is that it is under the control of the starter Cdk1 activity and is only involved in the autoamplification loop (Santoni *et al*, 2024; Dupre *et al*, 2002; Fisher *et al*, 1999). The phosphoproteomic data clearly support the latter.

Phosphorylation of key components of the nuclear envelope during breakdown

As a result of the massive activation of kinase activities under the control of Cdk1, hundreds of proteins are phosphorylated and orchestrate the structural events choreographing the mechanics of meiotic divisions. The first of these is the massive vesiculation of the nuclear envelope surrounding the enormous oocyte nucleus. During mitosis, nuclear pore proteins are extensively phosphorylated by Cdk1-Cyclin B, Plk1 and Nek6/7 to promote the breakdown of the nuclear envelope (Kutay *et al*, 2021). The *Xenopus* oocyte has the unusual feature of having an enormous nucleus (475 μm in diameter), and therefore a considerable surface area of the nuclear envelope (0.96 mm^2), as well as large stocks of annulate lamellae in the cytoplasm. Annulate lamellae are cytoplasmic stack cisternae of nuclear envelope perforated with nuclear pores, 10 times more abundant than in the nucleus in the *Xenopus* oocyte, but devoid of lamins (Bement & Capco, 1990; Miller & Forbes, 2000; Cordes *et al*, 1995). Their surface area also far exceeds that of the nuclear envelope surrounding the nucleus (Cordes *et al*, 1995). This correlates with the high protein concentrations of the nuclear pore proteins (0.1 to 0.7 μM) that we have measured (Fig. 7A). Annulate lamellae play a critical role as a reservoir for the formation of the 4000 of nuclei that form during the embryonic cell divisions leading up to the mid-blastula transition and the onset of transcription (Kessel *et al*, 1986; De Magistris & Antonin, 2018; Feldherr, 1974). During meiotic maturation, NEBD and vesiculation of annulate lamellae occur at the same time, in a progressive spatial manner, starting from the vegetal pole. Importantly, the nucleus and annulate lamellae do not re-form between the two meiotic divisions, reducing the risk that an S-phase can take place between MI and MII (Bement & Capco, 1990). A gene ontology analysis of our phosphoproteome highlights that the phosphorylation of nuclear pore components is enriched in Classes II, III and IV, displaying the highest level of enrichment in Class III, hence characteristic of MI (Fig. 7B). The nucleoporin Nup53 (also called Nup35) is a component of the soluble core region of the nuclear pore complex that is extensively phosphorylated in mitosis by Cdk1 and Plk1 (Linder *et al*, 2017). Phosphomimetic mutations of all Cdk1 and Plk1 sites in Nup53 slow down the reformation of nuclear pores in interphase and mutation to phospho-null amino acids impairs the nuclear breakdown during meiosis (Linder *et al*, 2017). Our

phosphoproteome reveals that Nup53 phosphorylation is more dynamic than previously believed (Fig. 7C). Indeed, 6 phosphopeptides are found to peak in MI (Class III), 9 phosphopeptides are phosphorylated both in MI and MII (Class II), and 2 phosphopeptides continuously increase in phosphorylation during meiotic maturation (Class IV) (Fig. 7C). We were able to calculate the phospho-occupancy of the S59 (S66 in human), showing that it increases from 30% in prophase to 90% in MI oocytes and stays constant until MII (Class II) (Fig. 7D). Several other transmembrane nucleoporins, notably NDC1 and POM121C, undergo dramatic increase of phosphorylation at transition to MI. Altogether, these observations indicate that dissociation of the nuclear envelope and the annulate lamellae occurring in MI might require either a specific set of phosphorylations and/or a general level of phosphorylation that is higher than the level of phosphorylation required to maintain the nucleus and the annulate lamellae dissociated during the MI-MII transition through MII.

The regulation of centrosomal proteins during oocyte maturation

An intriguing feature of oocytes in most, if not all, metazoan species is the elimination of their centrioles. This allows the sperm to contribute its centriole and thereby initiates the division cycle and the cell cycle. There is longstanding literature that proves that the oocyte or egg has retained its ability to generate centrioles. However, in nature, the female centrioles are lost and the sperm centriole is the main contributor. In *Xenopus*, oocytes entering prophase I contain a typical centrosome, including a pair of centrioles and pericentriolar material (PCM) containing γ-tubulin and pericentrin. Centrioles disappear at the end of the pachytene stage of prophase I and PCM disperses in multiple foci in the cytoplasm that are no longer functional as microtubule nucleation sites (Gard *et al*, 1995). At fertilization, the male gamete delivers two centrioles but does not provide the PCM (Delattre & Gönczy, 2004). Therefore, in most species (with the exception of rodents), the complete centrosome of the one-cell stage embryo is a bi-parental inheritance, reconstituted from paternal centrioles and maternal PCM (Delattre & Gönczy, 2004). In *Xenopus*, oocytes store enough quiescent centrosomal building blocks for duplicating and assembling 1000 to 2000 centrosomes (Gard *et al*, 1990). This implies that oocytes should comprise an enormous reserve of centrosomal proteins, *i.e.* centriolar and PCM proteins, that sustain the reconstitution of a functional centrosome at fertilization and its subsequent rounds of duplication in the early embryo.

Centriolar proteins. The centriole is formed by a polarized cylinder of microtubule triplets, decorated along the proximal to distal axis with several appendages that define the three main regions of the organelle: the proximal part, the central core, and the distal region (LeGuennec *et al*, 2021). In

agreement with a published RNA-seq and proteome of *Xenopus* eggs (Session *et al*, 2016; Wühr *et al*, 2014), our proteome reveals that most of the centriolar proteins are expressed in the oocyte (Table 1). The components of the proximal part, as SAS-6 and CPAP/CENPJ, and of the central core, as POC1B, POC5 and Centrin 1, are either constant or accumulate during meiotic maturation (Table 1). In contrast, proteins of distal and subdistal appendages are present at lower concentration, either constant or decreasing during meiotic maturation (Table 1). Indeed, the appendages are critical for the docking of mature centrioles at the plasma membrane and ciliogenesis (Tanos *et al*, 2013), a process that is not functional in the oocyte and during the early embryonic divisions (Drysdale & Elinson, 1992).

Besides the basic building blocks forming the centriole, the oocyte is expected to provide the machinery for its duplication, the first cycle occurring immediately after fertilization. The key regulators of centriole duplication, including Plk4, SAS-6 and STIL, are generally expressed at very low levels (Bauer *et al*, 2016). While Plk4 is expressed at the mRNA level in oocytes but escaped our proteomic detection, SAS-6 and STIL are expressed at a constant level during meiotic maturation (Table 1). The estimated concentrations of both proteins are in agreement with the previous predictions, that cartwheels comprise one molecule of STIL for every SAS-6 dimer (Bauer *et al*, 2016). Other important regulators of centriole duplication, such as CEP192, CEP152, CEP63, RTTN, CEP110/CCP110, CEP97 and CEP76 were also detected, and are either constant or accumulate during meiotic divisions (Table 1). Interestingly, our phosphoproteome reveals that several of these proteins are phosphorylated during meiotic maturation. STIL is phosphorylated at S554, which is located in a Cdk1 phosphorylation consensus (Appendix Fig. S5A), an interesting observation since phosphorylation of STIL by Cdk1-Cyclin reduces the efficiency of daughter centriole assembly. This phosphorylation provides an explanation why centrioles cannot duplicate during M-phase (Zitouni *et al*, 2016; Steinacker *et al*, 2022). A massive CEP97 phosphorylation occurs at MI at 8 distinct sites, only 3 of them lying within a Cdk1 consensus motif (Appendix Fig. S5B). Remarkably, one of the phosphosites of CEP97, S633, has been recently shown to be phosphorylated by the kinase Dyrk1a in multiciliated cells of *Xenopus* embryos (Lee *et al*, 2022); it is required for centriole duplication. Therefore, although centrioles are not assembled, all centriolar proteins are expressed in the full-grown oocyte and these components serve as a stock for the biogenesis of the centrioles of the embryo. Our results suggest that specific phosphorylations of proteins regulating centriole assembly could prevent the *de novo* establishment of centrioles in the oocyte.

PCM proteins. The core element of the PCM is the γ-tubulin ring complex (γ-TuRC) which is the basic element for nucleation of microtubules from microtubule-organizing centers (MTOCs) (Oakley &

Oakley, 1989). It includes γ-tubulin that is combined with other proteins known as GCP2/tubgcp2 to GCP6/tubgcp6. Some PCM proteins or regulators of PCM assembly have been described in functional studies to be present in the oocyte and then recruited to the zygotic centrosome as maternal components. These include γ-tubulin (Stearns & Kirschner, 1994; Gard, 1994; Félix *et al*, 1994), pericentrin (Dictenberg *et al*, 1998), Nek2B (Fry *et al*, 2000; Uto, 2000), SSX2IP (Bärenz *et al*, 2013),TPX2, PRC1, Kif4A, Eg5/Kif11, CLASP1/Xorbit and Kif22/Xkid, CEP152 (Hatch *et al*, 2010), NEDD1 (Liu & Wiese, 2008), Maskin/TACC3 (Stebbins-Boaz *et al*, 1999; Peset *et al*, 2005), XMAP215/CKAP5 (Popov *et al*, 2002; Kinoshita *et al*, 2002) and Nercc1/NEK9 (Roig *et al*, 2005).

Most of the PCM proteins were detected in our proteomic dataset and either accumulate or stay constant during meiotic divisions (Table 1). Our dataset highlights that γ-tubulin accumulates during meiotic divisions at the time the oocytes enter MII (Table 1; Appendix Fig. S5C). GCP2 and 4 are expressed at a lower level than γ-tubulin (Table 1), in agreement with the expected stoichiometry of GCPs-γ-tubulin in the γ-TuRC (Sulimenko *et al*, 2022). The phosphorylation of γ-TuRC components is known to affect the stability and the activation of the complex (Sulimenko *et al*, 2022). We detected the phosphorylation of GCP3 at S814 (Class IV) and GCP6 at S1173 (Class III) (Appendix Fig. S5D). This second phosphosite is well conserved in the human protein and targeted by Plk4, which regulates centriole duplication (Bahtz *et al*, 2012). These results indicate that the oocyte, despite the absence of centrioles, prepares a functional centrosomal machinery by accumulating and/or phosphorylating some of the PCM proteins. Apart of the γ-TuRC complex, we found that 10 other PCM proteins are phosphorylated during meiotic maturation (CEP192, SSX2IP, CEP41, TACC3/Maskin, Nucleophosmin, Katanin, Kif11, Kif15/Eg5, Numa and Dynein). CEP192 is a coiled-coil scaffolding protein that recruits γ-TuRC, Aurora-A and Plk1 to the centrosome for its maturation. Our phosphoproteome reveals that CEP192, a Class II protein, is phosphorylated at 7 sites between prophase and MI, 5 of them corresponding to Cdk1 phosphorylation sites (Appendix Fig. S5E). Plk1 is recruited to its many different locations in the cell through its Polo-Box-Domain (PBD), which binds to phosphorylated S-S/T(p) motifs (Elia *et al*, 2003b, 2003a; Lee *et al*, 1998; Reynolds & Ohkura, 2003). Two of the CEP192 sites identified in our phosphoproteome, S991 and S1227, correspond to such motifs. Therefore, by attracting Plk1, CEP192 phosphorylation could prepare the reconstitution of a functional centrosome at fertilization.

Assembly of microtubule spindles and microtubule dynamics

Xenopus prophase oocytes are inefficient in their ability to support microtubule polymerization (Jessus *et al*, 1984; Gard & Kirschner, 1987; Heidemann & Kirschner, 1975), although microtubules are formed

at the cortical and nuclear envelope level, where γ-tubulin foci are also localized (Gard, 1994; Jessus *et al*, 1988). The ability to assemble microtubule asters is acquired at the time of NEBD, when a giant disk-shaped MTOC generates a large microtubular monoaster at the basal region of the disintegrating nucleus (Huchon *et al*, 1981; Gard, 1994). Therefore, MTOC and microtubule-associated proteins (MAPs) must be finely regulated by post-translational modifications at time of NEBD. The transient microtubule monoaster transports the meiotic chromosomes to the animal cortex, where the first meiotic spindle is assembled (Huchon *et al*, 1981; Gard, 1992). Due to the absence of centrioles, meiotic spindles are barrel-shaped and are formed by centrosome-independent microtubule nucleation originating from the chromosomes and involving chromatin and the Ran GTPase (Gruss & Vernos, 2004), much like spindles of vascular plant cells. Moreover, the two successive spindles are differentially regulated. The MI spindle is a transient and dynamic structure while the MII spindle is stable for hours, anchored to the plasma membrane until fertilization (Gard, 1992). One can therefore expect that MAPs are specifically and differentially regulated at MI and MII (Classes III and V). Finally, a major change in microtubule assembly occurs during the transition from meiosis to embryonic mitosis. The assembly of the first embryonic spindle integrates the meiotic chromosome-dependent pathway with the newly formed centrosomes (Cavazza *et al*, 2016). Thereafter, subsequent embryonic spindles depend solely on the microtubule nucleating activity of the centrosomes (Kirschner, 1986). All these critical transitions in the way of assembling a microtubular spindle depend on the proteins stored in the oocyte.

At least 5 microtubule regulatory proteins undergo specific patterns of phosphorylation that deserve attention (Fig. 8). Katanin, which is responsible for the majority of M-phase severing activity in *Xenopus* eggs and is activated by Cdk1 (McNally & Thomas, 1998), displays a bi-modal pattern of phosphorylation, increasing at the time of formation of the monoaster-MTOC and MI spindle, decreasing during MI-MII transition and increasing again at MII (Fig. 8). Kif11/Eg5 phosphorylation occurs at T936 and T937 starting NEBD (Fig. 8). Both phosphosites were reported in a broad range of models, and the second site was shown to be phosphorylated by Cdk1 (Blangy *et al*, 1995; Cahu *et al*, 2008; Giet *et al*, 1999) (Fig. 8). Kif11/Eg5 controls the relative stability of bipolar versus monopolar organization of spindles in *Xenopus* egg extracts (Mitchison *et al*, 2005) but also centrosome disjunction and/or separation. Hence, Kif11 is a good candidate to be an important player regulating the original changes in microtubule dynamics and organization of the two successive spindles. Kif15, also known as XKlp2, a plus end-directed kinesin protein required for centrosome separation and maintenance of spindle bipolarity in *Xenopus* egg extracts (Boleti *et al*, 1996), is phosphorylated at S681 and S692 during meiotic maturation. S681 is rather phosphorylated at MI while S692 is specific of MII (Fig. 8), suggesting

a potential distinct regulation of Kif15 on microtubule dynamics at MI and MII. Dyneins are a family of motor proteins that move to microtubules in an opposed direction to kinesins. Among this family, the dynein light intermediate chain (DynC1LI) plays important roles in mitosis, including positioning the spindle and focusing the MTs into poles. Our phosphoproteome reveals multiple phosphorylations of this protein, starting in MI and remaining constant or progressively increasing until MII, as for S197 (S207 in human) (Fig. 8). This agrees with previous data showing that S197 is phosphorylated by Cdk1 (Dell *et al*, 2000; Addinall *et al*, 2001) and that DynC1LI becomes hyperphosphorylated at the time of NEBD and remains hyperphosphorylated throughout the rest of meiosis (Huang *et al*, 1999). Additionally, our phosphoproteome reveals that 3 sites (495, 498 and 501) are phosphorylated around NEBD and get dephosphorylated after MI (Class III), hence being correlated with the 1st meiotic division and not the 2nd one, while 6 other sites (197,396, 409,446, 452, and 467) are phosphorylated both in MI and MII (Class II) (Fig. 8). Dynein is required for organization of the original microtubule/MTOC array that is organized at NEBD, together with XMAP215, XKCM1 and Numa (Becker *et al*, 2003). The formation of this oocyte original monoaster/MTOC could involve the dynein phosphorylations that transiently take place precisely at this period.

Strikingly, MI and MII spindles segregate chromosomes and chromatids in a very different way. In MI, the homologous chromosomes are segregated, whereas in MII the sister chromatids are displaced in the daughter cells, due to a specific organization of kinetochores and regulation of cohesins. In MI, arm cohesins are phosphorylated and degraded whereas centromeric cohesins are protected from cleavage by Sugoshin (Sgo1)-PP2A. This allows the separation of chromosomes, but chromatids are still attached together. In MII, centromeric cohesins are fully degraded, allowing the segregation of sister chromatids, as during mitosis (Wassmann, 2022). How a fraction of cohesins is protected from cleavage in MI but not MII is still not entirely clear since the phosphorylation of cohesins and their partners, which are not very abundant proteins, is difficult to be detected with conventional shotgun phosphoproteomics. Notably, our phosphoproteomic studies highlight new sites differentially phosphorylated between MI and MII within these proteins. Sgo1 and two components of the cohesin complex, Pds5b and Wapl, are increasingly phosphorylated during meiotic divisions (Class IV) (Appendix Fig. S6). Noteworthy, S1069 of Wapl is a putative Plk1 site (Grosstessner-Hain *et al*, 2011; Kettenbach *et al*, 2011). By highlighting new sites differentially phosphorylated between MI and MII, our phosphoproteomic studies provide clues to elucidate the still unknown mechanisms of the meiotic mechanism of cohesion protection-deprotection.

DISCUSSION

The amphibian oocyte and egg have long been a source of inspiration and a source of experimental opportunity for important areas of biology, such as nuclear organization, spindle formation, cell polarity, fertilization, mitosis and meiosis, endocrine signaling and intracellular signal transduction. As experimental embryology gave way to genetic approaches in the late 20th century to study embryonic development, the attractiveness of amphibian oocytes declined. The more gene-centered approaches led quickly to an emphasis on gene expression and there was a further decline in work in amphibian oocytes. But the original advantages of the amphibian oocyte are arguably now more obvious, as the linkage between complex cellular processes like cellular reorganization, mitosis and signal transduction become more important. The study of transcriptional regulation, which has benefited by so many ingenious and sensitive tools, is of no use in the study of a cell type that does not transcribe RNA. Similarly, much of signal transduction involves post-translational modifications, which are hard to detect and where there is a dearth of scalable tools. Many important processes involve complex changes in distributed systems like the endoplasmic reticulum, the mitotic apparatus, the nuclear and plasma membranes, and the cytoskeleton.

It is in the study of these processes, which govern the meiotic and mitotic changes, the cell cycle, signal transduction, involving endocrine and intracellular posttranslational changes and proteolysis, surrounding the onset of meiosis and mitosis, fertilization, zygotic fusion, spindle formation, and cell division why we and others have returned to the awesome power of the amphibian oocyte and egg. These processes are not only complex and difficult to study but they speak to morphogenesis on the single cell level. This is particularly true for meiosis and mitosis, which occupy on a very short fraction of the life span of most germ and somatic cells. There is a need to tie the processes, described previously by histology, to molecular events. These processes are arguably simpler in that they do not involve transcription, but also more complicated because we lack general tools for identification and measurement. We are generally limited to measuring protein abundance and trying to infer rates of synthesis and degradation. We can also apply drugs, but their non-specificity and the complexity of pathways pose serious limitations. Mass spectrometry has had limited applications, as there are not yet widely applicable single cell tools. Nevertheless, much would be learned by mass spectrometry by gauging but sensitive single cell methods are now just under development. The current state is that the level of proteins and the level of phosphorylated proteins can today be measured accurately by mass spectrometry but not at the single cell level -except for the frog eggs and oocytes. Frog eggs and oocytes show exquisite synchrony for the very same processes, meiosis and mitosis that are hard to study in

cultured cells. There are well developed tools for protein abundance but they have to be performed carefully. Post-translational modifications, principally phosphorylations, can be traced to specific residues on specific proteins. In this paper, we have applied the current state of the art of quantitative mass spectrometry to oocyte maturation and meiosis using quantitative proteomics and quantitative phosphoproteomics. We have temporally correlated events with oocyte maturation induced naturally by progesterone to *Xenopus* full-grown oocytes and watched the progression through meiosis I to the natural arrest at the second meiotic metaphase. We have been able to correlate the proteomic measurements with the physiological changes as the oocyte, as it goes from an early prophase I state through to a second meiotic metaphase state. We find dramatic changes in the oocyte nucleus and the meiotic spindles and drastic modifications to the standard cell cycle. These dramatic changes are choreographed principally by signaling pathways employing kinases and phosphatases. Oocyte maturation also includes major preparations for the rapid embryonic mitotic events, including changes in membrane trafficking, where the plasma membrane increases in total area 16-fold.

For years, phosphorylation events have been extensively studied using candidate-based approaches, as site-specific mutagenesis and phosphospecific antibodies. These targeted-approaches have several caveats. The selection of the putative sites of phosphorylation is based on *in silico* evidence, limiting the analysis to proteins bearing canonical consensus sequences and hence our knowledge of novel phosphorylation motifs. When multiple putative phosphorylation sites are present in the same protein, mutagenesis of individual sites or combinations of sites becomes too complex, impairing identification of the phosphorylation sites used *in vivo* and their interdependency or redundancy. Moreover, the time-consuming production of phospho-specific antibodies is not scalable to high throughput applications. The recently developed field of quantitative phosphoproteomics bypasses the limitations of the targeted-approaches and is particularly well suited to the study of physiological processes based on a massive system of protein phosphorylation, such as oocyte meiotic maturation. Indeed, in all animals, meiotic maturation relies on the dynamics of phosphorylation events, either during the signaling pathway that leads to Cdk1 activation or during the Cdk1 downstream period that orchestrates the structural events of the two meiotic divisions. Oocyte meiotic maturation is a key biological process. First, it transforms the oocyte into a fertilizable cell at the origin of life of any animal. Second, since meiosis derives from mitosis, thanks to cellular adaptations that were necessary to produce a haploid gamete (preventing an S-phase between the two divisions, modifying the functioning of the spindle during meiosis I, establishing division arrests needed for the oocyte to grow or to wait for sperm, performing asymmetrical divisions to save nutrient reserves, etc.), its study provides the

opportunity to understand how cell division can adapt and diversify in living systems, depending on specific cellular organization and specialized functions. The candidate-based approaches have provided a global scheme of this process based on the knowledge of a few kinases that have been extensively studied for years. However, this scheme still does not provide a very comprehensive picture of the meiotic process, since it does not take into account hundreds of unknown critical kinases, substrates and phosphosites. Quantitative proteomics and phosphoproteomics allowed us to obtain a much deeper and comprehensive dynamic picture of the phosphorylated sites during meiotic maturation. This has enabled us to describe and support with biochemical precision the various processes in the oocyte, determine the relative timing of various site phosphorylations and molecular processes, thereby challenging or suggesting the epistatic sequences of specific molecular pathways. We have also confirmed the importance of certain previously known phosphosites, identified the likely kinases or in some cases the kinase families responsible for substrate phosphorylation, and established connections between phosphorylation events and intracellular remodeling, as well as regulatory mechanisms such as translation and protein degradation. In addition to explaining the order of very the diverse events of chromatin remodeling, nuclear organization, plasma membrane transformations, cytoskeletal changes of meiosis, our proteomic and phospho-proteomic datasets should provide a large number of experimental avenues for exploring similar events in both mitotic and meiotic stages of diverse organisms. This molecular data will enable us to better understand regulatory pathways involving chromosome behavior, spindle formation, nuclear and plasma membrane regulation, and signal transduction and derive insights far beyond the scope of meiosis and oocyte maturation. One such insight might come from a closer analysis of the quality control mechanisms in the oocyte. Both nucleopore remodeling (King et al., 2019) and E2/E3 ubiquitin ligases are involved in housekeeping and quality control, specifically in the removal of aggregated and orphan complex proteins, as the germ cell of an organism prepares to become the next generation.

METHODS

Oocytes collection and *in vitro* maturation

The research with *Xenopus laevis* was performed under the oversight of the Harvard Medical Area Institutional Animal Care and Use Committee. Mature *Xenopus laevis* females were used after priming with pregnant mare serum gonadotropin (PMSG, 50 IU per frog). A sample of ovary tissue was surgically removed, rinsed in 1× Marc's modified Ringer's (MMR) and placed in OR2 buffer (83 mM NaCl, 2.5 mM KCl, 1 mM $CaCl_2$, 1 mM $MgCl_2$, 1 mM Na_2HPO_4, 5 mM HEPES, pH 7.8) and oocytes were manually defolliculated. Stage VI oocytes were selected and kept in dishes with agar beds to avoid sticking to the dish. Maturation was induced by incubation at 18°C with 10µg/mL progesterone in OR2 buffer.

Eggs were flash frozen with liquid nitrogen in bunches of ten or fifty for protein and phospho-proteomics measurements respectively. All samples were taken in triplicates, each biological replicate was performed with different frogs. The first sample was taken from untreated oocytes at the time of progesterone treatment, the second timepoint 2 hours after progesterone treatment, with hourly timepoints past that, up to 9 hours post treatment.

Embryo lysis and digestion into peptides

For each condition the embryos were lysed at a ratio of 6 µL buffer/embryo in the same buffer as (Presler *et al*, 2017) (0.25 M sucrose, 1% replacement NP-40, 10 mM EDTA, 25 mM HEPES, 1 mM TCEP, 10 µM Combretastatin, 10 µM Cytochalasin D, Roche Protease Inhibitor Mini EDTA free, and Phosstop inhibitor (Roche) at pH 7.2). The yolk was removed by spinning the samples at 4,000 g for 4 minutes at 4°C. Both the supernatant and all lipids were transferred for a new tube. The concentration of HEPES was raised to 0.1 M and SDS was added to 20%. After addition of DTT to 5 mM, the samples were denatured in a 60°C water bath for 20 minutes. After the samples temperatures return to room temperature, N-Ethylmaleimide (NEM) was added to 15 mM, tubes were mixed thoroughly, and the reaction proceeded for 1 hour. Then additional DTT was added to 5 mM to quench the excess NEM. The samples were flash frozen and stored at -80°C until the methanol chloroform precipitation (Wessel *et al*, 1984). Protein was precipitated by methanol-chloroform precipitation. Due to the large volume of lysate (~1 mL), the precipitation was performed in glass 15 mL Corex tubes (No. 8441). The tubes were cleaned for a two-hour chromic acid incubation and rinsed extensively in filtered water. Then they were autoclaved and before use for the precipitation, they were rinsed with HPLC H_20. The centrifugations were done in a JA 50 30 Ti rotor in a Beckman Avanti J-30I centrifuge at 21,000 g for either 6 minutes or 15 minutes. After the last supernatant was removed, the pellets were air dried for 15 minutes and

resuspended in 0.6 mL of 6 M guanidine, 50 M EPPS pH 8.5 and transferred to a 2 mL eppendorf tube. The samples were incubated for 5 minutes at 65°C and the protein amount was determined by a BCA Assay. The solution was diluted to 2 M guanidine with 10 mM EPPS pH 8.5. Lysyl endopeptidase (FUJIFILM WAKO (129-02541) resuspended with HPLC H_20 to ~2 mg/mL) was added to a concentration of 20 ng/mL and the initial digestion proceeded for 12 hours at room temperature with gentle shaking. The samples were further diluted to 0.5 M guanidine with 10 mM EPPS pH 8.5 and Trypsin protease (Sequencing Grade Modified Trypsin, Promega) was added to a final concentration of 10 ng/mL along with an additional 20 ng/mL of LysC. The samples were incubated in a 37°C room for 8 hours on a nutator.

Phospho-peptide enrichment

To carry out the phosphoproteomic analysis, we made the conventional steps of digesting the proteins from each time sample with trypsin and specifically labeling them with isobaric tags (TMT-10 reagents McAlister *et al*, 2012). Tagged samples and the phosphopeptides were enriched on an IMAC column. Importantly, we chose to multiplex peptides before the phosphopeptide enrichment to improve data quality. There is a tradeoff of decreased yield and therefore depth, as it is not economical to label more than a few milligrams of material. We used 2.5-4 mgs of TMT-labeled peptides per replicate, enriched with 5 µm Titanium Dioxide microspheres (GL Sciences 5020-75000) and fractioned as previously described (Presler *et al*, 2017). A typical yield of 50-80 µg of peptides eluted from the column, with a median phosphopeptide enrichment of ~80%.

Phosphatase treatment of *Xenopus* samples prepared for parallel phospho-enrichment

We adapted the method that we used to phosphatase-treat digested peptides (Presler *et al*, 2017) for the larger samples used here for the parallel phospho-enrichment. We chose to phosphatase treat when proteases were present in the samples (but after the protease digestion sequence described above) to enable the de-phosphorylated peptides to have the cleavage pattern expected if they were present initially in the de-phosphorylated state. We used the heat-labile Alkaline Shrimp Phosphatase (Affymetrix Inc, USA). We used a 3k Amicon Centrifugal Filter to exchange the enzyme storage buffer to 10 mM EPPS pH 8.5 instead of Tris-HCl pH 7.5. We also concentrated the phosphatase to between 3-4 U/µL (confirmed by p-nitrophenyl phosphate assay). We added an estimated 833 units of phosphatase to two of the samples built to contain representative mixture of peptides (TMT 131N, channel 10: 100 oocytes collected at the latest timepoint, and TMT 131C, channel 11: 50 oocytes collected at the first

timepoint combined with 50 oocytes collected at the last timepoint). To samples that were not phosphatase-treated, we added the same volume of blank phosphatase buffer: 5 mM EPPS pH 8, 50% glycerol. To all samples, we added $MgCl_2$ to 10 mM and EDTA to 0.1 mM (to chelate metals that might compete with the magnesium necessary for enzymatic activity). All the samples were incubated with gentle shaking at room temperature for 12 hours. The phosphatase was then inactivated by incubation with gentle shaking in an air-incubator at 65°C for 15 minutes. Peptide fractionation and TMT-MS3 LC/MS were carried out as done previously (Presler *et al*, 2017).

Computing phospho-occupancy systematically

We grouped phospho-peptides by unique phospho-site identifiers. In order to rigorously reflect the measurement accuracy and to take advantage of many measurements of the same phospho-site (including on peptides with different missed-cleavages or oxidized methionines), we used BACIQ (Peshkin *et al*, 2019) to compute the estimated trend with confidence intervals. Then, we created phospho-site sets to connect phospho-sites on residues that could be on the same peptide. We made these assignments based on whether the individual phospho-sites were ever measured with another phospho-site as a composite phospho-site. In order to determine occupancy, we needed to measure the phospho-site as a different form (usually not-phosphorylated). To do this, we identified non-phosphorylated peptides measured from the same experimental conditions that include the residue(s) of the phospho-site. Again, multiple non-phosphorylated peptides can include the residues of interest and the same peptide sequences can be measured multiple times. Therefore, we again use BACIQ (Peshkin *et al*, 2019) to aggregate these measurements in a trend with confidence intervals.

Mass spectrometry data mapping and analysis

Peptide-Spectra matches were performed as previously described (Sonnett *et al*, 2018). Assignment of MS2 spectra was performed using the SEQUEST (Eng *et al*, 1994) algorithm by searching the data against the appropriate proteome reference set acquired from Xenbase (*Xenopus laevis* assembly 9.1) along with common contaminants: human keratins and trypsin. The target-decoy strategy was used to construct a second database of reversed sequences that were used to estimate the false discovery rate on the peptide level. SEQUEST searches were performed using a 20 ppm precursor ion tolerance with the requirement that both N- and C-terminal peptide ends are consistent with the protease specificities of LysC and Trypsin. TMT (+229.162932 Da) was set as a static modification on N-termini and lysines peptides, and N-ethyl maleimide (+125.047679 Da) was set as a static modification on cysteine residues.

Oxidation of methionine (+15.99492 Da) was set as a variable modification. A peptide level MS2 spectral assignment false discovery rate of 1% was obtained by applying the target-decoy strategy with linear discriminant analysis. Peptides of 7 amino acids length or longer were ranked by linear discriminant analysis score and were filtered to a ratio of 1% reverses/forwards + reverses. Peptides were assigned to proteins and a second filtering step to obtain a 1% FDR on the protein level was applied. Peptides that matched multiple proteins were assigned to the proteins with the most unique peptides. We only used Isolation Specificity > 0.75 spectra.

Estimation of the absolute abundance of proteins

The absolute protein concentration was estimated according previously published methods (Wühr *et al*, 2014; Peshkin *et al*, 2015), based here on ion current prorated to the isobarically labeled fractions. The respective sample fractions were estimated using our previously published Bayesian approach (Peshkin *et al*, 2019), which integrates peptide signal and peptide-level measurement agreement into a maximum likelihood estimate of the true protein ratio and the associated confidence interval (Peshkin *et al*, 2019). See Appendix Supplementary Methods.

Data availability

The mass spectrometry proteomics raw data and reference set of sequences have been deposited to the ProteomeXchange consortium via the PRIDE partner repository with the dataset identifier MassIVE MSV000094498. In addition, we developed a multi-functional Web portal to release the data and enable interactive interrogation (https://xenopus.hms.harvard.edu/index_oocyte.html). All of the aspects from overall protein trends to individual clusters to specific phosphosites and stoichiometry information are easily available. The portal provides per-protein link to external information about each human protein by symbol from GeneCards (https://www.genecards.org/) and respective *Xenopus* protein at Xenbase (https://www.xenbase.org/xenbase/).

ACKNOWLEDGMENTS

This work was supported by the National Center for Scientific Research (CNRS) and Sorbonne University, the National Research Agency (ANR) grants 18-CE13-0013-01 (CJ) and ANR-23-CE12-0045-01 (EMD), Sorbonne University Emergence grant (EMD), the ARC foundation grant ARCPJA2023080006901 (EMD), Amaranth Foundation (LP) and the NIH OD award R24 OD031956 (LP and MWK).

AUTHOR CONTRIBUTIONS

Leonid Peshkin: Conceptualization; Methodology; Experiments; Software; Formal Analysis; Data Curation; Writing; Supervision. **Enrico M Daldello**: Formal Analysis; Writing. **Elizabeth Van Itallie**: Software; Formal Analysis; Data Curation; Writing. **Matthew Sonnett**: Methodology; Formal Analysis. **Johannes Kreuzer**: Formal Analysis; Data Curation. **Wilhelm Haas**: Methodology; Formal Analysis. **Marc W Kirschner**: Conceptualization; Methodology; Experiments; Writing; Supervision. **Catherine Jessus**: Writing; Formal Analysis; Supervision.

DISCLOSURE AND COMPETING INTERESTS STATEMENT

The authors declare no competing interests.

REFERENCES

Addinall SG, Mayr PS, Doyle S, Sheehan JK, Woodman PG & Allan VJ (2001) Phosphorylation by cdc2-CyclinB1 Kinase Releases Cytoplasmic Dynein from Membranes. *Journal of Biological Chemistry* 276: 15939–15944

Angres B, Müller AHJ, Kellermann J & Hausen P (1991) Differential expression of two cadherins in *Xenopus laevis*. *Development* 111: 829–844

Araki K, Naito K, Haraguchi S, Suzuki R, Yokoyama M, Inoue M, Aizawa S, Toyoda Y & Sato E (1996) Meiotic Abnormalities of c-mos Knockout Mouse Oocytes: Activation after First Meiosis or Entrance into Third Meiotic Metaphase1. *Biol Reprod* 55: 1315–1324

Babiano R, Gamalinda M, Woolford JL & de la Cruz J (2012) Saccharomyces cerevisiae ribosomal protein L26 is not essential for ribosome assembly and function. *Mol Cell Biol* 32: 3228–3241

Bahtz R, Seidler J, Arnold M, Haselmann-Weiss U, Antony C, Lehmann WD & Hoffmann I (2012) GCP6 is a substrate of Plk4 and required for centriole duplication. *Journal of Cell Science* 125: 486–496

Bansal S & Tiwari S (2019) Mechanisms for the temporal regulation of substrate ubiquitination by the anaphase-promoting complex/cyclosome. *Cell Div* 14: 14

Bärenz F, Inoue D, Yokoyama H, Tegha-Dunghu J, Freiss S, Draeger S, Mayilo D, Cado I, Merker S, Klinger M, *et al* (2013) The centriolar satellite protein SSX2IP promotes centrosome maturation. *Journal of Cell Biology* 202: 81–95

Barnard DC, Cao Q & Richter JD (2005) Differential Phosphorylation Controls Maskin Association with Eukaryotic Translation Initiation Factor 4E and Localization on the Mitotic Apparatus. *Molecular and Cellular Biology* 25: 7605–7615

Bauer M, Cubizolles F, Schmidt A & Nigg EA (2016) Quantitative analysis of human centrosome architecture by targeted proteomics and fluorescence imaging. *The EMBO Journal* 35: 2152–2166

Becker BE, Romney SJ & Gard DL (2003) XMAP215, XKCM1, NuMA, and cytoplasmic dynein are required for the assembly and organization of the transient microtubule array during the maturation of Xenopus oocytes. *Developmental Biology* 261: 488–505

Bement WM & Capco DG (1990) Transformation of the amphibian oocyte into the egg: Structural and biochemical events. *J Elec Microsc Tech* 16: 202–234

Bhatt RR & Ferrell JE (2000) Cloning and Characterization of Xenopus Rsk2, the Predominant p90 Rsk Isozyme in Oocytes and Eggs. *Journal of Biological Chemistry* 275: 32983–32990

Blangy A, Lane HA, d'Hérin P, Harper M, Kress M & Niggt EA (1995) Phosphorylation by p34cdc2 regulates spindle association of human Eg5, a kinesin-related motor essential for bipolar spindle formation in vivo. *Cell* 83: 1159–1169

Blomen VA, Májek P, Jae LT, Bigenzahn JW, Nieuwenhuis J, Staring J, Sacco R, Van Diemen FR, Olk N, Stukalov A, *et al* (2015) Gene essentiality and synthetic lethality in haploid human cells. *Science* 350: 1092–1096

Bluemink JG, Hage WJ, van den Hoef MH & Dictus WJ (1983) Freeze-fracture electron microscopy of membrane changes in progesterone-induced maturing oocytes and eggs of Xenopus laevis. *Eur J Cell Biol* 31: 85–93

Bodart J-FL, Baert FY, Sellier C, Duesbery NS, Flament S & Vilain J-P (2005) Differential roles of p39Mos–Xp42Mpk1 cascade proteins on Raf1 phosphorylation and spindle morphogenesis in Xenopus oocytes. *Developmental Biology* 283: 373–383

Boke E, Ruer M, Wühr M, Coughlin M, Lemaitre R, Gygi SP, Alberti S, Drechsel D, Hyman AA & Mitchison TJ (2016) Amyloid-like Self-Assembly of a Cellular Compartment. *Cell* 166: 637–650

Boleti H, Karsenti E & Vernos I (1996) Xklp2, a Novel Xenopus Centrosomal Kinesin-like Protein Required for Centrosome Separation during Mitosis. *Cell* 84: 49–59

Bouftas N, Schneider L, Halder M, Demmig R, Baack M, Cladière D, Walter M, Al Abdallah H, Kleinhempel C, Messaritaki R, *et al* (2022) Cyclin B3 implements timely vertebrate oocyte arrest for fertilization. *Developmental Cell* 57: 2305-2320.e6

Cahu J, Olichon A, Hentrich C, Schek H, Drinjakovic J, Zhang C, Doherty-Kirby A, Lajoie G & Surrey T (2008) Phosphorylation by Cdk1 Increases the Binding of Eg5 to Microtubules In Vitro and in Xenopus Egg Extract Spindles. *PLoS ONE* 3: e3936

Campanella C, Andreuccetti P, Taddei C & Talevi R (1984) The modifications of cortical endoplasmic reticulum during in vitro maturation of *Xenopus laevis* oocytes and its involvement in cortical granule exocytosis. *J Exp Zool* 229: 283–293

Cao Q, Zhao C, Wang C, Cai L, Xia M, Zhang X, Han J, Xu Y, Zhang J, Ling X, *et al* (2021) The Recurrent Mutation in PATL2 Inhibits Its Degradation Thus Causing Female Infertility Characterized by Oocyte Maturation Defect Through Regulation of the Mos-MAPK Pathway. *Front Cell Dev Biol* 9: 628649

Castro A, Mandart E, Lorca T & Galas S (2003) Involvement of Aurora A Kinase during Meiosis I-II Transition in Xenopus Oocytes. *J Biol Chem* 278: 2236–2241

Cavazza T, Peset I & Vernos I (2016) From meiosis to mitosis: the sperm centrosome defines the kinetics of spindle assembly after fertilization. *Journal of Cell Science*: jcs.183624

Celebic D, Polat I, Legros V, Chevreux G, Wassmann K & Touati SA (2024) Qualitative rather than quantitative phosphoregulation shapes the end of meiosis I in budding yeast. *EMBO J*

Charbonneau M & Grey RD (1984) The onset of activation responsiveness during maturation coincides with the formation of the cortical endoplasmic reticulum in oocytes of Xenopus laevis. *Developmental Biology* 102: 90–97

Charlesworth A, Yamamoto TM, Cook JM, Silva KD, Kotter CV, Carter GS, Holt JW, Lavender HF, MacNicol AM, Ying Wang Y, *et al* (2012) Xenopus laevis zygote arrest 2 (zar2) encodes a zinc finger RNA-binding protein that binds to the translational control sequence in the maternal Wee1 mRNA and regulates translation. *Dev Biol* 369: 177–190

Chen J, Melton C, Suh N, Oh JS, Horner K, Xie F, Sette C, Blelloch R & Conti M (2011) Genome-wide analysis of translation reveals a critical role for deleted in azoospermia-like (Dazl) at the oocyte-to-zygote transition. *Genes Dev* 25: 755–766

Cheng K-Y (2003) The crystal structure of the human polo-like kinase-1 polo box domain and its phospho-peptide complex. *The EMBO Journal* 22: 5757–5768

Chew TG, Peaston A, Lim AK, Lorthongpanich C, Knowles BB & Solter D (2013) A Tudor Domain Protein SPINDLIN1 Interacts with the mRNA-Binding Protein SERBP1 and Is Involved in Mouse Oocyte Meiotic Resumption. *PLoS ONE* 8: e69764

Choi T, Fukasawa K, Zhou R, Tessarollo L, Borror K, Resau J & Vande Woude GF (1996) The Mos/mitogen-activated protein kinase (MAPK) pathway regulates the size and degradation of the first polar body in maturing mouse oocytes. *Proc Natl Acad Sci USA* 93: 7032–7035

Christou-Kent M, Kherraf Z, Amiri-Yekta A, Le Blévec E, Karaouzène T, Conne B, Escoffier J, Assou S, Guttin A, Lambert E, *et al* (2018) PATL 2 is a key actor of oocyte maturation whose invalidation causes infertility in women and mice. *EMBO Mol Med* 10

Cohen-Fix O, Peters JM, Kirschner MW & Koshland D (1996) Anaphase initiation in Saccharomyces cerevisiae is controlled by the APC-dependent degradation of the anaphase inhibitor Pds1p. *Genes Dev* 10: 3081–3093

Colman A, Jones EA & Heasman J (1985) Meiotic maturation in Xenopus oocytes: a link between the cessation of protein secretion and the polarized disappearance of Golgi apparati. *The Journal of cell biology* 101: 313–318

Cordes VC, Reidenbach S & Franke WW (1995) High content of a nuclear pore complex protein in cytoplasmic annulate lamellae of Xenopus oocytes. *Eur J Cell Biol* 68: 240–255

Daldello EM, Le T, Poulhe R, Jessus C, Haccard O & Dupré A (2015) Control of Cdc6 accumulation by Cdk1 and MAPK is essential for completion of oocyte meiotic divisions in *Xenopus*. *J Cell Sci* 128: 2482–2496

De Magistris P & Antonin W (2018) The Dynamic Nature of the Nuclear Envelope. *Current Biology* 28: R487–R497

De Matteis MA, Wilson C & D'Angelo G (2013) Phosphatidylinositol-4-phosphate: The Golgi and beyond. *BioEssays* 35: 612–622

Delattre M & Gönczy P (2004) The arithmetic of centrosome biogenesis. *Journal of Cell Science* 117: 1619–1630

Dell KR, Turck CW & Vale RD (2000) Mitotic Phosphorylation of the Dynein Light Intermediate Chain is Mediated by cdc2 Kinase. *Traffic* 1: 38–44

Deng J, Lang S, Wylie C & Hammes SR (2008) The Xenopus laevis Isoform of G Protein-Coupled Receptor 3 (GPR3) Is a Constitutively Active Cell Surface Receptor that Participates in Maintaining Meiotic Arrest in X. laevis Oocytes. *Molecular Endocrinology* 22: 1853–1865

Dictenberg JB, Zimmerman W, Sparks CA, Young A, Vidair C, Zheng Y, Carrington W, Fay FS & Doxsey SJ (1998) Pericentrin and γ-Tubulin Form a Protein Complex and Are Organized into a Novel Lattice at the Centrosome. *The Journal of Cell Biology* 141: 163–174

Drysdale TA & Elinson RP (1992) Cell Migration and Induction in the Development of the Surface Ectodermal Pattern of the *Xenopus laevis* Tadpole: (*Xenopus* /ciliated cell/hatching gland/cement gland/ectodermal differentiation). *Dev Growth Differ* 34: 51–59

Dumont JN (1972) Oogenesis inXenopus laevis (Daudin). I. Stages of oocyte development in laboratory maintained animals. *J Morphol* 136: 153–179

Dupré A, Daldello EM, Nairn AC, Jessus C & Haccard O (2014) Phosphorylation of ARPP19 by protein kinase A prevents meiosis resumption in Xenopus oocytes. *Nat Commun* 5: 3318

Dupre A, Jessus C, Ozon R & Haccard O (2002) Mos is not required for the initiation of meiotic maturation in Xenopus oocytes. *EMBO J* 21: 4026–4036

Elia AEH, Cantley LC & Yaffe MB (2003a) Proteomic Screen Finds pSer/pThr-Binding Domain Localizing Plk1 to Mitotic Substrates. *Science* 299: 1228–1231

Elia AEH, Rellos P, Haire LF, Chao JW, Ivins FJ, Hoepker K, Mohammad D, Cantley LC, Smerdon SJ & Yaffe MB (2003b) The Molecular Basis for Phosphodependent Substrate Targeting and Regulation of Plks by the Polo-Box Domain. *Cell* 115: 83–95

El-Jouni W, Haun S, Hodeify R, Hosein Walker A & Machaca K (2007) Vesicular traffic at the cell membrane regulates oocyte meiotic arrest. *Development* 134: 3307–3315

Ems-McClung SC, Emch M, Zhang S, Mahnoor S, Weaver LN & Walczak CE (2020) RanGTP induces an effector gradient of XCTK2 and importin α/β for spindle microtubule cross-linking. *Journal of Cell Biology* 219: e201906045

Eng JK, McCormack AL & Yates JR (1994) An approach to correlate tandem mass spectral data of peptides with amino acid sequences in a protein database. *J Am Soc Mass Spectrom* 5: 976–989

Feldherr CM (1974) The binding characteristics of the nuclear annuli. *Experimental Cell Research* 85: 271–277

Félix M, Antony C, Wright M & Maro B (1994) Centrosome assembly in vitro: role of gamma-tubulin recruitment in Xenopus sperm aster formation. *The Journal of cell biology* 124: 19–31

Fisher DL, Brassac T, Galas S & Dorée M (1999) Dissociation of MAP kinase activation and MPF activation in hormone-stimulated maturation of Xenopus oocytes. *Development* 126: 4537–4546

Frank-Vaillant M, Jessus C, Ozon R, Maller JL & Haccard O (1999) Two Distinct Mechanisms Control the Accumulation of Cyclin B1 and Mos in *Xenopus* Oocytes in Response to Progesterone. *MBoC* 10: 3279–3288

Fry AM, Descombes P, Twomey C, Bacchieri R & Nigg EA (2000) The NIMA-related kinase X-Nek2B is required for efficient assembly of the zygotic centrosome in Xenopus laevis. *Journal of Cell Science* 113: 1973–1984

Furuno N, Nishizawa M, Okazaki K, Tanaka H, Iwashita J, Nakajo N, Ogawa Y & Sagata N (1994) Suppression of DNA replication via Mos function during meiotic divisions in Xenopus oocytes. *EMBO J* 13: 2399–2410

Gaffré M, Martoriati A, Belhachemi N, Chambon J-P, Houliston E, Jessus C & Karaiskou A (2011) A critical balance between Cyclin B synthesis and Myt1 activity controls meiosis entry in *Xenopus* oocytes. *Development* 138: 3735–3744

Gard DL (1992) Microtubule organization during maturation of Xenopus oocytes: Assembly and rotation of the meiotic spindles. *Developmental Biology* 151: 516–530

Gard DL (1994) γ-Tubulin Is Asymmetrically Distributed in the Cortex of Xenopus Oocytes. *Developmental Biology* 161: 131–140

Gard DL (1999) Confocal microscopy and 3-D reconstruction of the cytoskeleton ofXenopus oocytes. *Microsc Res Tech* 44: 388–414

Gard DL, Affleck D & Error BM (1995) Microtubule Organization, Acetylation, and Nucleation in Xenopus laevis Oocytes: II. A Developmental Transition in Microtubule Organization during Early Diplotene. *Developmental Biology* 168: 189–201

Gard DL, Hafezi S, Zhang T & Doxsey SJ (1990) Centrosome duplication continues in cycloheximide-treated Xenopus blastulae in the absence of a detectable cell cycle. *The Journal of cell biology* 110: 2033–2042

Gard DL & Kirschner MW (1987) Microtubule assembly in cytoplasmic extracts of Xenopus oocytes and eggs. *The Journal of cell biology* 105: 2191–2201

Gavin A-C, Ainle AN, Chierici E, Jones M & Nebreda AR (1999) A p90 ^{rsk} Mutant Constitutively Interacting with MAP Kinase Uncouples MAP Kinase from p34 ^{cdc2} /Cyclin B Activation in *Xenopus* Oocytes. *MBoC* 10: 2971–2986

Gawantka V, Ellinger-Ziegelbauer H & Hausen P (1992) β-integrin is a maternal protein that is inserted into all newly formed plasma membranes during early *Xenopus* embryogenesis. *Development* 115: 595–605

Gerhart J, Wu M & Kirschner M (1984) Cell cycle dynamics of an M-phase-specific cytoplasmic factor in Xenopus laevis oocytes and eggs. *The Journal of cell biology* 98: 1247–1255

Giet R, Uzbekov R, Cubizolles F, Le Guellec K & Prigent C (1999) The Xenopus laevis Aurora-related Protein Kinase pEg2 Associates with and Phosphorylates the Kinesin-related Protein XIEg5. *Journal of Biological Chemistry* 274: 15005–15013

Glotzer M, Murray AW & Kirschner MW (1991) Cyclin is degraded by the ubiquitin pathway. *Nature* 349: 132–138

Groisman I, Jung M-Y, Sarkissian M, Cao Q & Richter JD (2002) Translational Control of the Embryonic Cell Cycle. *Cell* 109: 473–483

Gromley A, Yeaman C, Rosa J, Redick S, Chen C-T, Mirabelle S, Guha M, Sillibourne J & Doxsey SJ (2005) Centriolin Anchoring of Exocyst and SNARE Complexes at the Midbody Is Required for Secretory-Vesicle-Mediated Abscission. *Cell* 123: 75–87

Grosstessner-Hain K, Hegemann B, Novatchkova M, Rameseder J, Joughin BA, Hudecz O, Roitinger E, Pichler P, Kraut N, Yaffe MB, *et al* (2011) Quantitative Phospho-proteomics to Investigate the Polo-like Kinase 1-Dependent Phospho-proteome. *Molecular & Cellular Proteomics* 10: M111.008540

Gruss O (2018) Animal Female Meiosis: The Challenges of Eliminating Centrosomes. *Cells* 7: 73

Gruss OJ & Vernos I (2004) The mechanism of spindle assembly. *The Journal of Cell Biology* 166: 949–955

Gwon Y, Maxwell BA, Kolaitis RM, Zhang P, Kim HJ, Taylor JP. Ubiquitination of G3BP1 mediates stress granule disassembly in a context-specific manner. Science. 2021 Jun 25;372(6549):eabf6548. doi: 10.1126/science.abf6548. Epub 2021 Aug 5. PMID: 34739333; PMCID: PMC8574224.

Haccard O & Jessus C (2006) Oocyte Maturation, Mos and Cyclins—A Matter of Synthesis: Two Functionally Redundant Ways to Induce Meiotic Maturation. *Cell Cycle* 5: 1152–1159

Hansen DV, Tung JJ & Jackson PK (2006) CaMKII and Polo-like kinase 1 sequentially phosphorylate the cytostatic factor Emi2/XErp1 to trigger its destruction and meiotic exit. *Proceedings of the National Academy of Sciences* 103: 608–613

Hatch EM, Kulukian A, Holland AJ, Cleveland DW & Stearns T (2010) Cep152 interacts with Plk4 and is required for centriole duplication. *Journal of Cell Biology* 191: 721–729

Heidemann SR & Kirschner MW (1975) Aster formation in eggs of Xenopus laevis. Induction by isolated basal bodies. *The Journal of cell biology* 67: 105–117

Heim A, Niedermeier ML, Stengel F & Mayer TU (2022) The translation regulator Zar1l controls timing of meiosis in *Xenopus* oocytes. *Development* 149: dev200900

Hochegger H, Klotzbücher A, Kirk J, Howell M, le Guellec K, Fletcher K, Duncan T, Sohail M & Hunt T (2001) New B-type cyclin synthesis is required between meiosis I and II during Xenopus oocyte maturation. *Development* 128: 3795–3807

Houliston E, Le Guellec R, Kress M, Philippe M & Le Guellec K (1994) The kinesin-related protein Eg5 associates with both interphase and spindle microtubules during Xenopus early development. *Dev Biol* 164: 147–159

Huang C-YF, Chang C-PB, Huang C-L & Ferrell JE (1999) M Phase Phosphorylation of Cytoplasmic Dynein Intermediate Chain and p150Glued. *Journal of Biological Chemistry* 274: 14262–14269

Huchon D, Crozet N, Cantenot N & Ozon R (1981) Germinal vesicle breakdown in the Xenopus laevis oocyte: description of a transient microtubular structure. *Reprod Nutr Dévelop* 21: 135–148

Huchon D, Rime H, Jessus C & Ozon R (1993) Control of metaphase I formation in *Xenopus* oocyte: Effects of an indestructible cyclin B and of protein synthesis. *Biology of the Cell* 77: 133–141

Hyman LE & Wormington WM (1988) Translational inactivation of ribosomal protein mRNAs during Xenopus oocyte maturation. *Genes Dev* 2: 598–605

Isobe K, Jung HJ, Yang C-R, Claxton J, Sandoval P, Burg MB, Raghuram V & Knepper MA (2017) Systems-level identification of PKA-dependent signaling in epithelial cells. *Proc Natl Acad Sci USA* 114

Jamieson-Lucy A & Mullins MC (2019) The vertebrate Balbiani body, germ plasm, and oocyte polarity. In *Current Topics in Developmental Biology* pp 1–34. Elsevier

Jessus C (2010) MPF and the Control of Meiotic Divisions: Old Problems, New Concepts. In *Oogenesis*, Verlhac M & Villeneuve A (eds) pp 227–265. Wiley

Jessus C, Friederich E, Francon J & Ozon R (1984) In vitro inhibition of tubulin assembly by a ribonucleoprotein complex associated with the free ribosome fraction isolated from Xenopus laevis oocytes: effect at the level of microtubule-associated proteins. *Cell Differentiation* 14: 179–187

Jessus C, Thibier C, Huchon D & Ozon R (1988) Taxol reveals cortical sites of microtubule assembly in Xenopus oocytes. Role of the nucleus. *Cell Differentiation and Development* 25: 57–63

Jia J, Tang S, Yue X, Jing S, Zhu L, Tan C, Gao J, Du Y, Lee I & Qian Y (2023) An A-kinase anchoring protein (ACBD3) coordinates traffic-induced PKA activation at the Golgi. *Journal of Biological Chemistry* 299: 104696

Josefsberg Ben-Yehoshua L, Lewellyn AL, Thomas P & Maller JL (2007) The Role of Xenopus Membrane Progesterone Receptor β in Mediating the Effect of Progesterone on Oocyte Maturation. *Molecular Endocrinology* 21: 664–673

Kado RT, Marcher K & Ozon R (1981) Electrical membrane properties of the Xenopus laevis oocyte during progesterone-induced meiotic maturation. *Developmental Biology* 84: 471–476

Kaufman OH, Lee K, Martin M, Rothhämel S & Marlow FL (2018) rbpms2 functions in Balbiani body architecture and ovary fate. *PLoS Genet* 14: e1007489

Kessel RG, Tung HN, Beams HW & Lin JJ-C (1986) Is the nuclear envelope a?generator? of membrane?: Developmental sequences in cytomembrane elaboration. *Cell Tissue Res* 245

Kettenbach AN, Schweppe DK, Faherty BK, Pechenick D, Pletnev AA & Gerber SA (2011) Quantitative Phosphoproteomics Identifies Substrates and Functional Modules of Aurora and Polo-Like Kinase Activities in Mitotic Cells. *Sci Signal* 4

Keuss MJ, Thomas Y, Mcarthur R, Wood NT, Knebel A & Kurz T (2016) Characterisation of the mammalian family of DCN-type NEDD8 E3 ligases. *Journal of Cell Science*: jcs.181784

King GA, Goodman JS, Schick JG, Chetlapalli K, Jorgens DM, McDonald KL, Ünal E. Meiotic cellular rejuvenation is coupled to nuclear remodeling in budding yeast. Elife. 2019 Aug 9;8:e47156. doi: 10.7554/eLife.47156. PMID: 31397671; PMCID: PMC6711709.

Kinoshita K, Habermann B & Hyman AA (2002) XMAP215: a key component of the dynamic microtubule cytoskeleton. *Trends in Cell Biology* 12: 267–273

Kinterová V, Kaňka J, Bartková A & Toralová T (2022) SCF Ligases and Their Functions in Oogenesis and Embryogenesis—Summary of the Most Important Findings throughout the Animal Kingdom. *Cells* 11: 234

Kirschner M (1986) Beyond self-assembly: From microtubules to morphogenesis. *Cell* 45: 329–342

Kishimoto T (2003) Cell-cycle control during meiotic maturation. *Current Opinion in Cell Biology* 15: 654–663

Klima M, Tóth DJ, Hexnerova R, Baumlova A, Chalupska D, Tykvart J, Rezabkova L, Sengupta N, Man P, Dubankova A, *et al* (2016) Structural insights and in vitro reconstitution of membrane targeting and activation of human PI4KB by the ACBD3 protein. *Sci Rep* 6: 23641

Kobayashi H (1991) On the synthesis and destruction of A- and B-type cyclins during oogenesis and meiotic maturation in Xenopus laevis. *J Cell Biol* 114: 755–765

Koch LB, Spanos C, Kelly V, Ly T & Marston AL (2024) Rewiring of the phosphoproteome executes two meiotic divisions in budding yeast. *EMBO J* 43: 1351–1383

Kraft C (2003) Mitotic regulation of the human anaphase-promoting complex by phosphorylation. *The EMBO Journal* 22: 6598–6609

Kufer TA, Silljé HHW, Körner R, Gruss OJ, Meraldi P & Nigg EA (2002) Human TPX2 is required for targeting Aurora-A kinase to the spindle. *The Journal of Cell Biology* 158: 617–623

Kumar H, Pushpa K, Kumari A, Verma K, Pergu R & Mylavarapu SVS (2019) The exocyst complex and Rab5 are required for abscission by localizing ESCRT III subunits to the cytokinetic bridge. *Journal of Cell Science* 132: jcs226001

Kutay U, Jühlen R & Antonin W (2021) Mitotic disassembly and reassembly of nuclear pore complexes. *Trends in Cell Biology* 31: 1019–1033

Larabell CA & Chandler DE (1989) The coelomic envelope of Xenopus laevis eggs: A quick-freeze, deep-etch analysis. *Developmental Biology* 131: 126–135

Leaf DS, Roberts SJ, Gerhart JC & Moore H-P (1990) The secretory pathway is blocked between the trans-Golgi and the plasma membrane during meiotic maturation in Xenopus oocytes. *Developmental Biology* 141: 1–12

Lee KS, Grenfell TZ, Yarm FR & Erikson RL (1998) Mutation of the polo-box disrupts localization and mitotic functions of the mammalian polo kinase Plk. *Proc Natl Acad Sci USA* 95: 9301–9306

Lee M, Nagashima K, Yoon J, Sun J, Wang Z, Carpenter C, Lee H-K, Hwang Y-S, Westlake CJ & Daar IO (2022) CEP97 phosphorylation by Dyrk1a is critical for centriole separation during multiciliogenesis. *Journal of Cell Biology* 221: e202102110

LeGuennec M, Klena N, Aeschlimann G, Hamel V & Guichard P (2021) Overview of the centriole architecture. *Current Opinion in Structural Biology* 66: 58–65

Lemaître J-M, Bocquet S & Méchali M (2002) Competence to replicate in the unfertilized egg is conferred by Cdc6 during meiotic maturation. *Nature* 419: 718–722

Lemonnier T, Dupré A & Jessus C (2020) The G2-to-M transition from a phosphatase perspective: a new vision of the meiotic division. *Cell Div* 15: 9

Linder MI, Köhler M, Boersema P, Weberruss M, Wandke C, Marino J, Ashiono C, Picotti P, Antonin W & Kutay U (2017) Mitotic Disassembly of Nuclear Pore Complexes Involves CDK1- and PLK1-Mediated Phosphorylation of Key Interconnecting Nucleoporins. *Developmental Cell* 43: 141-156.e7

Liu L & Wiese C (2008) *Xenopus* NEDD1 is required for microtubule organization in *Xenopus* egg extracts. *Journal of Cell Science* 121: 578–589

Lorenzo-Orts L, Strobl M, Steinmetz B, Leesch F, Pribitzer C, Roehsner J, Schutzbier M, Dürnberger G & Pauli A (2023) eIF4E1b is a non-canonical eIF4E protecting maternal dormant mRNAs. *EMBO Rep*

Macůrek L, Lindqvist A, Lim D, Lampson MA, Klompmaker R, Freire R, Clouin C, Taylor SS, Yaffe MB & Medema RH (2008) Polo-like kinase-1 is activated by aurora A to promote checkpoint recovery. *Nature* 455: 119–123

Maller J, Wu M & Gerhart JC (1977) Changes in protein phosphorylation accompanying maturation of Xenopus laevis oocytes. *Developmental Biology* 58: 295–312

Marnef A, Maldonado M, Bugaut A, Balasubramanian S, Kress M, Weil D & Standart N (2010) Distinct functions of maternal and somatic Pat1 protein paralogs. *RNA* 16: 2094–2107

Maton G, Lorca T, Girault J-A, Ozon R & Jessus C (2005) Differential regulation of Cdc2 and Aurora-A in *Xenopus* oocytes: a crucial role of phosphatase 2A. *Journal of Cell Science* 118: 2485–2494

Maton G, Thibier C, Castro A, Lorca T, Prigent C & Jessus C (2003) Cdc2-Cyclin B Triggers H3 Kinase Activation of Aurora-A in Xenopus Oocytes. *J Biol Chem* 278: 21439–21449

McAlister GC, Huttlin EL, Haas W, Ting L, Jedrychowski MP, Rogers JC, Kuhn K, Pike I, Grothe RA, Blethrow JD, Gygi SP. Increasing the multiplexing capacity of TMTs using reporter ion isotopologues with isobaric masses. Anal Chem. 2012 Sep 4;84(17):7469-78. doi: 10.1021/ac301572t. Epub 2012 Aug 20. PMID: 22880955; PMCID: PMC3715028.

McNally FJ & Thomas S (1998) Katanin Is Responsible for the M-Phase Microtubule-severing Activity in *Xenopus* Eggs. *MBoC* 9: 1847–1861

McPhail JA, Lyoo H, Pemberton JG, Hoffmann RM, Van Elst W, Strating JR, Jenkins ML, Stariha JT, Powell CJ, Boulanger MJ, *et al* (2020) Characterization of the c10orf76-PI4KB complex and its necessity for Golgi PI4P levels and enterovirus replication. *EMBO Reports* 21: e48441

Mendez R, Barnard D & Richter JD (2002) Differential mRNA translation and meiotic progression require Cdc2-mediated CPEB destruction. *EMBO J* 21: 1833–1844

Meneau F, Dupré A, Jessus C & Daldello EM (2020) Translational Control of Xenopus Oocyte Meiosis: Toward the Genomic Era. *Cells* 9: 1502

Miller BR & Forbes DJ (2000) Purification of the Vertebrate Nuclear Pore Complex by Biochemical Criteria. *Traffic* 1: 941–951

Miller KE, Session AM & Heald R (2019) Kif2a Scales Meiotic Spindle Size in Hymenochirus boettgeri. *Current Biology* 29: 3720-3727.e5

Mitchison TJ, Maddox P, Gaetz J, Groen A, Shirasu M, Desai A, Salmon ED & Kapoor TM (2005) Roles of Polymerization Dynamics, Opposed Motors, and a Tensile Element in Governing the Length of *Xenopus* Extract Meiotic Spindles. *MBoC* 16: 3064–3076

Mueller PR, Coleman TR & Dunphy WG (1995) Cell cycle regulation of a Xenopus Wee1-like kinase. *MBoC* 6: 119–134

Müller H -Arno J (2001) Of mice, frogs and flies: Generation of membrane asymmetries in early development. *Dev Growth Differ* 43: 327–342

Mulner-Lorillon O, Bellé R, Cormier P, Drewing S, Minella O, Poulhe R & Schmalzing G (1995) Brefeldin A Provokes Indirect Activation of cdc2 Kinase (MPF) in Xenopus Oocytes, Resulting in Meiotic Cell Division. *Developmental Biology* 170: 223–229

Nader N, Dib M, Courjaret R, Hodeify R, Machaca R, Graumann J & Machaca K (2018) VLDL receptor regulates membrane progesterone receptor trafficking and non-genomic signaling. *Journal of Cell Science*: jcs.212522

Nader N, Dib M, Daalis A, Kulkarni RP & Machaca K (2014) Role for endocytosis of a constitutively active GPCR (GPR185) in releasing vertebrate oocyte meiotic arrest. *Developmental Biology* 395: 355–366

Nader N, Dib M, Hodeify R, Courjaret R, Elmi A, Hammad AS, Dey R, Huang X-Y & Machaca K (2020) Membrane progesterone receptor induces meiosis in Xenopus oocytes through endocytosis into signaling endosomes and interaction with APPL1 and Akt2. *PLoS Biol* 18: e3000901

Nakahata S, Kotani T, Mita K, Kawasaki T, Katsu Y, Nagahama Y & Yamashita M (2003) Involvement of Xenopus Pumilio in the translational regulation that is specific to cyclin B1 mRNA during oocyte maturation. *Mechanisms of Development* 120: 865–880

Nakajo N, Yoshitome S, Iwashita J, Iida M, Uto K, Ueno S, Okamoto K & Sagata N (2000) Absence of Wee1 ensures the meiotic cell cycle in Xenopus oocytes. *Genes Dev* 14: 328–338

Nakamura Y, Tanaka KJ, Miyauchi M, Huang L, Tsujimoto M & Matsumoto K (2010) Translational repression by the oocyte-specific protein P100 in Xenopus. *Dev Biol* 344: 272–283

Nguyen AT, Prado MA, Schmidt PJ, Sendamarai AK, Wilson-Grady JT, Min M, Campagna DR, Tian G, Shi Y, Dederer V, *et al* (2017) UBE2O remodels the proteome during terminal erythroid differentiation. *Science* 357: eaan0218

Oakley CE & Oakley BR (1989) Identification of γ-tubulin, a new member of the tubulin superfamily encoded by mipA gene of Aspergillus nidulans. *Nature* 338: 662–664

Okano-Uchida T, Sekiai T, Lee K, Okumura E, Tachibana K & Kishimoto T (1998) In VivoRegulation of Cyclin A/Cdc2 and Cyclin B/Cdc2 through Meiotic and Early Cleavage Cycles in Starfish. *Developmental Biology* 197: 39–53

Ota R, Kotani T & Yamashita M (2011) Biochemical Characterization of Pumilio1 and Pumilio2 in Xenopus Oocytes. *Journal of Biological Chemistry* 286: 2853–2863

Padmanabhan K (2006) Regulated Pumilio-2 binding controls RINGO/Spy mRNA translation and CPEB activation. *Genes Dev* 20: 199–209

Pascreau G, Delcros J-G, Cremet J-Y, Prigent C & Arlot-Bonnemains Y (2005) Phosphorylation of Maskin by Aurora-A Participates in the Control of Sequential Protein Synthesis during Xenopus laevis Oocyte Maturation. *Journal of Biological Chemistry* 280: 13415–13423

Patra D & Dunphy WG (1998) Xe-p9, a *Xenopus* Suc1/Cks protein, is essential for the Cdc2-dependent phosphorylation of the anaphase- promoting complex at mitosis. *Genes Dev* 12: 2549–2559

Payne DM, Rossomando AJ, Martino P, Erickson AK, Her JH, Shabanowitz J, Hunt DF, Weber MJ & Sturgill TW (1991) Identification of the regulatory phosphorylation sites in pp42/mitogen-activated protein kinase (MAP kinase). *The EMBO Journal* 10: 885–892

Peset I, Seiler J, Sardon T, Bejarano LA, Rybina S & Vernos I (2005) Function and regulation of Maskin, a TACC family protein, in microtubule growth during mitosis. *The Journal of Cell Biology* 170: 1057–1066

Peshkin L, Gupta M, Ryazanova L & Wühr M (2019) Bayesian Confidence Intervals for Multiplexed Proteomics Integrate Ion-statistics with Peptide Quantification Concordance*[S]. *Molecular & Cellular Proteomics* 18: 2108–2120

Peshkin L, Wühr M, Pearl E, Haas W, Freeman RM, Gerhart JC, Klein AM, Horb M, Gygi SP & Kirschner MW (2015) On the Relationship of Protein and mRNA Dynamics in Vertebrate Embryonic Development. *Developmental Cell* 35: 383–394

Peuchen EH, Cox OF, Sun L, Hebert AS, Coon JJ, Champion MM, Dovichi NJ & Huber PW (2017) Phosphorylation Dynamics Dominate the Regulated Proteome during Early Xenopus Development. *Sci Rep* 7: 15647

Piqué M, López JM, Foissac S, Guigó R & Méndez R (2008) A Combinatorial Code for CPE-Mediated Translational Control. *Cell* 132: 434–448

Popov AV, Severin F & Karsenti E (2002) XMAP215 Is Required for the Microtubule-Nucleating Activity of Centrosomes. *Current Biology* 12: 1326–1330

Presler M, Van Itallie E, Klein AM, Kunz R, Coughlin ML, Peshkin L, Gygi SP, Wühr M & Kirschner MW (2017) Proteomics of phosphorylation and protein dynamics during fertilization and meiotic exit in the *Xenopus* egg. *Proc Natl Acad Sci USA* 114: E10838–E10847

Reimann JDR, Freed E, Hsu JY, Kramer ER, Peters J-M & Jackson PK (2001) Emi1 Is a Mitotic Regulator that Interacts with Cdc20 and Inhibits the Anaphase Promoting Complex. *Cell* 105: 645–655

Rempel RE, Sleight SB & Maller JL (1995) Maternal Xenopus Cdk2-Cyclin E Complexes Function during Meiotic and Early Embryonic Cell Cycles That Lack a G1 Phase. *Journal of Biological Chemistry* 270: 6843–6855

Reverte CG, Ahearn MD & Hake LE (2001) CPEB Degradation during Xenopus Oocyte Maturation Requires a PEST Domain and the 26S Proteasome. *Dev Biol* 231: 447–458

Reynolds N & Ohkura H (2003) Polo boxes form a single functional domain that mediates interactions with multiple proteins in fission yeast polo kinase. *Journal of Cell Science* 116: 1377–1387

Ríos-Cardona D, Ricardo-González RR, Chawla A & Ferrell JE (2008) A role for GPRx, a novel GPR3/6/12-related G-protein coupled receptor, in the maintenance of meiotic arrest in Xenopus laevis oocytes. *Dev Biol* 317: 380–388

Roig J, Groen A, Caldwell J & Avruch J (2005) Active Nercc1 Protein Kinase Concentrates at Centrosomes Early in Mitosis and Is Necessary for Proper Spindle Assembly. *MBoC* 16: 4827–4840

Rong Y, Ji S-Y, Zhu Y-Z, Wu Y-W, Shen L & Fan H-Y (2019) ZAR1 and ZAR2 are required for oocyte meiotic maturation by regulating the maternal transcriptome and mRNA translational activation. *Nucleic Acids Research* 47: 11387–11402

Ross J (1997) A hypothesis to explain why translation inhibitors stabilize mRNAs in mammalian cells: mRNA Stability and mitosis. *BioEssays* 19: 527–529

Sadler SE & Maller JL (1985) Inhibition of Xenopus oocyte adenylate cyclase by progesterone: a novel mechanism of action. *Adv Cyclic Nucleotide Protein Phosphorylation Res* 19: 179–194

Sagata N, Daar I, Oskarsson M, Showalter S & Vande Woude G (1989a) The product of the mos proto-oncogene as a candidate 'initiator' for oocyte maturation. *Science* 245: 643–646

Sagata N, Oskarsson M, Copeland T, Brumbaugh J & Woude GFV (1988) Function of c-mos proto-oncogene product in meiotic maturation in Xenopus oocytes. *Nature* 335: 519–525

Sagata N, Watanabe N, Vande Woude GF & Ikawa Y (1989b) The c-mos proto-oncogene product is a cytostatic factor responsible for meiotic arrest in vertebrate eggs. *Nature* 342: 512–518

Santoni M, Meneau F, Sekhsoukh N, Castella S, Le T, Miot M & Daldello EM (2024) Unraveling the interplay between PKA inhibition and Cdk1 activation during oocyte meiotic maturation. *Cell Reports* 43: 113782

Sasaki J, Ishikawa K, Arita M & Taniguchi K (2012) ACBD3-mediated recruitment of PI4KB to picornavirus RNA replication sites: Picornaviral protein/ACBD3/PI4KB complex. *The EMBO Journal* 31: 754–766

Session AM, Uno Y, Kwon T, Chapman JA, Toyoda A, Takahashi S, Fukui A, Hikosaka A, Suzuki A, Kondo M, *et al* (2016) Genome evolution in the allotetraploid frog Xenopus laevis. *Nature* 538: 336–343

Setoyama D, Yamashita M & Sagata N (2007) Mechanism of degradation of CPEB during Xenopus oocyte maturation. *Proc Natl Acad Sci USA* 104: 18001–18006

Solc P, Kitajima TS, Yoshida S, Brzakova A, Kaido M, Baran V, Mayer A, Samalova P, Motlik J & Ellenberg J (2015) Multiple Requirements of PLK1 during Mouse Oocyte Maturation. *PLoS ONE* 10: e0116783

Sonnett M, Gupta M, Nguyen T & Wühr M (2018) Quantitative Proteomics for Xenopus Embryos II, Data Analysis. In *Xenopus*, Vleminckx K (ed) pp 195–215. New York, NY: Springer New York

Stearns T & Kirschner M (1994) In vitro reconstitution of centrosome assembly and function: The central role of γ-tubulin. *Cell* 76: 623–637

Stebbins-Boaz B, Cao Q, de Moor CH, Mendez R & Richter JD (1999) Maskin Is a CPEB-Associated Factor that Transiently Interacts with eIF-4E. *Molecular Cell* 4: 1017–1027

Steinacker TL, Wong S-S, Novak ZA, Saurya S, Gartenmann L, Van Houtum EJH, Sayers JR, Lagerholm BC & Raff JW (2022) Centriole growth is limited by the Cdk/Cyclin-dependent phosphorylation of Ana2/STIL. *Journal of Cell Biology* 221: e202205058

Sulimenko V, Dráberová E & Dráber P (2022) γ-Tubulin in microtubule nucleation and beyond. *Front Cell Dev Biol* 10: 880761

Swartz SZ, Nguyen HT, McEwan BC, Adamo ME, Cheeseman IM & Kettenbach AN (2021) Selective dephosphorylation by PP2A-B55 directs the meiosis I-meiosis II transition in oocytes. *eLife* 10: e70588

Taieb FE, Gross SD, Lewellyn AL & Maller JL (2001) Activation of the anaphase-promoting complex and degradation of cyclin B is not required for progression from Meiosis I to II in Xenopus oocytes. *Current Biology* 11: 508–513

Takagi M, Absalon MJ, McLure KG & Kastan MB (2005) Regulation of p53 Translation and Induction after DNA Damage by Ribosomal Protein L26 and Nucleolin. *Cell* 123: 49–63

Tanos BE, Yang H-J, Soni R, Wang W-J, Macaluso FP, Asara JM & Tsou M-FB (2013) Centriole distal appendages promote membrane docking, leading to cilia initiation. *Genes Dev* 27: 163–168

Tavernier N, Noatynska A, Panbianco C, Martino L, Van Hove L, Schwager F, Léger T, Gotta M & Pintard L (2015) Cdk1 phosphorylates SPAT-1/Bora to trigger PLK-1 activation and drive mitotic entry in *C. elegans* embryos. *Journal of Cell Biology* 208: 661–669

Tavernier N, Sicheri F & Pintard L (2021) Aurora A kinase activation: Different means to different ends. *Journal of Cell Biology* 220: e202106128

Terasaki M, Runft LL & Hand AR (2001) Changes in Organization of the Endoplasmic Reticulum during *Xenopus* Oocyte Maturation and Activation. *MBoC* 12: 1103–1116

Thibier C, De Smedt V, Poulhe R, Huchon D, Jessus C & Ozon R (1997) In Vivo Regulation of Cytostatic Activity inXenopusMetaphase II-Arrested Oocytes. *Developmental Biology* 185: 55–66

Thillaiappan NB, Smith HA, Atakpa-Adaji P & Taylor CW (2021) KRAP tethers IP3 receptors to actin and licenses them to evoke cytosolic Ca2+ signals. *Nat Commun* 12: 4514

Thomas Y, Cirillo L, Panbianco C, Martino L, Tavernier N, Schwager F, Van Hove L, Joly N, Santamaria A, Pintard L, *et al* (2016) Cdk1 Phosphorylates SPAT-1/Bora to Promote Plk1 Activation in C. elegans and Human Cells. *Cell Reports* 15: 510–518

Tzeng Y-W, Li D-Y, Chen Y, Yang C-H, Chang C-Y & Juang Y-L (2018) LMO7 exerts an effect on mitosis progression and the spindle assembly checkpoint. *The International Journal of Biochemistry & Cell Biology* 94: 22–30

Uto K (2000) Nek2B, a novel maternal form of Nek2 kinase, is essential for the assembly or maintenance of centrosomes in early Xenopus embryos. *The EMBO Journal* 19: 1816–1826

Vigneron S, Sundermann L, Labbé J-C, Pintard L, Radulescu O, Castro A & Lorca T (2018) Cyclin A-cdk1-Dependent Phosphorylation of Bora Is the Triggering Factor Promoting Mitotic Entry. *Developmental Cell* 45: 637-650.e7

Vik TA & Ryder JW (1997) Identification of Serine 380 as the Major Site of Autophosphorylation of Xenopus pp90rsk. *Biochemical and Biophysical Research Communications* 235: 398–402

Virant-Klun I, Leicht S, Hughes C & Krijgsveld J (2016) Identification of Maturation-Specific Proteins by Single-Cell Proteomics of Human Oocytes. *Molecular & Cellular Proteomics* 15: 2616–2627

Walczak CP, Leto DE, Zhang L, Riepe C, Muller RY, DaRosa PA, Ingolia NT, Elias JE & Kopito RR (2019) Ribosomal protein RPL26 is the principal target of UFMylation. *Proc Natl Acad Sci USA* 116: 1299–1308

Warner JR & McIntosh KB (2009) How Common Are Extraribosomal Functions of Ribosomal Proteins? *Molecular Cell* 34: 3–11

Wassmann K (2022) Separase Control and Cohesin Cleavage in Oocytes: Should I Stay or Should I Go? *Cells* 11: 3399

Wessel D, Flügge UI. A method for the quantitative recovery of protein in dilute solution in the presence of detergents and lipids. Anal Biochem. 1984 Apr;138(1):141-3. doi: 10.1016/0003-2697(84)90782-6. PMID: 6731838.

Whitmire E, Khan B & Coué M (2002) Cdc6 synthesis regulates replication competence in Xenopus oocytes. *Nature* 419: 722–725

Wilk K, Bilinski S, Dougherty MT & Kloc M (2005) Delivery of germinal granules and localized RNAs via the messenger transport organizer pathway to the vegetal cortex of Xenopus oocytes occurs through directional expansion of the mitochondrial cloud. *Int J Dev Biol* 49: 17–21

Wind M, Kelm O, Nigg EA & Lehmann WD (2002) Identification of phosphorylation sites in the polo-like kinases Plx1 and Plk1 by a novel strategy based on element and electrospray high resolution mass spectrometry. *Proteomics* 2: 1516–1523

Woodland HR (1974) Changes in the polysome content of developing Xenopus laevis embryos. *Dev Biol* 40: 90–101

Wu X-J, Thomas P & Zhu Y (2018) Pgrmc1 Knockout Impairs Oocyte Maturation in Zebrafish. *Front Endocrinol* 9: 560

Wühr M, Freeman RM, Presler M, Horb ME, Peshkin L, Gygi SP & Kirschner MW (2014) Deep Proteomics of the Xenopus laevis Egg using an mRNA-Derived Reference Database. *Current Biology* 24: 1467–1475

Yamamoto TM, Cook JM, Kotter CV, Khat T, Silva KD, Ferreyros M, Holt JW, Knight JD & Charlesworth A (2013) Zar1 represses translation in Xenopus oocytes and binds to the TCS in maternal mRNAs with different characteristics than Zar2. *Biochimica et Biophysica Acta (BBA) - Gene Regulatory Mechanisms* 1829: 1034–1046

Yanagitani K, Juszkiewicz S, Hegde RS. UBE2O is a quality control factor for orphans of multiprotein complexes. Science. 2017 Aug 4;357(6350):472-475. doi: 10.1126/science.aan0178. PMID: 28774922; PMCID: PMC5549844.

Yang C, Dominique GM, Champion MM & Huber PW (2022) Remnants of the Balbiani body are required for formation of RNA transport granules in Xenopus oocytes. *iScience* 25: 103878

Yang M, Jin Y, Fan S, Liang X, Jia J, Tan Z, Huang T, Li Y, Ma T & Li M (2019) Inhibition of neddylation causes meiotic arrest in mouse oocyte. *Cell Cycle* 18: 1254–1267

Yew N, Mellini ML, Martinez CK & Woude GFV (1992) Meiotic initiation by the mos protein in Xenopus. *Nature* 355: 649–652

Zhang M, Zhang J, Yan W & Chen X (2016) p73 expression is regulated by ribosomal protein RPL26 through mRNA translation and protein stability. *Oncotarget* 7: 78255–78268

Zhang Z, Liu R, Zhou H, Li Q, Qu R, Wang W, Zhou Z, Yu R, Zeng Y, Mu J, *et al* (2023) PATL2 regulates mRNA homeostasis in oocytes by interacting with EIF4E and CPEB1. *Development* 150: dev201572

Zitouni S, Francia ME, Leal F, Montenegro Gouveia S, Nabais C, Duarte P, Gilberto S, Brito D, Moyer T, Kandels-Lewis S, *et al* (2016) CDK1 Prevents Unscheduled PLK4-STIL Complex Assembly in Centriole Biogenesis. *Current Biology* 26: 1127–1137

FIGURE LEGENDS

Figure 1. Molecular events coordinating *Xenopus laevis* oocyte meiotic divisions.

From top to bottom: The prophase arrest is maintained by high PKA activity due to the constitutively expressed GPR185 receptor. The exocytic pathway is active while the endocytic pathway is downregulated. Cdk1-Cyclin B2 complexes are present under an inactive state due to Cdk1 phosphorylation. Progesterone activates the mPRβ receptor, GPR185 is inactivated, the exocytosis and endocytosis pathways are inverted. PKA is inactivated and promotes translation and/or accumulation of new proteins, among them Mos (that does not accumulate due to its instability) and Cyclin B1 (due to its stabilization). New Cyclin B1 proteins associate with Cdk1 and form a starter amount of Cdk1 activity. This Cdk1 starter stabilizes Mos and promotes Cdk1-Cyclin B2 activation through the regulation of Myt1, Cdc25, Gwl and PP2A. An autoamplification loop is launched, whereby more Cdk1 is activated, more it activates kinases as Mos-MAPK, Aurora-A and Plk1, all of them contributing with Cdk1 to regulate Myt1 and Cdc25, hence accelerating Cdk1 activation. Phosphorylated substrates trigger NEBD and the MI spindle assembly as well as protein translation. APC is inhibited under the control of Cdk1 and leads to Cyclin B degradation. The Cdk1 activity decreases and allows anaphase I and expulsion of the 1st polar body. Under the Mos/MAPK control, Emi2/Erp1 inactivates APC, halting Cyclin B degradation. The re-accumulation of Cyclin B increases Cdk1 activity that triggers the formation of the MII spindle, avoiding the assembly of a nucleus and DNA replication. APC remains inhibited by Emi2/Erp1, what ensures the oocyte arrest in MII. Color code: red: inactivated proteins; green: activated proteins; red arrow: inhibition; green arrow: activation; yellow highlight: accumulated protein; blue highlight: protein synthesized but not accumulated.

Figure 2. Changes in the protein levels during meiotic divisions.

(**A**) The relative changes in the concentration of proteins whose accumulation/degradation has been reported to correlate with the critical stages of *Xenopus* meiotic divisions have been plotted. (**B**) Changes of protein stoichiometry during meiotic maturation. The log2 fold changes between the concentration of each protein in PRO-arrested oocytes and MII-arrested oocytes was plotted. The red line marks the 1.5-fold change used as a threshold to identify accumulating proteins. The blue line marks the 0.75-fold change used as threshold to distinguish proteins that are degraded during meiosis. Proteins, whose changes in homeostasis during meiotic divisions are documented in the literature, are marked with the following color code: red, for proteins accumulating; black, for proteins which are expressed at a stable level; and blue, for proteins that are degraded. (**C-D**) Gene ontology analysis of the

biological processes enriched among the proteins found to accumulate (in red, panel **C**) or degraded (in blue, panel **D**) during meiosis. The statistical significance of the enrichment is expressed as false discovery rate (FDR). A representative subset of the proteins belonging to each group is displayed.

Figure 3. Changes in protein phosphorylation during meiotic divisions.

(**A**) Relative phosphopeptide signals were normalized for the changes in the total level of the proteins. The changes in the phosphopeptides were measured between the three biological stages of meiotic divisions (PRO = 0hr, MI = average of 3 and 4 hours, and MII = average of 7 to 9 hours). Class I (n=136 - 2%, in blue) includes proteins bearing a phosphosite whose occupancy decreases during meiosis resumption (Log2FC(MI/PRO)<-1). Class II (n=2167 - 39%, in green) contains proteins that are highly phosphorylated from MI (Log2FC(MI/PRO)>1) to MII (-1<Log2FC(MII/MI)<1). Class III (n=267 - 5%, in red) consists of proteins whose phosphorylation is specific of MI (Log2FC(MI/PRO)>1, Log2FC(MII/MI)<-1). Class IV (n=507 - 9%, yellow) is composed of proteins whose phosphorylation increases from MI (Log2FC(MI/PRO)>1) to MII, picking in MII (Log2FC(MII/MI)> 1). Class V (n=301 – 5%, orange) comprises proteins whose phosphorylation does not vary in MI (-1<Log2FC(MI/PRO)<1) but are phosphorylated only in MII (Log2FC(MII/MI)>1). The average signal of each Class was plotted with a thick and dark line. (**B**) Table summarizing the proteins bearing phosphosites belonging to Class I.

Figure 4. RNA-binding proteins and translation initiation factors are dynamically phosphorylated during meiotic divisions.

(**A**) Gene ontology enrichment analysis of the biological process "translation" (GO:0006412) among the phosphopeptides found in each class defined in Fig. 3. (**B-C**) Graphical representation of the phosphorylation dynamics of RBPs (**B**) and translation initiation factors (**C**) during meiotic divisions. Proteins are color-coded to highlight the changes in protein abundance during meiotic divisions: unchanged=white, decreased=blue, increased=light orange. The phosphorylated sites are color-coded: unchanged, grey; Class I, blue; Class II, green; Class III, red; Class IV, yellow; Class V, orange. The numbering is referred to the iso-allele which has higher number of phosphorylation sites detected.

Figure 5. E2 and E3 ubiquitin ligases are highly regulated by phosphorylation.

(**A**) Gene ontology enrichment analysis of the biological process "protein polyubiquitination" (GO:0000209) among the phosphopeptides found in each class defined in Fig. 3. (**B-C**) Graphical representation of the phosphorylation dynamics of the components of two E3 ubiquitin ligases, the

anaphase promoting complex (APC) (**B**) and the Skp, Cullin, F-box containing complex (SCF) (**C**) during meiotic divisions. Proteins are color-coded to highlight changes in protein abundance during meiotic divisions: unchanged=white, decreased=blue, increased=light orange. The phosphorylated sites are color-coded: unchanged, grey; Class I, blue; Class II, green; Class III, red; Class IV, yellow; Class V, orange. The numbering is referred to the iso-allele which has higher number of phosphorylation sites detected.

Figure 6. The network of phosphorylations regulating Cdk1 and the Mos/MAPK pathway.

(**A**) Gene ontology enrichment analysis of the biological process "mitotic cell cycle" (GO:0000278) among the phosphopeptides found in each class defined in Fig. 3. (**B**) Graphical representation of the network of phosphorylations of cell cycle regulators controlling Cdk1 activation (**upper panel**) and the Mos/MAPK pathway (**lower panel**). The human nomenclature numbering has been used for the phospho-sites. The phosphosites are displayed by dots and color-coded: yellow background, new sites identified in this paper and never described elsewhere; grey background, phosphosites already documented in vertebrates by low throughput papers and not identified in this paper; grey-yellow background, phosphosites already documented in vertebrates by low throughput papers and also identified in this paper. The functional effect of the phosphorylation is indicated by the color of the dot contour line: green, activatory; red, inhibitory; black, unknown.

Figure 7. The phosphorylation pattern of nuclear pore components during meiotic divisions.

(**A**) Absolute concentration (nM) of nucleoporins in prophase and metaphase II oocytes. (**B**) Gene ontology enrichment analysis of the biological process "nuclear pore organization" (GO:0006999) among the phosphopeptides found in each class defined in Fig. 3. (**C**) Phosphorylation patterns of Nup35/Nup53. The phosphorylation curves are color-coded: Class II, green; Class III, red; Class IV, yellow. (**D**) High precision phospho-occupancy calculation of S59 phosphorylation pattern of Nup35/Nup53.

Figure 8. Microtubule-interacting proteins phosphorylation during meiotic divisions.

Graphic representation of the phosphorylation dynamics of kinesins (Kif15, Kif11), dyneins (DYNC1LI1, DYNC1LI2) and katanin (KATNB1) during meiotic divisions. The sites of the phosphorylation detected are marked above each panel.

Table 1. Centrosomal components during meiotic divisions.

Expression patterns of the components of the centrioles and the pericentriolar material. The changes in protein abundance are color-coded: unchanged=white, decreased=blue, increased=light orange. The estimation of the protein and mRNA concentrations was derived by published datasets and color-coded on a white-green scale for protein concentrations and on a white-yellow scale for mRNA concentrations.

EXPANDED VIEW FIGURE LEGENDS

Figure EV1. Validation of the proteomic dataset.

(**A**) Table summarizing proteins whose changes in protein level have been documented using Western blot. The PMID of the original publication displaying the Western blot is reported. The changes in abundance detected in our dataset are color-coded with a scale from green to red. Log2 fold changes between prophase and metaphase II from our dataset are compared to another dataset previously published (Peuchen, 2017). (**B**) Proteome-wide comparison of our dataset with (Peuchen, 2017). Proteins whose abundance was previously published are color-coded in red for the ones that accumulate, black for the constant, and blue for the ones that are degraded. (**C**) Changes in protein abundance between prophase and metaphase II were calculated for each protein were we could distinguish the .S and .L isoforms, and plotted. The Pearson correlation between the isoforms was calculated with Prism. (**D**) Table summarizing the comparison between .S and .L isoforms presented in panel **C**. (**E**) Correlation plot between the changes in protein abundance occurring during the prophase to metaphase II transition and the relative abundance in prophase oocytes.

Figure EV2. Phosphorylation patterns of Cdk1 regulators during meiotic divisions

(**A**-**D** and **F**) Levels of phosphorylation sites of Plk1 (**A**), Bora (**B**), Cdc25 (**C**), Gwl/MASTL (**D**) and Wee2 (**F**) during meiotic divisions are plotted. The peptide sequences are reported with the phosphorylation sites marked in bold. The number of the residue phosphorylated is reported between breakers according to the *Xenopus* and human nomenclature. (**E**) The phosphorylation occupancy for S428 of Cdc27 is plotted with its confidence intervals.

Figure EV3. Phosphorylation patterns of the mos/MAPK pathway during meiotic divisions

(**A**-**E**) Levels of phosphorylation sites of Erk1 (**A**), Bora (**B**), MEK1 (**C**), MEK2 (**D**) and Rsk2 (**E**) during meiotic divisions are plotted. The peptide sequences are reported with the phosphorylation sites marked in bold. The number of the residue phosphorylated is reported between breakers according to the *Xenopus* and human nomenclature. (**F**) The phosphorylation occupancy for S381 of Rsk1 is plotted with its confidence intervals.

Fig. 1

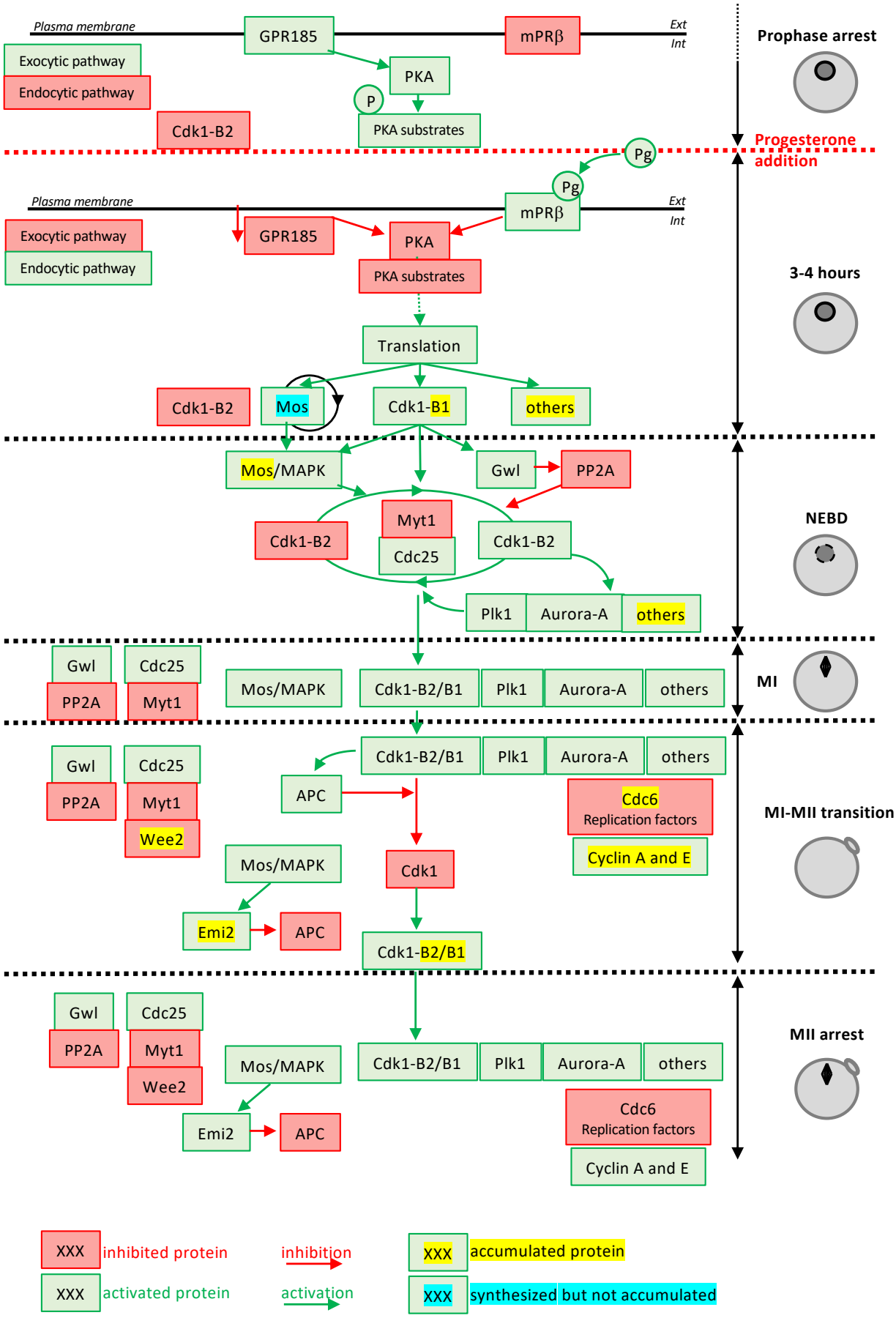
Plasma membrane
GPR185
mPRβ
Ext
Int
Prophase arrest
Exocytic pathway
Endocytic pathway
PKA
P
PKA substrates
Cdk1-B2
Progesterone addition
Pg
Pg
Plasma membrane
mPRβ
Ext
Int
Exocytic pathway
Endocytic pathway
GPR185
PKA
PKA substrates
3-4 hours
Translation
Cdk1-B2
Mos
Cdk1-B1
others
Mos/MAPK
Gwl
PP2A
Myt1
Cdk1-B2
Cdc25
Cdk1-B2
NEBD
Plk1
Aurora-A
others
Gwl
Cdc25
PP2A
Myt1
Mos/MAPK
Cdk1-B2/B1
Plk1
Aurora-A
others
MI
Gwl
Cdc25
PP2A
Myt1
Wee2
Cdk1-B2/B1
Plk1
Aurora-A
others
APC
Cdc6
Replication factors
Cyclin A and E
MI-MII transition
Mos/MAPK
Cdk1
Emi2
APC
Cdk1-B2/B1
Gwl
Cdc25
PP2A
Myt1
Wee2
Mos/MAPK
Cdk1-B2/B1
Plk1
Aurora-A
others
MII arrest
Emi2
APC
Cdc6
Replication factors
Cyclin A and E
XXX
inhibited protein
inhibition
XXX
accumulated protein
XXX
activated protein
activation
XXX
synthesized but not accumulated

Fig. 2

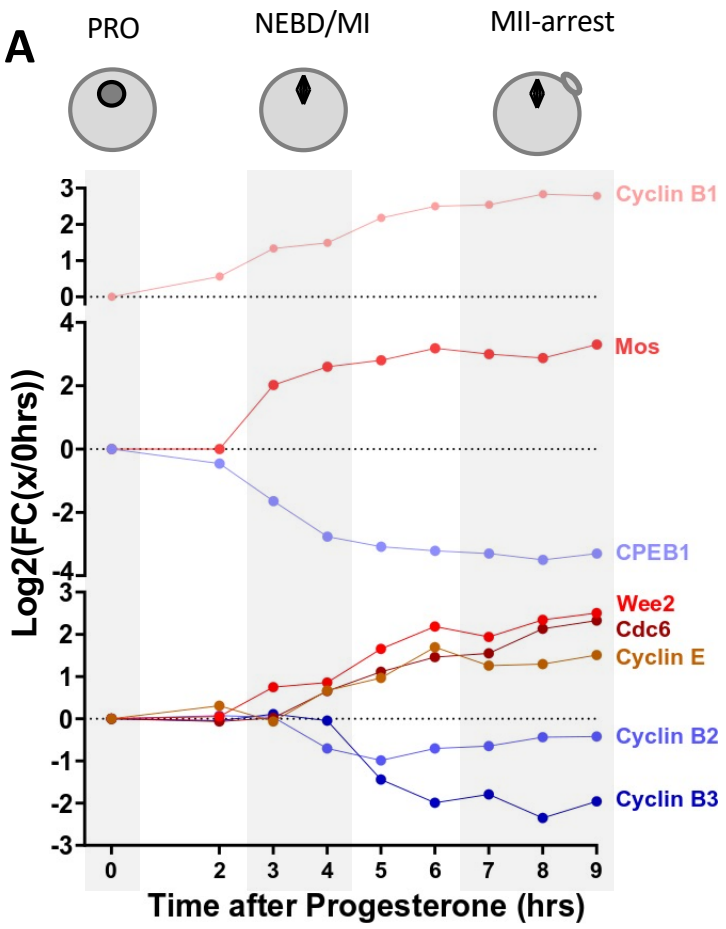
A
PRO
NEBD/MI
MII-arrest
Cyclin B1
Mos
CPEB1
Wee2
Cdc6
Cyclin E
Cyclin B2
Cyclin B3
Log2(FC(x/0hrs))
Time after Progesterone (hrs)

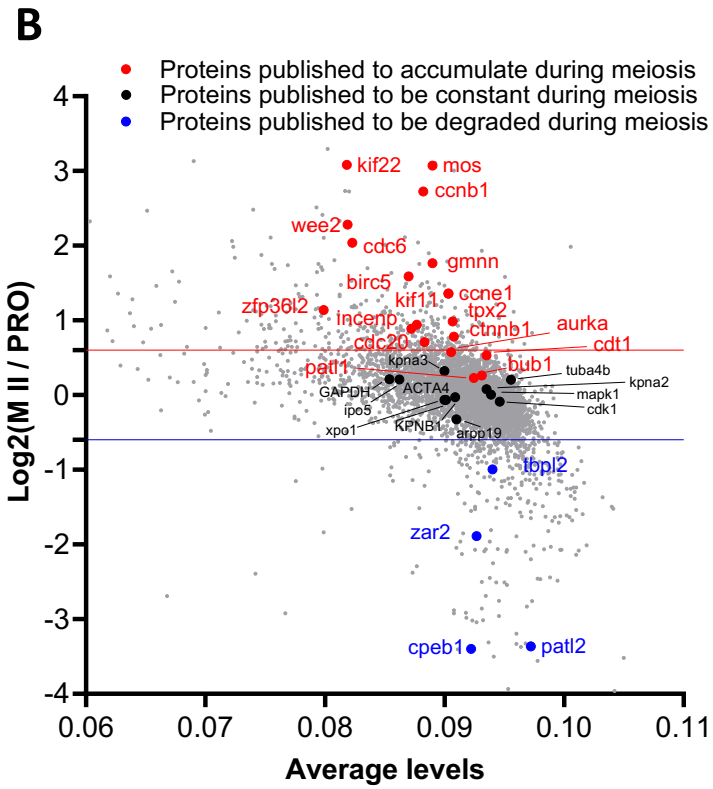
B
Proteins published to accumulate during meiosis
Proteins published to be constant during meiosis
Proteins published to be degraded during meiosis
kif22
mos
ccnb1
wee2
cdc6
gmnn
birc5
ccne1
zfp36l2
kif11
incenp
tpx2
ctnnb1
aurka
cdc20
cdt1
patl1
kpna3
bub1
tuba4b
kpna2
GAPDH
ACTA4
mapk1
cdk1
ipo5
xpo1
KPNB1
arpp19
tbpl2
zar2
cpeb1
patl2
Log2(M II / PRO)
Average levels

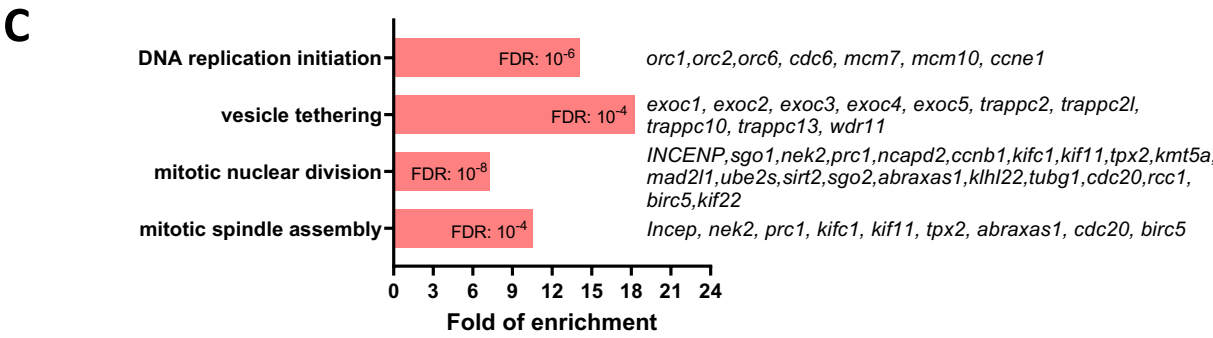
C
DNA replication initiation
FDR: 10-6
orc1,orc2,orc6, cdc6, mcm7, mcm10, ccne1
vesicle tethering
FDR: 10-4
exoc1, exoc2, exoc3, exoc4, exoc5, trappc2, trappc2l, trappc10, trappc13, wdr11
mitotic nuclear division
FDR: 10-8
INCENP,sgo1,nek2,prc1,ncapd2,ccnb1,kifc1,kif11,tpx2,kmt5a, mad2l1,ube2s,sirt2,sgo2,abraxas1,klhl22,tubg1,cdc20,rcc1, birc5,kif22
mitotic spindle assembly
FDR: 10-4
Incep, nek2, prc1, kifc1, kif11, tpx2, abraxas1, cdc20, birc5
Fold of enrichment

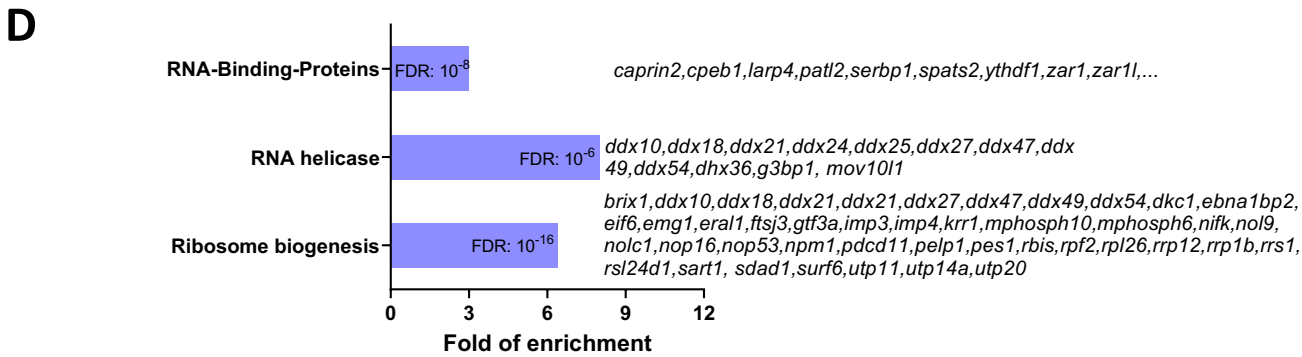
D
RNA-Binding-Proteins
FDR: 10-8
caprin2,cpeb1,larp4,patl2,serbp1,spats2,ythdf1,zar1,zar1l,...
RNA helicase
FDR: 10-6
ddx10,ddx18,ddx21,ddx24,ddx25,ddx27,ddx47,ddx 49,ddx54,dhx36,g3bp1, mov10l1
Ribosome biogenesis
FDR: 10-16
brix1,ddx10,ddx18,ddx21,ddx21,ddx27,ddx47,ddx49,ddx54,dkc1,ebna1bp2, eif6,emg1,eral1,ftsj3,gtf3a,imp3,imp4,krr1,mphosph10,mphosph6,nifk,nol9, nolc1,nop16,nop53,npm1,pdcd11,pelp1,pes1,rbis,rpf2,rpl26,rrp12,rrp1b,rrs1, rsl24d1,sart1, sdad1,surf6,utp11,utp14a,utp20
Fold of enrichment

Fig. 3

A

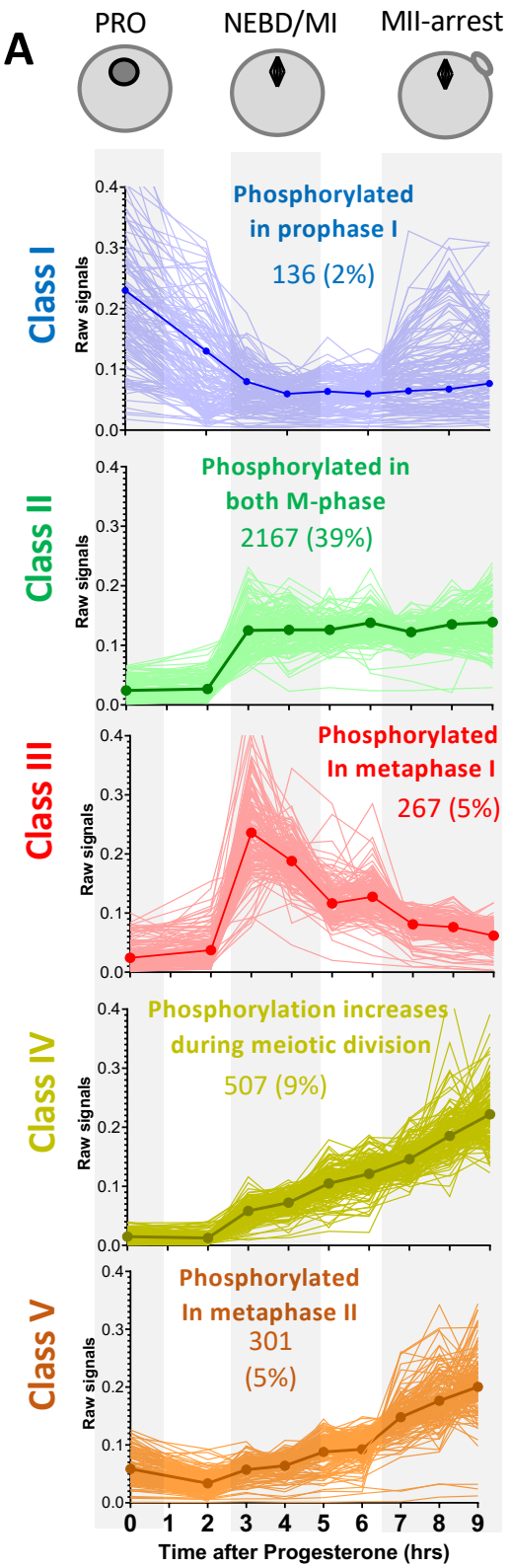

B

	gene name	description	PMID
Vessicle trafficking and membrane organization	C2CD2L	an endoplasmic reticulum protein that functions both as membrane tether to the plasma membrane and as phospholipid transporter	32693056
	MAGI1	a scaffolding protein localized at the plasma membrane	35389514
	NKTR	a membrane-anchored protein with function in protein folding	7906541
	LDLRAP1	interacts with the cytoplasmic tail of the LDL receptor and facilitates the clathrin-mediated endocytosis of LDLR and other members of this family	15728179
	PI4KB	PKA substrate that regulates Golgi reorganization during mitosis, and is involved in Golgi-to-plasma membrane trafficking	23712958
Actin cytoskeleton	WIPF2	induces reorganization of the actin filament network around the plasma membrane by cooperating with WASP/WASL88	21785420
	SPTBN1	an actin crosslinking and molecular scaffold protein that is involved in Ca2+ and calmodulin-dependent exocytosis	32601107
	ITPRID2	tethers IP3 receptors to the actin under the plasma membrane to mediate Ca2+ signalling	34301929
Translation	PATL1	RNA binding protein involved in mRNA stabilization and translation repression	20826699
	eIF4ENIF1	binds and sequesters eIF4E inhibiting protein translation initiation.	16157702
	Maskin	component of the translation repression complex nucleated by CPEB1 that is involved in mantaining translation repression in Prophase arrested oocytes.	10635326
Ubiquitn ligases	Ube2O	E2/E3 ubiquitin-protein ligase with both E2 and E3 ligase activities.	30468556
	Faf2	endoplasmic reticulum–associated protein involved in the dissolution of RNA stress granules	34739333
	Ube4b	E3-ubiquitin ligase, with unknow function.	
	DCUN1D5	catalyzes the neddylation of cullins that is required for the activation of the cullin-E3 ubiquitin ligase.	26906416

Fig. 4

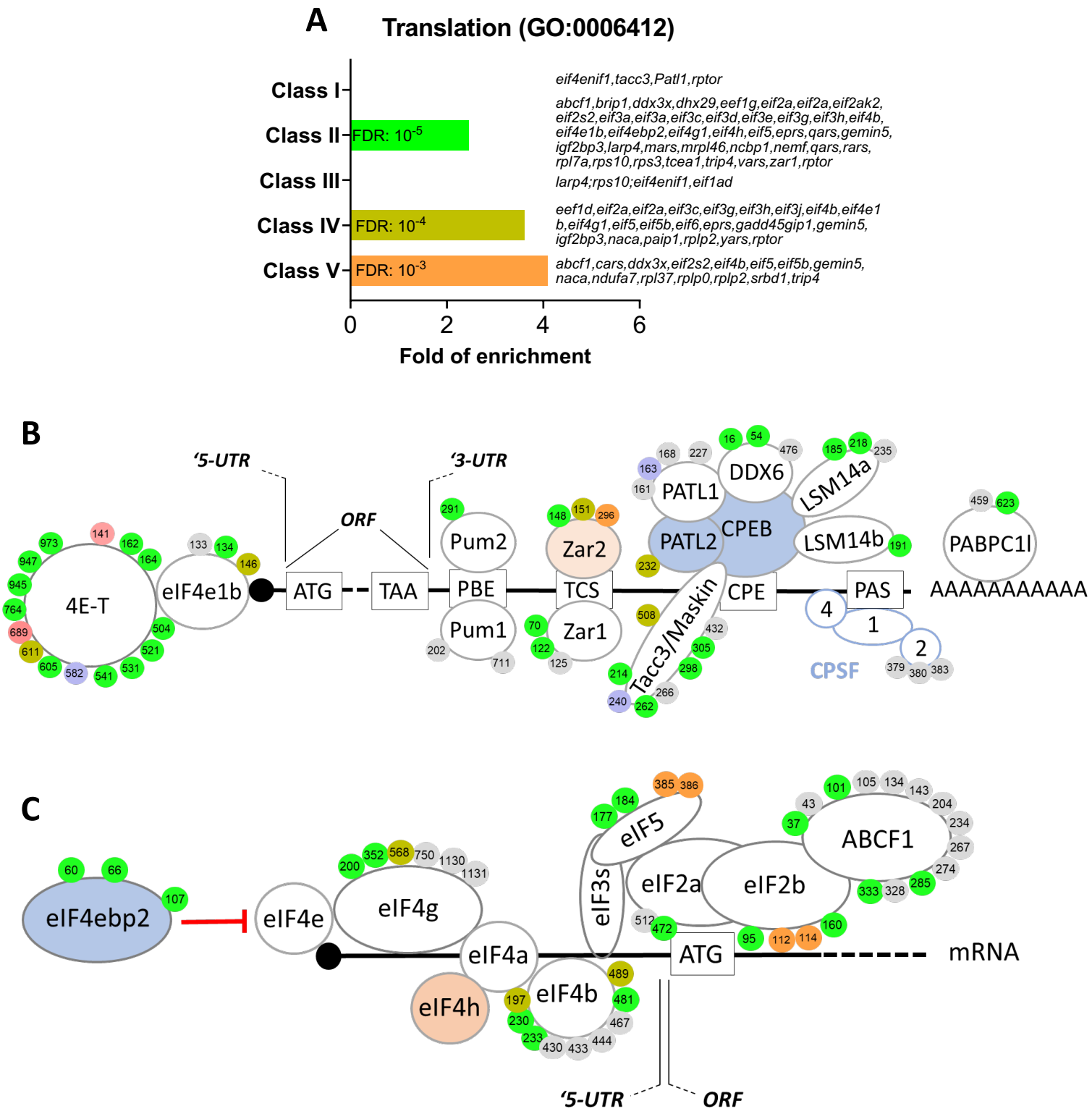
A
Translation (GO:0006412)
Class I
Class II
Class III
Class IV
Class V
FDR: 10-5
FDR: 10-4
FDR: 10-3
eif4enif1,tacc3,Patl1,rptor
abcf1,brip1,ddx3x,dhx29,eef1g,eif2a,eif2a,eif2ak2,
eif2s2,eif3a,eif3a,eif3c,eif3d,eif3e,eif3g,eif3h,eif4b,
eif4e1b,eif4ebp2,eif4g1,eif4h,eif5,eprs,qars,gemin5,
igf2bp3,larp4,mars,mrpl46,ncbp1,nemf,qars,rars,
rpl7a,rps10,rps3,tcea1,trip4,vars,zar1,rptor
larp4;rps10;eif4enif1,eif1ad
eef1d,eif2a,eif2a,eif3c,eif3g,eif3h,eif3j,eif4b,eif4e1
b,eif4g1,eif5,eif5b,eif6,eprs,gadd45gip1,gemin5,
igf2bp3,naca,paip1,rplp2,yars,rptor
abcf1,cars,ddx3x,eif2s2,eif4b,eif5,eif5b,gemin5,
naca,ndufa7,rpl37,rplp0,rplp2,srbd1,trip4
0
2
4
6
Fold of enrichment
B
'5-UTR
'3-UTR
ORF
4E-T
eIF4e1b
ATG
TAA
PBE
Pum2
Pum1
TCS
Zar2
Zar1
PATL1
PATL2
DDX6
CPEB
LSM14a
LSM14b
Tacc3/Maskin
CPE
PAS
PABPC1l
AAAAAAAAAAA
CPSF
C
eIF4ebp2
eIF4e
eIF4g
eIF4a
eIF4b
eIF4h
eIF3s
eIF5
eIF2a
eIF2b
ABCF1
ATG
mRNA
'5-UTR
ORF

Fig. 5

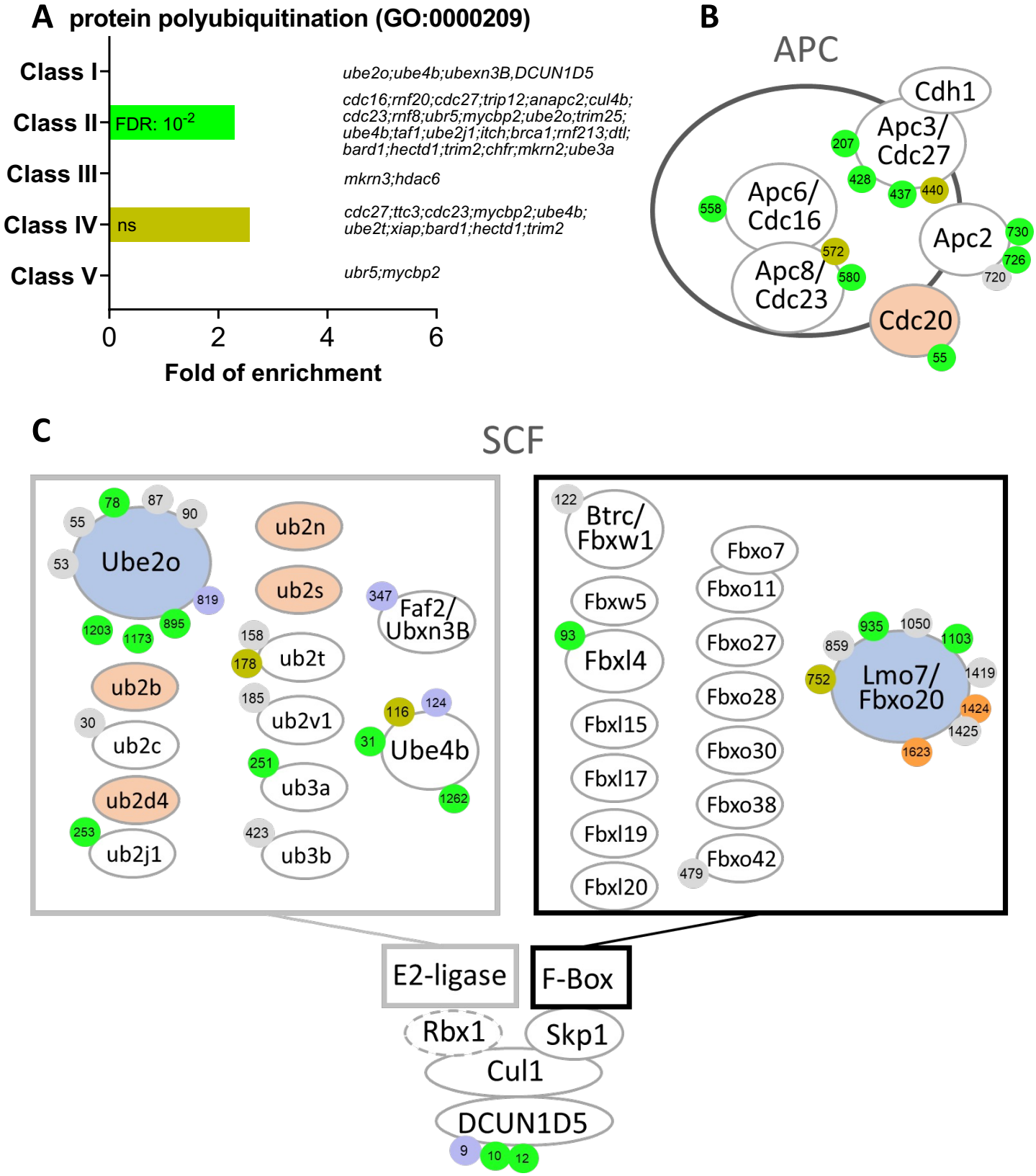
A
protein polyubiquitination (GO:0000209)
Class I
Class II
Class III
Class IV
Class V
FDR: 10-2
ns
ube2o;ube4b;ubexn3B,DCUN1D5
cdc16;rnf20;cdc27;trip12;anapc2;cul4b;
cdc23;rnf8;ubr5;mycbp2;ube2o;trim25;
ube4b;taf1;ube2j1;itch;brca1;rnf213;dtl;
bard1;hectd1;trim2;chfr;mkrn2;ube3a
mkrn3;hdac6
cdc27;ttc3;cdc23;mycbp2;ube4b;
ube2t;xiap;bard1;hectd1;trim2
ubr5;mycbp2
0
2
4
6
Fold of enrichment
B
APC
Cdh1
Apc3/
Cdc27
Apc6/
Cdc16
Apc8/
Cdc23
Apc2
Cdc20
207
428
437
440
558
572
580
730
726
720
55
C
SCF
Ube2o
78
87
90
55
53
819
895
1203
1173
ub2n
ub2s
347
Faf2/
Ubxn3B
158
178
ub2t
ub2b
185
ub2v1
30
ub2c
116
124
31
Ube4b
251
ub3a
1262
ub2d4
253
ub2j1
423
ub3b
122
Btrc/
Fbxw1
Fbxo7
Fbxw5
Fbxo11
93
Fbxl4
Fbxo27
Fbxo28
Fbxl15
Fbxo30
Fbxl17
Fbxo38
Fbxl19
Fbxo42
479
Fbxl20
935
1050
859
1103
752
Lmo7/
Fbxo20
1419
1424
1425
1623
E2-ligase
F-Box
Rbx1
Skp1
Cul1
DCUN1D5
9
10
12

Fig. 6

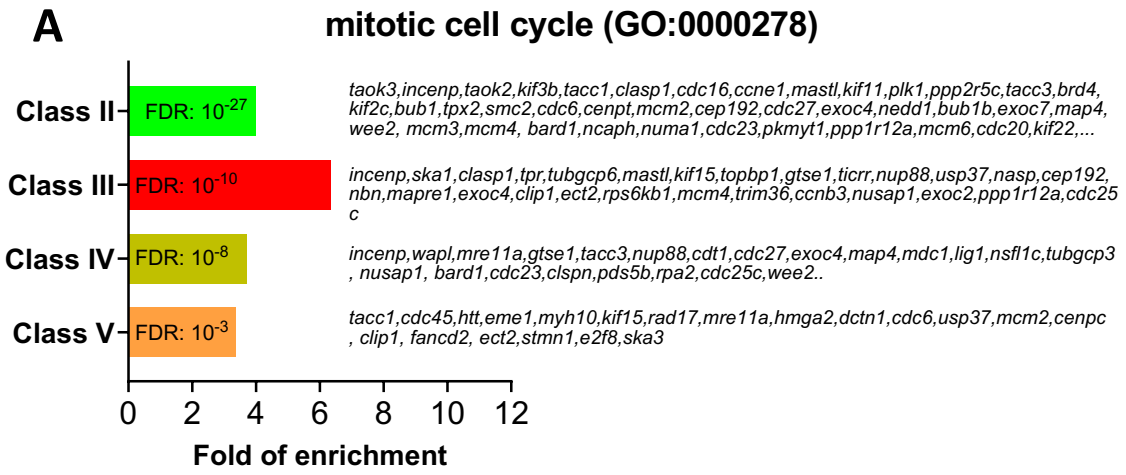
A
mitotic cell cycle (GO:0000278)
Class II
FDR: 10-27
taok3,incenp,taok2,kif3b,tacc1,clasp1,cdc16,ccne1,mastl,kif11,plk1,ppp2r5c,tacc3,brd4, kif2c,bub1,tpx2,smc2,cdc6,cenpt,mcm2,cep192,cdc27,exoc4,nedd1,bub1b,exoc7,map4, wee2, mcm3,mcm4, bard1,ncaph,numa1,cdc23,pkmyt1,ppp1r12a,mcm6,cdc20,kif22,...
Class III
FDR: 10-10
incenp,ska1,clasp1,tpr,tubgcp6,mastl,kif15,topbp1,gtse1,ticrr,nup88,usp37,nasp,cep192, nbn,mapre1,exoc4,clip1,ect2,rps6kb1,mcm4,trim36,ccnb3,nusap1,exoc2,ppp1r12a,cdc25 c
Class IV
FDR: 10-8
incenp,wapl,mre11a,gtse1,tacc3,nup88,cdt1,cdc27,exoc4,map4,mdc1,lig1,nsfl1c,tubgcp3 , nusap1, bard1,cdc23,clspn,pds5b,rpa2,cdc25c,wee2..
Class V
FDR: 10-3
tacc1,cdc45,htt,eme1,myh10,kif15,rad17,mre11a,hmga2,dctn1,cdc6,usp37,mcm2,cenpc , clip1, fancd2, ect2,stmn1,e2f8,ska3
0 2 4 6 8 10 12
Fold of enrichment

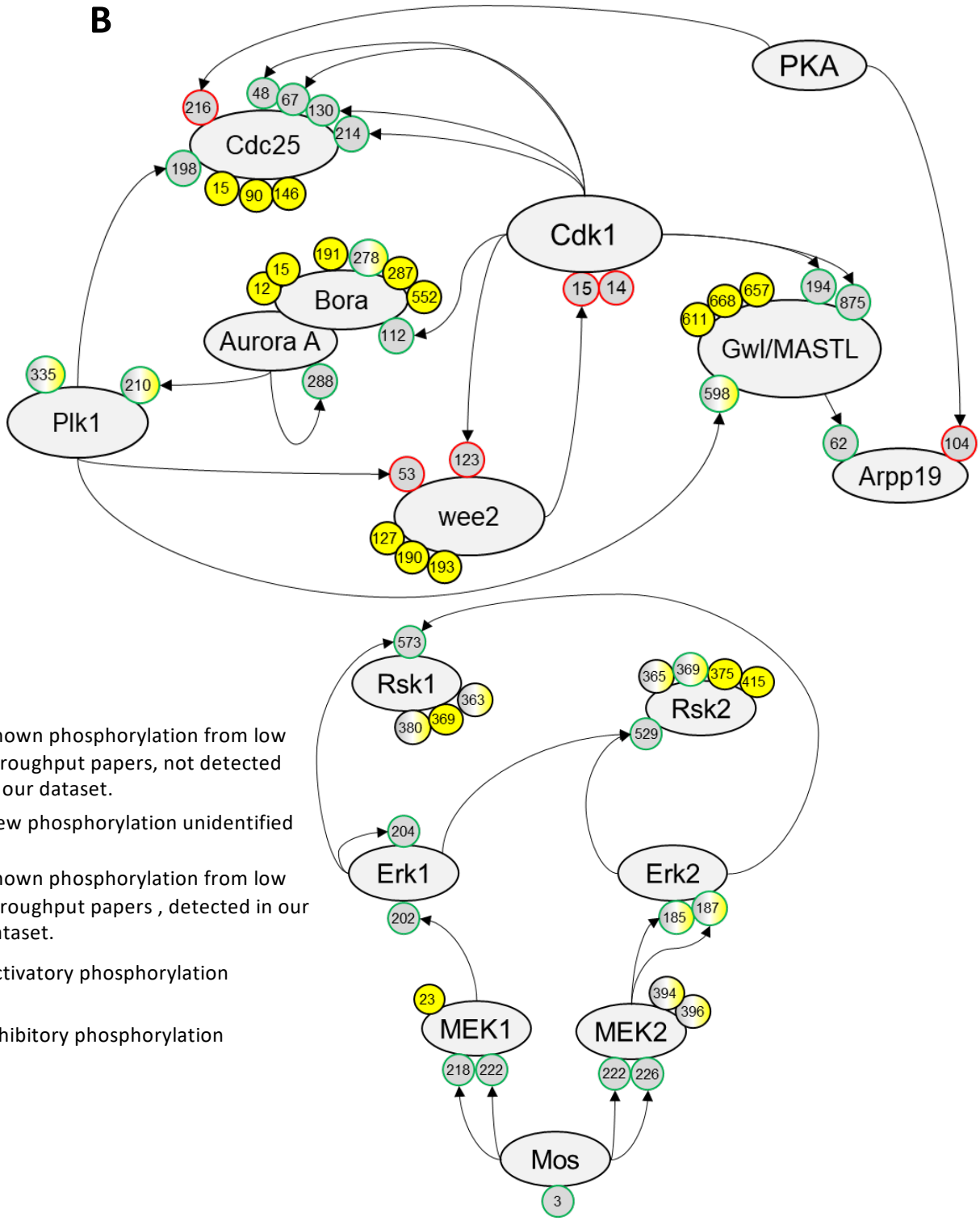
B
PKA
Cdc25
216
48
67
130
214
198
15
90
146
Cdk1
15
14
Bora
15
12
191
278
287
552
112
Aurora A
288
Plk1
335
210
Gwl/MASTL
611
668
657
194
875
598
Arpp19
62
104
wee2
53
123
127
190
193
Rsk1
573
363
380
369
Rsk2
365
369
375
415
529
Erk1
204
202
Erk2
185
187
MEK1
23
218
222
MEK2
394
396
222
226
Mos
3
Known phosphorylation from low throughput papers, not detected in our dataset.
New phosphorylation unidentified
Known phosphorylation from low throughput papers , detected in our dataset.
Activatory phosphorylation
Inhibitory phosphorylation

Fig. 7

A Nucleoporins concentration (nM)

	PRO	MII
NUP107	157	161
NUP133	166	172
NUP153	117	144
NUP155	186	191
NUP160	134	140
NUP188	120	124
NUP205	360	383
NUP210	97	119
NUP214	150	131
NUP35	327	308
NUP37	309	317
NUP43	218	237
NUP50	712	725
NUP54	160	166
NUP58	385	388
NUP62	440	440
NUP85	134	145
NUP88	110	110
NUP93	665	693
NUP98	476	442

B Nuclear pore organization (GO:0006999)

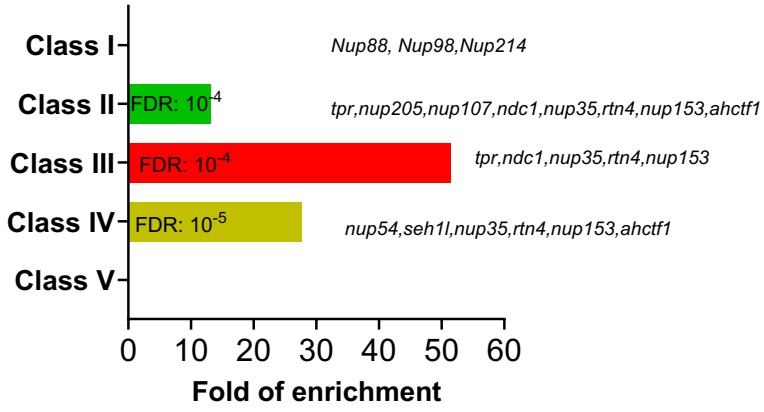

C

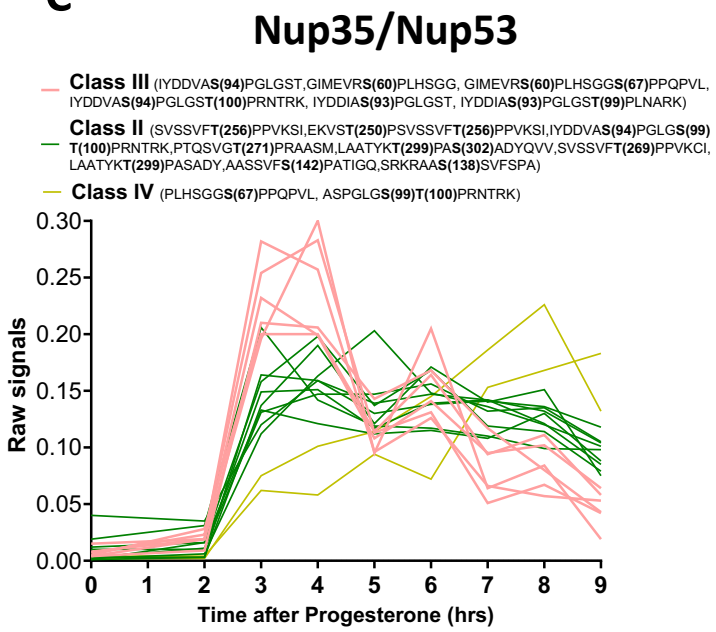

D

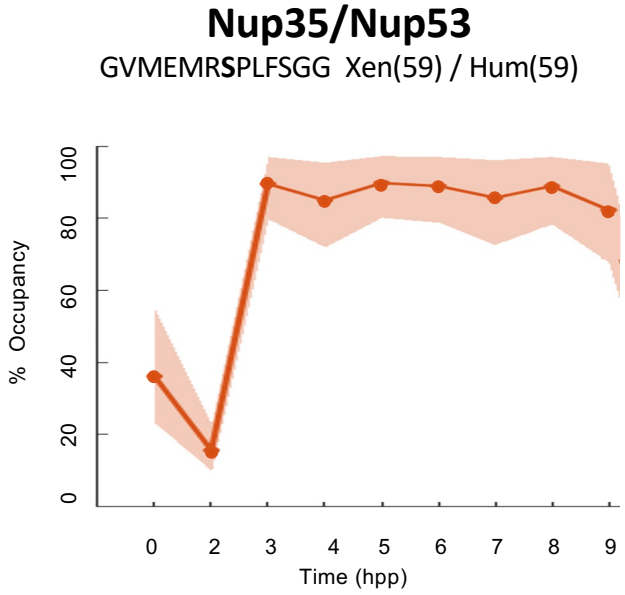

Fig. 8

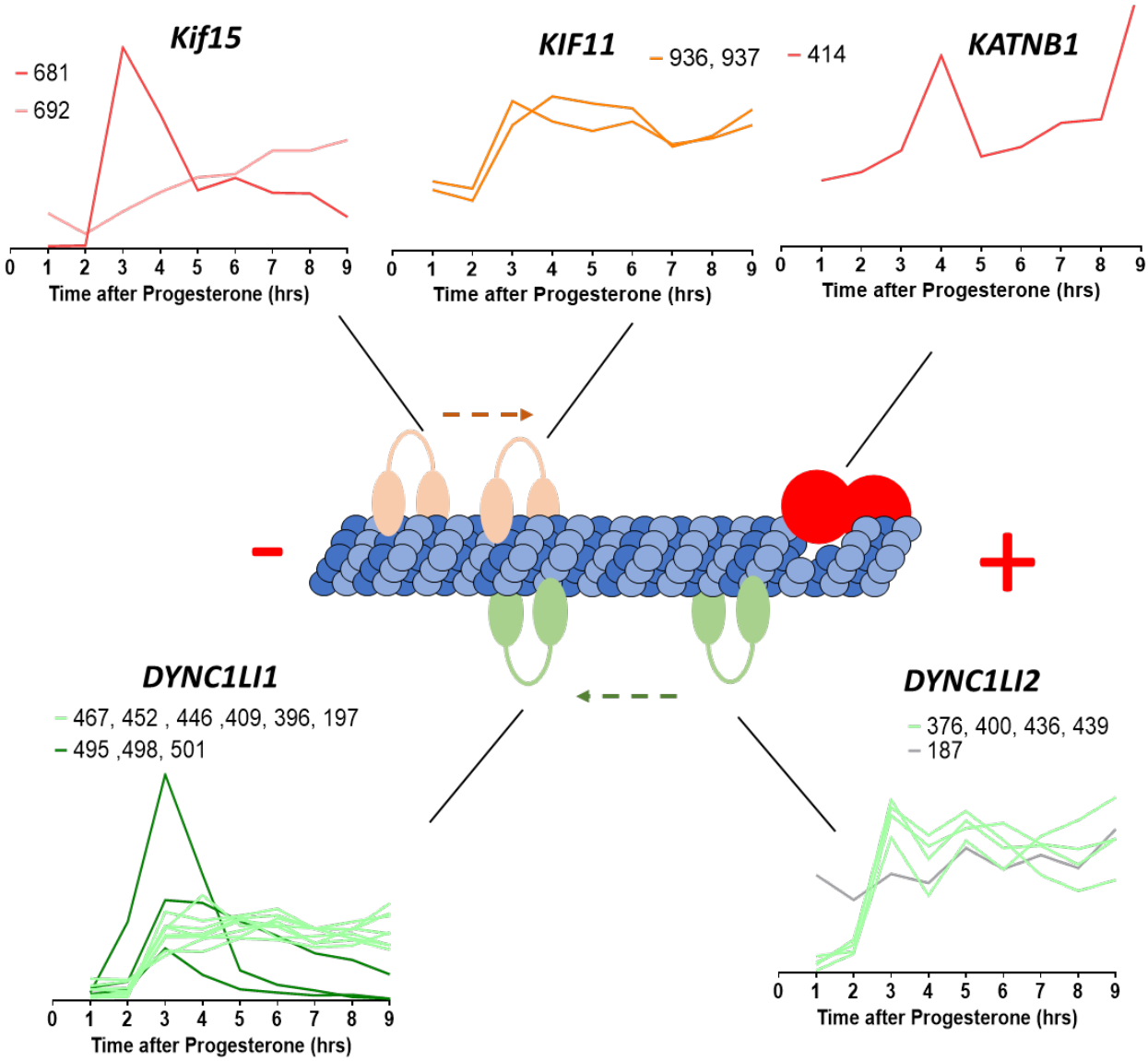
Kif15
681
692
0 1 2 3 4 5 6 7 8 9
Time after Progesterone (hrs)
KIF11
936, 937
414
0 1 2 3 4 5 6 7 8 9
Time after Progesterone (hrs)
KATNB1
0 1 2 3 4 5 6 7 8 9
Time after Progesterone (hrs)
-
+
DYNC1LI1
467, 452 , 446 ,409, 396, 197
495 ,498, 501
0 1 2 3 4 5 6 7 8 9
Time after Progesterone (hrs)
DYNC1LI2
376, 400, 436, 439
187
0 1 2 3 4 5 6 7 8 9
Time after Progesterone (hrs)

Table 1

		Proteome										(Whur,2014)	(Session,2016)
	Gene name	0	2	3	4	5	6	7	8	9	Log2 FC (MII/PRO)	Estimated concentration in MII-arrested oocytes (nM)	Count per Million (CPM) in PRO I
Proximal part	SAS-6	0.11	0.09	0.10	0.10	0.09	0.09	0.09	0.09	0.08	-0.3	36	20
	CENPJ	0.07	0.09	0.09	0.10	0.10	0.11	0.09	0.10	0.09	0.4	9	56
	Cep135	not detected										5	1
Central core	POC1B	0.05	0.05	0.07	0.08	0.09	0.14	0.11	0.10	0.11	1.2	7	96
	POC5	0.05	0.06	0.07	0.08	0.09	0.10	0.10	0.11	0.12	1.1	39	100
	CETN1	0.08	0.08	0.11	0.09	0.09	0.09	0.10	0.09	0.10	0.2	not detected	3
	SFI1	not detected										3	7
	POC1A	not detected										20	54
	CETN2	not detected										82	not detected
	WDR90	not detected										5	25
	FAM161A	not detected										not detected	34
Distal appendages	SCLT1	0.10	0.09	0.10	0.11	0.10	0.10	0.08	0.08	0.08	-0.4	13	2
	FBF1	0.11	0.12	0.11	0.12	0.11	0.11	0.08	0.07	0.06	-0.7	not detected	17
	CEP83	not detected										not detected	7
	CEP89	not detected										not detected	1
Sub-distal appendages	FBF1	0.11	0.12	0.11	0.12	0.11	0.11	0.08	0.07	0.06	-0.7	not detected	17
	CEP164	0.10	0.08	0.11	0.09	0.12	0.09	0.08	0.06	0.08	-0.4	1	not detected
	NIN	0.11	0.09	0.11	0.07	0.08	0.11	0.10	0.08	0.10	-0.2	4	27
	TUBE1	0.10	0.09	0.10	0.10	0.10	0.11	0.09	0.09	0.09	-0.1	7	8
	TUBD1	0.08	0.08	0.08	0.09	0.09	0.11	0.09	0.09	0.10	0.1	13	28
	ODF2	not detected										7	8
	CEP128	not detected										3	17
	CNTRL	not detected										6	26
	CEP170	not detected										4	3
	TCHP	not detected										2	16
	CCDC68	not detected										not detected	3
	tubz1	not detected										not detected	10
	CCDC120	not detected										not detected	not detected
Centriole duplication	CCP110	0.06	0.07	0.06	0.08	0.08	0.09	0.10	0.12	0.12	0.9	7	20
	CEP152	0.07	0.07	0.10	0.10	0.10	0.12	0.10	0.11	0.09	0.6	7	161
	CEP192	0.08	0.08	0.08	0.08	0.09	0.09	0.10	0.11	0.10	0.5	21	24
	STIL	0.08	0.08	0.07	0.08	0.10	0.11	0.10	0.11	0.12	0.5	14	100
	CEP63	0.07	0.06	0.11	0.11	0.13	0.12	0.10	0.09	0.09	0.5	4	33
	CEP76	0.07	0.07	0.07	0.08	0.09	0.14	0.10	0.07	0.12	0.5	12	57
	RTTN	0.09	0.09	0.09	0.10	0.10	0.11	0.09	0.09	0.08	0.0	18	14
	CEP97	0.10	0.10	0.10	0.10	0.09	0.10	0.10	0.09	0.09	-0.1	15	1
	SAS-6	0.11	0.09	0.10	0.10	0.09	0.09	0.09	0.09	0.08	-0.3	36	42
	Plk4	not detected										not detected	not detected
PCM	KIF22	0.02	0.02	0.04	0.05	0.07	0.09	0.12	0.14	0.19	3.1	33	464
	SSX2IP	0.03	0.03	0.05	0.07	0.09	0.11	0.11	0.13	0.16	2.1	20	10
	TUBG1	0.04	0.04	0.04	0.04	0.04	0.04	0.12	0.12	0.11	1.5	166	101
	tpx2	0.06	0.06	0.07	0.08	0.10	0.11	0.11	0.12	0.11	1.0	43	516
	kif11	0.06	0.06	0.07	0.08	0.09	0.10	0.10	0.11	0.12	0.9	44	185
	dync1li1	0.06	0.0735	0.0605	0.0675	0.062	0.0605	0.104	0.1185	0.087	0.8	169	38
	dync2h1	0.067	0.057	0.073	0.074	0.092	0.098	0.104	0.105	0.128	0.7	35	3
	prc1	0.06	0.07	0.08	0.09	0.10	0.12	0.09	0.10	0.10	0.7	32	13
	CEP152	0.07	0.07	0.10	0.10	0.10	0.12	0.10	0.11	0.09	0.6	7	33
	kif4a	0.08	0.07	0.08	0.09	0.09	0.09	0.10	0.10	0.10	0.4	100	120
	TUBGCP4	0.08	0.08	0.08	0.09	0.10	0.08	0.10	0.10	0.10	0.2	14	20
	nedd1	0.08	0.08	0.09	0.08	0.09	0.08	0.10	0.10	0.09	0.2	30	12
	dync2i1	0.0875	0.076	0.0915	0.088	0.0965	0.0975	0.0925	0.0935	0.101	0.1	not detected	11
	CKAP5	0.09	0.09	0.09	0.09	0.09	0.10	0.09	0.10	0.09	0.1	67	102
	dynll2	0.086	0.111	0.077	0.102	0.09	0.08	0.086	0.085	0.104	0.1	411	60
	dync2i2	0.089	0.081	0.1	0.099	0.106	0.098	0.09	0.087	0.095	0.0	not detected	35
	TUBGCP3	0.09	0.08	0.09	0.09	0.10	0.10	0.09	0.10	0.09	0.0	33	10
	KATNB1	0.09	0.09	0.10	0.10	0.10	0.10	0.09	0.09	0.09	0.0	20	108
	dynlt1	0.086	0.1	0.114	0.09	0.09	0.07	0.083	0.085	0.093	0.0	138	49
	dync1i2	0.091	0.104	0.104	0.073	0.081	0.106	0.091	0.089	0.092	0.0	232	48
	PCNT	0.09	0.09	0.09	0.10	0.10	0.10	0.09	0.09	0.09	0.0	16	23
	NPM2	0.08	0.10	0.08	0.12	0.08	0.08	0.07	0.07	0.09	0.0	1181	116
	dync2li1	0.086	0.074	0.084	0.086	0.089	0.091	0.082	0.081	0.091	0.0	43	4
	CLASP1	0.09	0.08	0.09	0.10	0.10	0.10	0.09	0.09	0.08	-0.1	15	48
	TUBGCP2	0.09	0.09	0.10	0.10	0.10	0.09	0.09	0.09	0.09	-0.1	59	22
	dync1li2	0.097	0.089	0.099	0.104	0.094	0.099	0.091	0.094	0.086	-0.1	26	27
	dynll1	0.099	0.101	0.094	0.096	0.092	0.105	0.089	0.093	0.089	-0.1	51	130
	NEK9	0.09	0.10	0.10	0.10	0.10	0.10	0.09	0.08	0.08	-0.2	45	27
	TACC3	0.10	0.10	0.10	0.10	0.10	0.10	0.09	0.09	0.08	-0.2	115	117
	TUBGCP6	0.10	0.09	0.11	0.10	0.10	0.10	0.08	0.08	0.08	-0.3	8	14
	NPM3	0.11	0.09	0.12	0.11	0.10	0.10	0.09	0.09	0.08	-0.3	150	70
	KATNA1	0.10	0.10	0.10	0.09	0.10	0.09	0.09	0.08	0.08	-0.3	63	30
	NPM1	0.12	0.09	0.12	0.10	0.09	0.09	0.08	0.08	0.08	-0.6	308	102
	TUBGCP5	not detected										24	not detected
	KATNAL1	not detected										5	not detected
	KATNAL2	not detected										not detected	22

Fig. EV1

A

	PRO I		MI				MII - arrest							
Gene name	0	2	3	4	5	6	7	8	9	FC (MII/PRO)	Log2- FC (MII/PRO)	FC (MII/PRO) (Peuchen, 2017)	Log2- FC (MII/PRO) (Peuchen, 2017)	PMID	
kif22 (XKid)	0.018	0.019	0.036	0.053	0.074	0.094	0.120	0.138	0.187	8.5	3.1	not detected	not detected	12360284	UP
mos	0.015	0.015	0.061	0.091	0.105	0.136	0.120	0.110	0.148	8.4	3.1	0.9	-0.2	2474853	
ccnb1	0.021	0.031	0.053	0.059	0.095	0.119	0.122	0.150	0.145	6.6	2.7	not detected	not detected	10512866	
wee2	0.027	0.028	0.045	0.048	0.084	0.121	0.102	0.135	0.151	4.9	2.3	not detected	not detected	10673504	
cdc6	0.034	0.033	0.035	0.054	0.074	0.094	0.100	0.149	0.171	4.1	2.0	0.5	-1.0	12384698, 12384699,26092930	
gmnn	0.037	0.038	0.056	0.072	0.099	0.122	0.105	0.130	0.142	3.4	1.8	1.2	0.3	19656945	
birc5 (survivin)	0.044	0.047	0.053	0.056	0.085	0.101	0.113	0.145	0.139	3.0	1.6	2.2	1.1	18378691	
ccne1	0.046	0.057	0.044	0.073	0.090	0.149	0.110	0.113	0.131	2.6	1.4	not detected	not detected	11413001	
zfp36l2	0.059	0.058	0.066	0.053	0.048	0.045	0.132	0.123	0.135	2.2	1.1	not detected	not detected	18385675	
tpx2	0.057	0.061	0.071	0.085	0.098	0.107	0.109	0.115	0.115	2.0	1.0	not detected	not detected	19121998	
kif11 (Eg5)	0.058	0.061	0.073	0.077	0.091	0.100	0.103	0.110	0.119	1.9	0.9	1.7	0.8	8026619	
incenp	0.059	0.065	0.069	0.075	0.096	0.093	0.101	0.101	0.126	1.9	0.9	1.5	0.5	18378691	
ctnnb1	0.064	0.051	0.078	0.088	0.097	0.109	0.105	0.118	0.107	1.7	0.8	1.0	0.0	9876185	
cdc20	0.064	0.058	0.082	0.091	0.097	0.089	0.111	0.102	0.101	1.6	0.7	0.5	-1.1	11413001	
aurka (Eg2)	0.067	0.069	0.088	0.089	0.099	0.104	0.094	0.098	0.108	1.5	0.6	1.3	0.3	10704364	
cdt1	0.072	0.071	0.081	0.098	0.098	0.114	0.096	0.115	0.100	1.4	0.5	1.0	0.0	19656945	
bub1	0.081	0.075	0.099	0.083	0.107	0.102	0.097	0.093	0.101	1.2	0.3	not detected	not detected	11231148	
patl1	0.085	0.075	0.089	0.089	0.095	0.100	0.096	0.104	0.099	1.2	0.2	4.6	2.2	20826699	
kpna3	0.081	0.088	0.075	0.085	0.087	0.09	0.1	0.106	0.098	1.3	0.3	0.6	-0.7	26399853	CONSTANT
gapdh	0.079	0.0885	0.0815	0.083	0.0795	0.0825	0.0905	0.0925	0.0915	1.2	0.2	0.5	-1.03398944	26399853	
ipo5	0.082	0.0845	0.0835	0.0735	0.088	0.08	0.093	0.0965	0.095	1.2	0.2	0.5	-0.9	26399853	
tuba4b	0.079	0.106	0.082	0.132	0.092	0.096	0.078	0.08	0.115	1.2	0.2	0.4	-1.5	20531391	
kpna2	0.09	0.0875	0.096	0.101	0.092	0.09	0.096	0.088	0.101	1.1	0.1	1.1	0.1	26399853	
mapk1	0.092	0.095	0.093	0.098	0.091	0.099	0.092	0.099	0.086	1.0	0.0	0.6	-0.7	26092930	
kpnb1	0.1	0.088	0.08	0.086	0.077	0.093	0.087	0.092	0.115	1.0	0.0	0.5	-1.1	26399853	
xpo1	0.093	0.093	0.086	0.086	0.094	0.092	0.089	0.092	0.086	1.0	-0.1	0.6	-0.8	26399853	
acta4	0.089	0.101	0.086	0.099	0.09	0.09	0.085	0.081	0.089	1.0	-0.1	not detected	not detected	20826699	
cdk1	0.0965	0.092	0.1005	0.0975	0.098	0.095	0.0915	0.0935	0.087	0.9	-0.1	1.0	0.0	26092930	
arpp19	0.1015	0.085	0.1125	0.0885	0.1025	0.086	0.085	0.075	0.083	0.8	-0.3	0.6	-0.7	24525567	
zar1	0.211	0.096	0.109	0.083	0.088	0.086	0.076	0.062	0.064	0.3	-1.6	0.3	-1.8	23827238	
tbpl2	0.135	0.123	0.132	0.089	0.093	0.071	0.075	0.055	0.073	0.5	-1.0	not detected	not detected	19650908	DOWN
zar2	0.218	0.0985	0.0935	0.0845	0.0835	0.0795	0.065	0.0525	0.059	0.3	-1.9	not detected	not detected	23827238	
patl2	0.273	0.286	0.108	0.057	0.036	0.033	0.028	0.025	0.029	0.1	-3.3	0.4	-1.3	20826699	
cpeb1	0.306	0.223	0.098	0.045	0.036	0.033	0.031	0.027	0.031	0.1	-3.4	0.4	-1.2	11237472, 11927567	

B

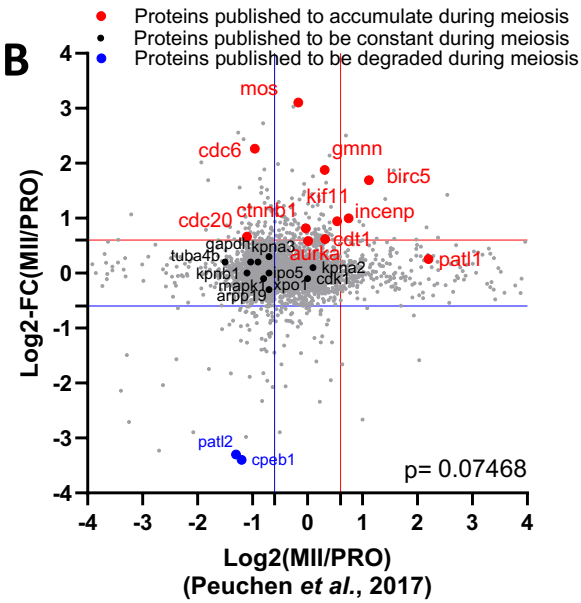

C

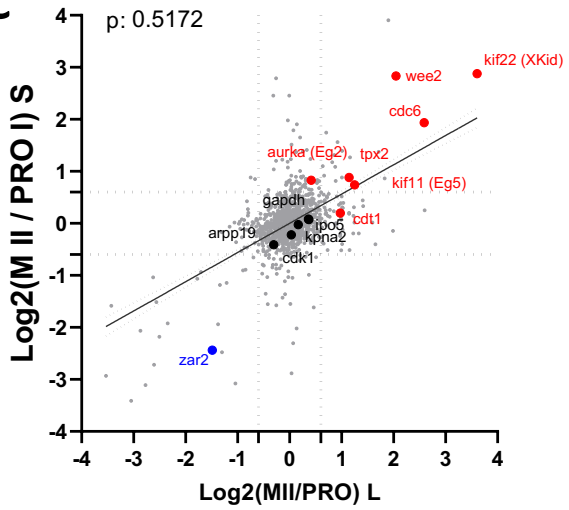

D

		S		
		UP	Constant	DOWN
L	UP	19	57	0
	Constant	62	1042	39
	DOWN	2	38	22

E

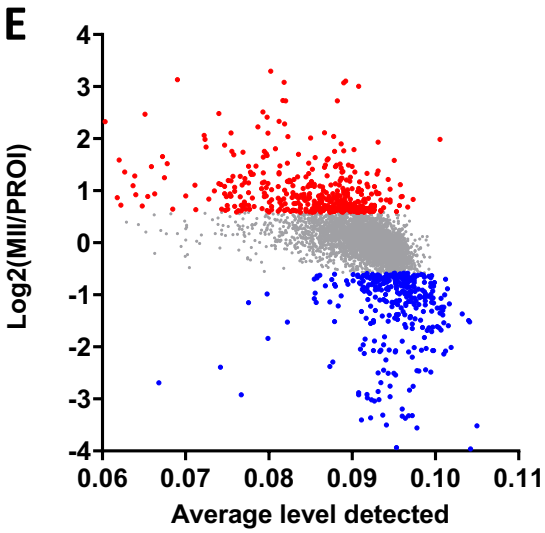

Fig. EV2

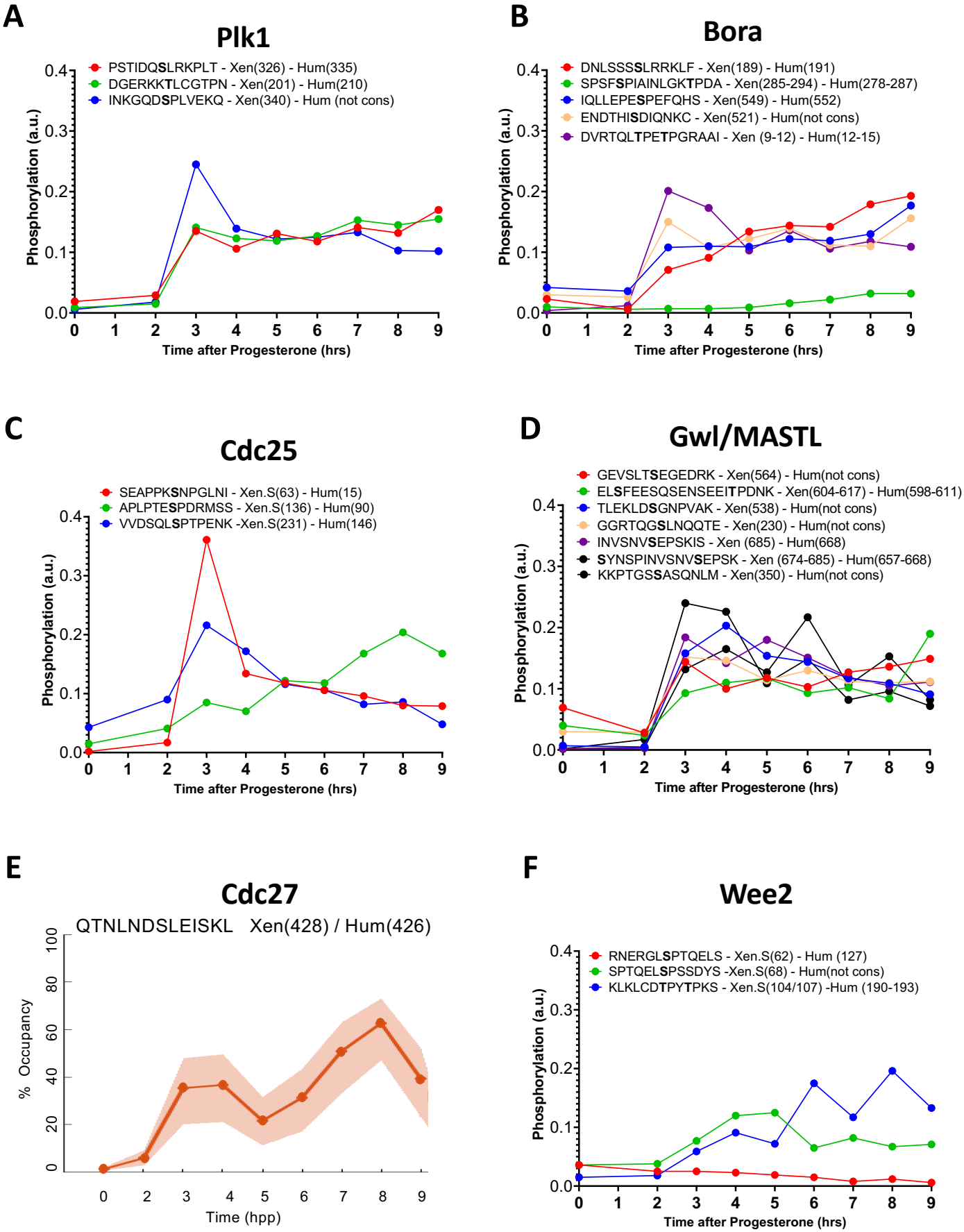
A
Plk1
PSTIDQSLRKPLT - Xen(326) - Hum(335)
DGERKKTLCGTPN - Xen(201) - Hum(210)
INKGQDSPLVEKQ - Xen(340) - Hum (not cons)
Phosphorylation (a.u.)
Time after Progesterone (hrs)
B
Bora
DNLSSSSLRRKLF - Xen(189) - Hum(191)
SPSFSPIAINLGKTPDA - Xen(285-294) - Hum(278-287)
IQLLEPESPEFQHS - Xen(549) - Hum(552)
ENDTHISDIQNKC - Xen(521) - Hum(not cons)
DVRTQLTPETPGRAAI - Xen (9-12) - Hum(12-15)
Phosphorylation (a.u.)
Time after Progesterone (hrs)
C
Cdc25
SEAPPKSNPGLNI - Xen.S(63) - Hum(15)
APLPTESPDRMSS - Xen.S(136) - Hum(90)
VVDSQLSPTPENK -Xen.S(231) - Hum(146)
Phosphorylation (a.u.)
Time after Progesterone (hrs)
D
Gwl/MASTL
GEVSLTSEGEDRK - Xen(564) - Hum(not cons)
ELSFEESQSENSEEITPDNK - Xen(604-617) - Hum(598-611)
TLEKLDSGNPVAK - Xen(538) - Hum(not cons)
GGRTQGSLNQQTE - Xen(230) - Hum(not cons)
INVSNVSEPSKIS - Xen (685) - Hum(668)
SYNSPINVSNVSEPSK - Xen (674-685) - Hum(657-668)
KKPTGSSASQNLM - Xen(350) - Hum(not cons)
Phosphorylation (a.u.)
Time after Progesterone (hrs)
E
Cdc27
QTNLNDSLEISKL Xen(428) / Hum(426)
% Occupancy
Time (hpp)
F
Wee2
RNERGLSPTQELS - Xen.S(62) - Hum (127)
SPTQELSPSSDYS -Xen.S(68) - Hum(not cons)
KLKLCDTPYTPKS - Xen.S(104/107) -Hum (190-193)
Phosphorylation (a.u.)
Time after Progesterone (hrs)

Fig. EV3

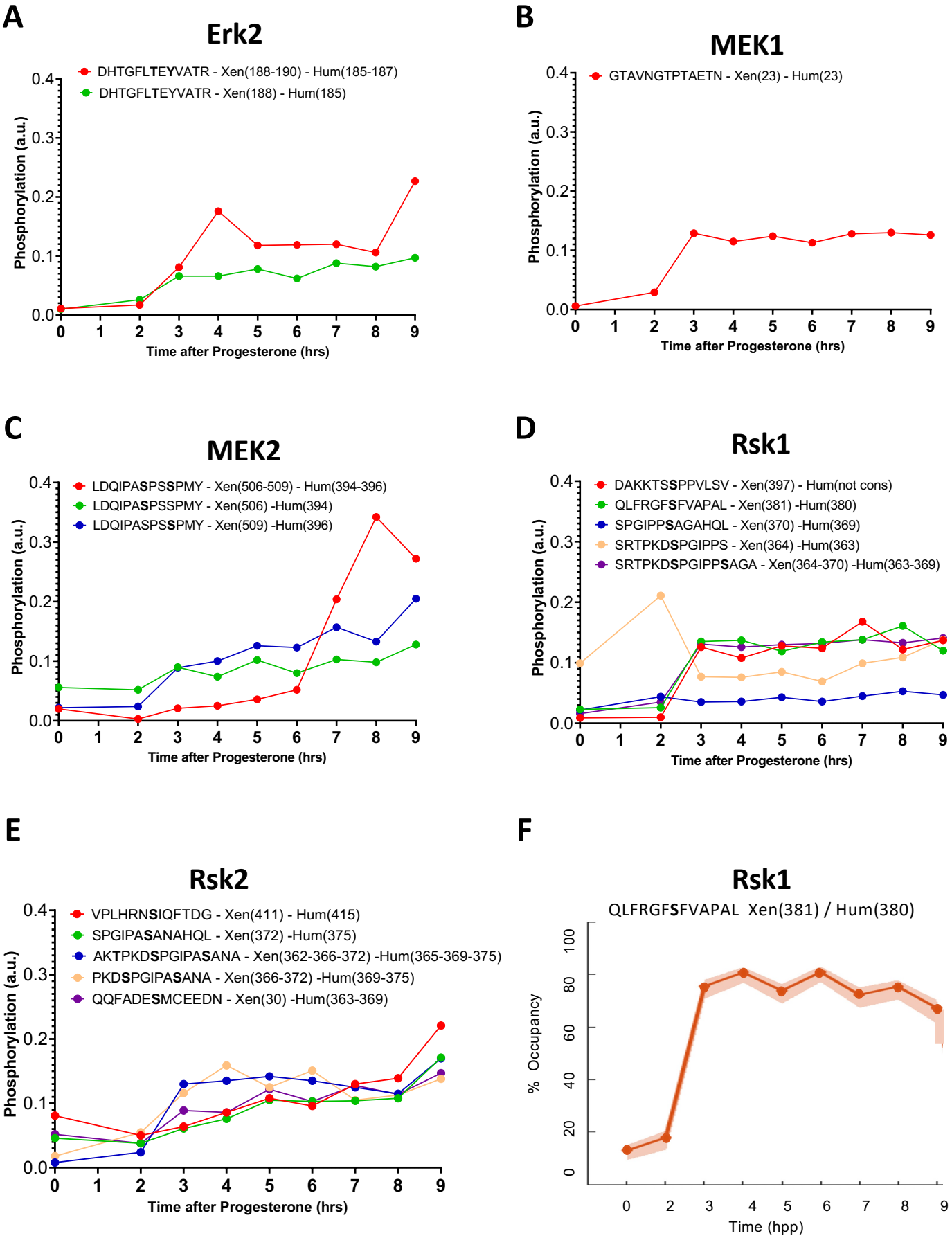
A
Erk2
DHTGFLTEYVATR - Xen(188-190) - Hum(185-187)
DHTGFLTEYVATR - Xen(188) - Hum(185)
Phosphorylation (a.u.)
Time after Progesterone (hrs)
B
MEK1
GTAVNGTPTAETN - Xen(23) - Hum(23)
Phosphorylation (a.u.)
Time after Progesterone (hrs)
C
MEK2
LDQIPASPSSPMY - Xen(506-509) - Hum(394-396)
LDQIPASPSSPMY - Xen(506) -Hum(394)
LDQIPASPSSPMY - Xen(509) -Hum(396)
Phosphorylation (a.u.)
Time after Progesterone (hrs)
D
Rsk1
DAKKTSSPPVLSV - Xen(397) - Hum(not cons)
QLFRGFSFVAPAL - Xen(381) -Hum(380)
SPGIPPSAGAHQL - Xen(370) -Hum(369)
SRTPKDSPGIPPS - Xen(364) -Hum(363)
SRTPKDSPGIPPSAGA - Xen(364-370) -Hum(363-369)
Phosphorylation (a.u.)
Time after Progesterone (hrs)
E
Rsk2
VPLHRNSIQFTDG - Xen(411) - Hum(415)
SPGIPASANAHQL - Xen(372) -Hum(375)
AKTPKDSPGIPASANA - Xen(362-366-372) -Hum(365-369-375)
PKDSPGIPASANA - Xen(366-372) -Hum(369-375)
QQFADESMCEEDN - Xen(30) -Hum(363-369)
Phosphorylation (a.u.)
Time after Progesterone (hrs)
F
Rsk1
QLFRGFSFVAPAL Xen(381) / Hum(380)
% Occupancy
Time (hpp)